TAMPEREEN TEKNILLINEN YLIOPISTO
TAMPERE UNIVERSITY OF TECHNOLOGY

Jussi Aaltonen

Interaction of Bootstrap Reservoir and Hydraulic Pump in Aircraft Hydraulic Systems

Julkaisu 1448 • Publication 1448

Tampere 2016

Tampereen teknillinen yliopisto. Julkaisu 1448
Tampere University of Technology. Publication 1448

Jussi Aaltonen

Interaction of Bootstrap Reservoir and Hydraulic Pump in Aircraft Hydraulic Systems

Thesis for the degree of Doctor of Science in Technology to be presented with due permission for public examination and criticism in Festia Building, Auditorium Pieni Sali 1 at Tampere University of Technology, on the 20th of December 2016, at 12 noon.

Tampereen teknillinen yliopisto - Tampere University of Technology
Tampere 2016

ISBN 978-952-15-3881-0 (printed)
ISBN 978-952-15-3886-5 (PDF)
ISSN 1459-2045

Aaltonen, J: Interaction of Bootstrap Reservoir and Hydraulic Pump in Aircraft Hydraulic Systems

Tampere University of Technology, 2016

Keywords: Axial piston pump, Bootstrap reservoir, Aircraft hydraulic system

ABSTRACT

This thesis focuses on studying system- and component-level phenomena in the fighter aircraft hydraulic power supply system in detail. The objective is to find out system-level root causes for premature failures of hydraulic pumps encountered in many modern fighter aircraft, and to study phenomena related to them. The thesis establishes a theoretically justified basis for understanding the interactions of the hydraulic system, bootstrap-type reservoir and axial piston hydraulic pump. It also presents a cost-effective and flexible method for studying system- and component-level phenomena in an aircraft hydraulic system by combining a theoretical approach with ground and laboratory testing.

The hydraulic pump and bootstrap reservoir are studied using computer simulations to find out how interactions in the system-level operation influence the internal loads of the pump. A hydraulic pump and bootstrap-type reservoir with pipework connecting them are modelled as analytical physical models. Other parts of the hydraulic system are modelled using empirical black box-type models. The models used are verified in the laboratory using a purpose-built test rig and field measurements made with a real aircraft. Root causes of failures and phenomena causing them are identified using simulations. On the basis of this, system and component design variables which affect these phenomena are determined. The results of the study prove that premature failures of the hydraulic pump encountered in certain types of high-performance fighter aircraft are related to hydraulic system design features and their service and maintenance practices. The thesis concludes with design recommendations for bootstrap-type reservoir and pump supply and drain lines.

PREFACE

This is not the first thesis I have begun to write, and it is far from the first thesis subject for me, but this definitely is the first thesis I will finish. Before your eyes lies the thesis "Interaction of Bootstrap Reservoir and Hydraulic Pump in Aircraft Hydraulic System", which has been written to fulfil the graduation requirements of the Doctoral programme in Engineering Sciences at Tampere University of Technology. This thesis is one product of a long series of research projects in which I have been involved since the early 2000s. Even though the research on the area is bound to continue in years to come, this thesis finally finishes one part of it.

I would like to express my sincere gratitude to the Finnish Air Force Headquarters and Finnish Defence Forces Logistics Command (formerly Finnish Air Force Materiel Command) for funding all of the research presented in this thesis.

I would like to express my sincere gratitude to certain persons for their support: Professor Kari T. Koskinen, whose advice and support has been invaluable throughout the whole process, and Captain Mika Siitonen from the Finnish Air Force, who has played a significant role in this research in many ways, from making the funding possible to providing input on technical questions along the way. I would also like to thank all of the team members, former and present, for their contribution to the research.

I would also like to express my sincere appreciation to Patria Aviation Oy, VTT Oy, Finnair Oyj, Eaton Ltd Aerospace Group, Parker Ltd Aerospace Systems and Technologies, the US Navy, the Royal Australian Air Force and (already gone but not forgotten) the Aerodynamics laboratory of Aalto University whose fruitful co-operation and kind assistance has been of great benefit throughout the years. Last but not least, I would like express my gratitude to my wife, Nina Aaltonen, for pushing me forward with this, always firmly, but not always gently. Without her, this probably would never have been finished.

Tampere 7.10.2016

Jussi Aaltonen

CONTENTS

NOMENCLATURE

ω	angular velocity	[1/s]
δ_s	friction type translation coefficient	
η	dynamic viscosity	[Ns/m^2]
ψ	inclination of barrel against valveplate	[deg, rad]
β	primary swashplate angle	[deg, rad]
α	secondary swashplate angle	[deg, rad]
τ	yield in slipper lubrication film	[Pa]
φ, φ_i	angular position of piston	[deg, rad]
η_{mh}	mechanical efficiency	
ω_s	angular velocity, swashplate	[1/s]
η_{tot}	total efficiency	
η_{vol}	volumetric efficiency	
A	area	[m^2]
A_0	flow area, cylinder discharge opening	[m^2]
A_{bs1}	reservoir low pressure piston area	[m^2]
A_{bs2}	reservoir high pressure piston area	[m^2]
A_{CP}	control piston area	[m^2]
A_k	piston area	[m^2]
a_{k1}	piston acceleration on the z-y plane	[m/s^2]
a_{k2}	piston acceleration on the z-x plane	[m/s^2]

A_p	opening area of pressure port of valveplate	[m^2]
A_s	opening area of suction port of valveplate	[m^2]
A'_p	nominal opening area of pressure port of valveplate	[m^2]
A'_s	nominal opening area of suction port of valveplate	[m^2]
A_v	area of an orifice	[m^2]
A_{vtot}	orifice area	[m^2]
B	bulk modulus	[Pa]
b_1	x-y and y-z plane projection of piston position	[m]
b_2	z-x plane projection of piston position	[m]
b_c	viscous friction coefficient	[Ns/m]
b_k	viscous friction coefficient, piston/barrel contact	[Ns/m]
b_{ks}	viscous friction coefficient, slipper	[Ns/m]
b_s	viscous friction coefficient, swashplate	[Ns/rad]
c	width of plane A_c	[m]
c_d	discharge coefficient	
D_{hp}	hydraulic diameter, pressure port opening	[m]
D_{hs}	hydraulic diameter, suction port opening	[m]
D_{hvtot}	hydraulic diameter, orifice	[m]
D_k	piston diameter	[m]
D_v	control valve spool diameter	[m]
e	eccentricity	[m]

e_1	effecting radius of F_{Ban} when z_v is odd	[m]
e_2	effecting radius of F_{Ban} when z_v is even	[m]
e_{ab}	effecting radius of F_{Bab}	[m]
e_{mi}	mean effecting radius of F_{Ban}	[m]
$F_{\omega k}$	piston centrifugal force on centre of gravity	[N]
F_{μ}	control piston spool friction	[N]
$F_{\mu BS}$	reservoir piston friction	[N]
$F'_{\omega k}$	piston centrifugal force on slipper	[N]
$F'_{\omega ky}$	piston centrifugal force, y-component	[N]
F'_{p}	control piston force, z-component	[N]
F'_{s}	return spring force, z-component	[N]
F_{Aki}	piston force against swashplate	[N]
F_{aki}	piston inertia	[N]
F_{Bab}	force caused by fluid field between barrel and valve plate	[N]
F_{Ban}	force caused on valve plate by cylinder pressure	[N]
F_C	coulomb friction force	[N]
F_{Dki}	pressure force on a piston	[N]
F_G	force caused by aircraft acceleration to reservoir piston	[N]
F_p	control piston force	[N]
F_{RBxi}	piston radial force, x-component	[N]
F_{RByi}	piston radial force, y-component	[N]

F_{Rki}	normal force between piston and barrel	[N]
F_s	return spring force	[N]
F_S	stiction friction force	[N]
F_{Sky}	piston reaction force on slipper, y-component	[N]
F_{TG}	friction force between slipper and swashplate	[N]
F_{TGy}	friction between slipper and swashplate, y-comp	[N]
F_{Tki}	friction force on piston	[N]
f_k	dry friction coefficient, piston/barrel contact	
h	clearance between valve plate and barrel	[m]
h_0	maximum clearance between valve plate and barrel	[m]
h_{0k}	clearance between piston and barrel	[m]
h_G	lubrication film thickness on slipper	[m]
L	length of a gap	[m]
L'_v	control orifice width projected to spool surface	[m]
L_F	length of the piston/barrel contact	[m]
L_{FA0}	bottom dead centre length of piston/barrel contact	[m]
$l_{F/2}$	distance of piston centre of gravity from piston head	[m]
l_K	length of piston	[m]
l_{KM}	distance of piston centre of gravity from slipper joint	[m]
l_{s1}	distance of piston centre of gravity from top dead centre	[m]
L_v	control valve orifice width	[m]

M	torque	[Nm]
M_μ	friction torque of swashplate	[Nm]
m_{bsTOT}	total mass of reservoir piston	[kg]
M_{Bz}	shaft torque caused by pistons	[Nm]
m_k	piston mass	[kg]
M_p	torque generated on swashplate by control piston	[Nm]
m_p	control piston mass	[kg]
M_s	torque generated on swashplate by return spring	[Nm]
M_{Sx}	swashplate torque, x-axis	[Nm]
p	pressure	[Pa, bar]
p_c	control pressure	[Pa, bar]
p_e	case pressure	[Pa, bar]
p_k	cylinder pressure	[Pa, bar]
p_{k0}	initial cylinder pressure	[Pa, bar]
p_s	supply pressure	[Pa, bar]
Q_{cL}	leakage flow between cylinder and piston	[l/min]
Q_{iL}	leakage flow on valveplate	[l/min]
Q_{kL}	cylinder leakage flow	[l/min]
Q_{kp}	volumetric flow, pressure port of valveplate	[l/min]
Q_{ks}	volumetric flow, suction port of valveplate	[l/min]
Q_p	pump delivery volumetric flow	[l/min]

Q_{sL}	Leakage through slipper bearing	[l/min]
r	radius of clearance between valve plate and barrel	[m]
R	radius of piston bores	[m]
r_g	slipper inner radius	[m]
R_g	slipper outer radius	[m]
r_i	mean radius of valveplate	[m]
s_k	piston position, z-component	[m]
s_{k1}	piston position on the z-y plane	[m]
s_{k2}	piston position on the z-x plane	[m]
v	velocity	[m/s]
v'_p	velocity of contact point of control piston and swashplate, z-component	[m/s]
v'_s	velocity of contact point of return spring and swashplate, z-component	[m/s]
V_{c0}	cylinder dead volume	[m^2]
V_c	cylinder volume	[m^2]
v_k	piston velocity	[m/s]
v_{pR}	velocity of contact point of control piston and swashplate	[m/s]
v_{sR}	velocity of contact point of return spring and swashplate	[m/s]
v_s	translation velocity stiction and coulomb friction	[m/s]
w	width of the clearance between valveplate and barrel	[m]
w_i	mean width of gap	[m]

x	pressure compensator spool displacement	[m]
x_{TOT}	pressure compensator spool maximum displacement	[m]
x_{bs}	reservoir piston displacement	[m]
x_p	control piston displacement	[m]
x_{ab1}	location of force resultant of plane A_1	[m]
x_{ab2}	location of force resultant of plane A_2	[m]
x_{abc}	location of force resultant of plane	[m]
x_{B1}	x-component of e_1	[m]
x_{B2}	x-component of e_2	[m]
x_{Dk}	piston position, x-coordinate	[m]
x_{Ri}	slipper, x-coordinate	[m]
x_v	spool lift	[m]
y_{B1}	y-component of e_1	[m]
y_{B2}	y-component of e_2	[m]
y_{Dk}	piston position, y-coordinate	[m]
y_{Ri}	slipper, y-coordinate	[m]
z_v	number of pistons on pressure stroke	
z_0	piston position, z-component	[m]
z_1	piston position on the z-y plane	[m]
z_2	piston position on the z-x plane	[m]
ΔQ	system flow variation	[l/min]

ABBREVIATIONS

ADG	Accessory drive gearbox
AMAD	Airframe mounted auxiliary drive
AR	Air refuelling system
CFD	Computational fluid dynamics
CSD	Constant speed drive
DAQ	Data acquisition
EDP	Engine-driven pump
EPU	Emergency power unit
FEA	Finite element method
FFP	Fuel flow proportioner
FLCS	Flight control system
HDU	Hydraulic drive unit
ISA	Integrated servo actuator
JFS	Jet fuel starter
LEF	Leading edge flap
LG	Landing gear
MBS	Multibody systems analysis
MLG	Main landing gear
NLG	Nose landing gear
NWS	Nose wheel steering
ODE	Ordinary differential equation
PDE	Partial differential equation
PMG	Permanent magnet generator
PTO	Power take-off

1 INTRODUCTION

The life span of military aircraft from the first specification of their design requirements to the end of operational service is very long, in some cases over 50 years. Just the design process before the first flying prototypes can take over ten years. Considering the speed at which technology develops, it is thus possible that some technical details can be considered outdated even before the aircraft enters operational service.

A modern aircraft typically goes through numerous updates during its operational service life. These updates usually concentrate on improving its mission-specific capabilities, adding new capabilities or extending its usable life. However, possibilities for improving reliability or lowering operating costs are often overlooked even though technical development opens possibilities for improving them as well.

The design concept of the 4th generation jet fighters, the generation to which most fighters in operational service today belong, dates back to the late 1960s. The hydraulic systems, as well as many other subsystems, of the 4th generation jet fighters are thus mainly based on 1960s and 1970s technology. Their design is based on the knowledge of the time and was done using the methods and tools available at the time. Therefore on the basis of current knowledge, numerous details of systems and components can be pointed out as outdated, even though at the time they were designed they were state-of-the-art. Improving these relatively small details can offer possibilities for significant improvements in reliability, as well as maintenance and operation costs.

Design and analysis methodologies and tools have also gone through remarkable development since the 4th generation fighters were on the design board. The most significant change has happened in the field of computer simulation. In the 1970s, this was still in its early infancy, but nowadays it has matured into an everyday tool used by every engineer. Computer simulation opens possibilities for easily and accurately studying phenomena which previously could only be studied by test flying or were impossible to study at all. Using modern methodologies enables a better understanding of the operation and especially interactions among subsystems, structures and environments.

1.1 Military Aircraft Hydraulic Systems

Hydraulic systems are used in aircraft for a wide variety of functions, such as flight controls, brake systems, door actuation, landing gear actuation, nose wheel steering and weapon systems.

The hydraulic system is usually considered to be a separate subsystem of the aircraft's structure, but it is actually an inseparable part of many other subsystems, as in modern aircraft, nearly all of the power stages of various actuators are hydraulic and thus powered by the hydraulic system. This means that the hydraulic system does not operate independently from other subsystems, but its operation is always defined by control inputs given by other subsystems. For example, a typical 4th generation fighter has more than ten independent flight control surfaces, each actuated by electro-hydraulic actuators on the basis of flight control system commands. Besides the flight control system actuators, there are also electro-hydraulic actuators of auxiliary systems (weapons systems, etc.) which are controlled by the control systems of each auxiliary system. In a modern fly-by-wire aircraft, the instantaneous load of the hydraulic system is not determined only by pilot command and manoeuvre, because there is no direct dependence between the pilot command and flight control surface deflections, but deflections are always also a function of the current flight state, load and environmental conditions (Terry, 1998) (Tuttle, et al., 1990).

Most of the load on the hydraulic system is generated by the flight control system. As fighters have become faster and their manoeuvrability demands have grown higher, the power of the hydraulic system has grown. In 4th generation fighters, the power of the hydraulic system is approx. 150–250 kW. In the 5th generation fighters, still mainly on the drawing board, the hydraulic power required for flight control and thrust vectoring is projected to be considerably higher (Zhanlin, et al., 2003).

Even though power-by-wire and electro-hydraulic actuators have been discussed for a long time and their benefits have been thoroughly proven, most military aircraft in operational service today (up to the 4.5th generation) use traditional central hydraulic systems, and due to the life span of aircraft, this will also be the case for several decades in the future (Busch & Aldana, 1993) (Bajpai, et al., 2001).

Even though the power demand has increased, the typical hydraulic system pressure used has not increased accordingly. During the Second World War, in aircraft utilising hydraulics the standard system pressure was 100–140 bar (1500–2000 psi). In 1st generation jet fighters, the typical system pressures were already 210 bar (3000 psi). The pressure level used remained the same through the 2nd and 3rd generations and even some 4th generation fighters mainly utilised 210 bar systems. During generations 4 and 4.5, the typical system pressure was raised to 280 bar (4000 psi). The 5th generation fighters are projected to utilise 550 bar (8000 psi) systems. System power requirements and system pressure have been evolving in an imbalance, which has caused flow demands to rise in disproportion. As power density requirements have also been rising, the disproportion in flow and pressure has caused several drawbacks and difficulties in component and system design.

Jet fighters up to generation 4.5 have so-called central hydraulic systems. In central hydraulic systems, the hydraulic system of the aircraft is divided into two or more separate systems which are each divided into multiple separate circuits. Each system and circuit is not dependant on the operation of the others. Systems and circuits are also redundant, to give the aircraft adequate fault tolerance and tolerance to battle damage.

Even though the hydraulic system has a parallel redundant structure, its reliability and usability is still an essential issue in the reliability and usability of the whole aircraft. The flight-worthiness of the aircraft is highly dependent on the flight-worthiness of the hydraulic system.

Specifications for the configuration of hydraulic systems are given in design standards such as SAE AS 5440. However, reliability and damage tolerance issues are mostly defined by flying quality requirements specified by other standards, such as MIL-F-8785. A typical requirement for fixed wing aircraft is that damage in one component or circuit, including the power source, should not cause loss of a certain level of manoeuvrability, and even with two damaged circuits or components, a complete loss of manoeuvrability is not allowed. This demand leads to hydraulic system configurations with commonly at least two separate pumps powering at least two separate hydraulic systems, each responsible for different functions but with the possibility to cross-connect systems in certain cases. In aircraft with multiple engines,

each hydraulic pump is driven by a different engine, which gives an adequate redundancy. In single engine aircraft, some other means is commonly used to provide an adequate power supply in case of engine malfunction if it is not possible to use engine wind milling, such as a ram-air turbine-driven pump.

Semi-closed hydraulic circuits are often used in aircraft. In a semi-closed circuit, the system return flow directly supplies the pump and the reservoir is only used to compensate fluid volume changes. The reason for using semi-closed circuits is the same as in other applications: making the system smaller and lighter.

The hydraulic pumps used in aircraft are typically variable displacement axial piston units with constant pressure regulators. The rotational speed of pumps is usually very high in order to enable the use of as small and light units as possible. Because of this, there are some small differences in typical aircraft pump design in comparison to generic hydraulic pumps.

Hydraulic fluid reservoirs in aircraft hydraulic systems differ a great deal from generic mobile hydraulic applications. The reservoir volumes are significantly smaller due to weight savings requirements, and reservoirs are always pressurised. Reservoir pressurising is necessary to guarantee adequate fluid supply for the hydraulic pump independent from the aircraft alignment, acceleration etc. There are several different ways to achieve reservoir pressurisation: Air charge using engine bleed air, inert gas (nitrogen) charge and bootstrap reservoir (self-pressurising using system pressure) (Figure 1-1).

Air-charged reservoirs are mainly used in commercial aircraft that use non-flammable synthetic ester-based hydraulic fluids. The hydrocarbon-based fluids commonly used in military aircraft mean that air-charged reservoirs are unusable in their systems, since the combination of hydrocarbon-based fluid, even if it is fire-resistant, and pressurised air poses a great fire hazard. Therefore, gas-pressurised reservoirs in military aircraft are charged with some inert gas, typically nitrogen. A common reservoir type in modern aircraft, both military and commercial, is the bootstrap reservoir, in which the reservoir is self-pressurised using the system's pressure.

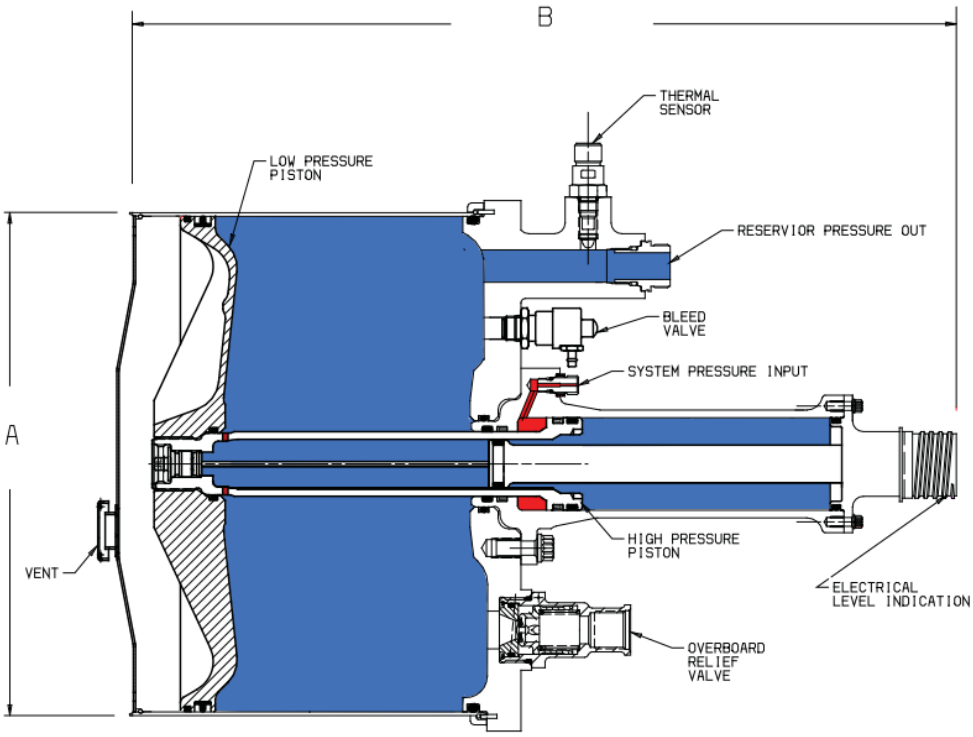

Figure 1-1Bootstrap-type hydraulic reservoir (Parker Aerospace, 2016)

Hydraulic pumps and reservoirs with their accessories form the backbone of an aircraft's hydraulic system, and they are therefore the most critical components of the system. Due to the nature of the flight control of a modern aircraft, the operating point of pumps and their stress level is in a continuously changing state which depends on the flight state, ambient conditions and flight control system commands. Thus an arbitrary operating point of the pump and the whole system cannot be reproduced in ground tests with real aircraft due to different ambient conditions, the lack of aerodynamic load and the limitations of the flight control system. This makes it impossible to study the system's operation using simple ground tests.

A more detailed overview to the typical fourth generation jet fighter hydraulic system is provided in Appendix 1. Due to the fact that detailed technical information of most of fourth generation fighters is still classified information the example used is Locheed Martin F-16A which documentation is publicly available from various sources. Description of the system is based on the flight manual.

1.2 Motivation and Justification for the Research

In aircraft applications, hydraulic pumps have varying lifetime expectancies: In commercial aviation their lifetimes can be tens of thousands flight hours and even in the most demanding military aircraft applications they are expected to live over a thousand hours. However it is commonly known that hydraulic pumps tend to be the Achilles heel of some fighter aircrafts for no obvious or easily explainable reason.

Probably the most common cause of premature failure of hydraulic pumps in fighter aircraft is excessive wear caused by cavitation erosion in one of the critical components inside the pump. Common explanations for the root causes of these failures vary from the operating conditions and properties of hydraulic fluid to system and component design flaws. However, under closer examination it is usually impossible to pinpoint the exact unambiguous root cause. Nevertheless, these failures occur in certain aircraft types more often than in others.

The exact root cause for this type of failure cannot be reliably studied by using traditional causal analysis, but requires the ability to study system- and component-level phenomena in operating points encountered during flight operations. The traditional approach to studying hydraulic system behaviour in such arbitrary in-flight operating points is laboratory tests using a functional simulator (*ironbird*), or test flights with suitable test instrumentation installed in the aircraft. Both of these approaches, however, have serious shortcomings in terms of the expenses, availability of equipment and risks involved in testing. Test flights are technically very challenging to realise, involve high risks and are thus extremely expensive. Testing with a functional simulator involves fewer risks and is cheaper, but a functional simulator is very often not available. Therefore a systematic and cost-efficient approach to studying the behaviour of aircraft hydraulic systems without an ironbird or flight testing is needed.

A cost-effective and -efficient and flexible method for studying system- and component-level phenomena in aircraft hydraulic system is used in this study. The method combines a theoretical approach, i.e. simulation, with ground and laboratory testing in a way which enables the accurate and reliable study of phenomena occurring at arbitrary in-flight operating points without conducting actual flight testing. A

closely reminiscent method has earlier been successfully used by Tumarkian & Casey to investigate hydraulic pump failures of Ukrainian Air Force MIG-23 fighters. Unfortunately, Tumarkian & Casey's investigations have never been published completely or in scientifically relevant media (Casey, 2007).

1.3 Objective of the Thesis

In this thesis, system- and component-level phenomena in fighter aircraft hydraulic power supply systems are studied in detail. The objective is to discover the phenomena causing premature failures of axial piston hydraulic pumps typically encountered in some fighter aircraft and to study these phenomena. On the basis of these studies, improvements in system and component design principles are proposed.

Hypothesis:

System-level component interactions have an effect on the premature failures of the swashplate-type axial piston hydraulic pump through their effect on its internal load.

Research questions:

1. How do **bootstrap-type reservoir and supply line dynamics affect** the internal forces of the swashplate-type axial piston hydraulic pump in a semi-closed circuit?
2. What kind of **effects do drain line pressure losses** have on the internal forces of the swashplate-type axial piston hydraulic pump?
3. How does **free air in the bootstrap-type** reservoir affect the internal forces of the swashplate-type axial piston hydraulic pump?

1.4 Scientific Contribution

The primary field of scientific contributions of this thesis is establishing a basis for understanding system level phenomena in fighter aircraft hydraulic power supply systems. This is achieved through studying system- and component-level phenomena and interactions in hydraulic power supply system with computer simulations and laboratory and field tests. These results are used to isolate root causes and to give

scientifically justified explanation for premature pump failures. Primary scientific contributions are:

Establishing basis for understanding the interactions between variable displacement swash plate type axial piston pump and bootstrap-type reservoir in semi-closed hydraulic system
Identifying root causes for hydraulic pump failures and phenomena triggering them
Identifying freely variable design parameters in system and components and establishing their relationships and their effect on the pump's supply line pressure dynamics
Qualitative analysis of the sensitivity of the system and component design variables which have an effect on these phenomena

The secondary field of contribution is hydraulic system and component modelling and simulation. In the model used in the simulations hydraulic pump and bootstrap-type reservoir with pipework connecting them are modelled using analytical physical equations. Other parts of the hydraulic system are modelled using empirical black box-type empirical or semi-empirical models. The models are verified in the laboratory using laboratory and field measurements. Secondary scientific contributions are:

A detailed analytical model of a variable displacement swashplate-type axial piston pump with secondary swashplate angle
A detailed analytical model of a bootstrap-type hydraulic reservoir
Empirical black-box type system models

Furthermore, the systematic methodology utilising modelling and computer simulation alongside laboratory and field testing to eliminate the need for flight testing or the use of an ironbird is novel in the aerospace context.

1.5 Research Methods

Mathematical modelling and computer simulation are selected for the main research method in this study. The mathematical modelling of the aircraft pump, bootstrap and hydraulic system is based on common equations presented in the general literature.

Laboratory measurements and field tests with a real on-ground fighter aircraft are carried out to verify the simulation model.

Laboratory measurements are carried out using specific test rig developed for studying static and dynamic pump operation in different conditions. Field tests with real fighter aircraft are carried out in a test hangar, which enables operating aircraft with full thrust.

Simulation is utilised for studying system operation in in-flight situations, which are too risky and expensive to study using measurements. Because it is also very complicated to measure internal loads in hydraulic pumps, simulation models are used to derive connections between external measurable variables and internal phenomena.

Synthesis is used to derive design guidelines based on the measurements and simulation studies.

1.6 Structure of the Thesis

This thesis is divided into seven chapters.

Chapter 1 is an introduction giving the background for the study and introducing the objectives, scientific contribution and methods used. In Chapter 2, a short literature study on swashplate-type hydraulic pump modelling and aircraft hydraulic systems is presented.

Chapter 3 concentrates on the mathematical modelling of the aircraft hydraulic pump and its system. The pump model consists of submodels of a rotating group, swashplate, port plate and controller and these are explained in detail. The complete simulation model also includes the hydraulic system and bootstrap models, which are presented.

In Chapter 4 the verification of the developed simulation model is presented. The verification is carried out against laboratory measurements from a specific test rig and field measurements from real fighter aircraft.

Chapter 5 presents the simulation study of the influence of system operation on pumps' internal loads. The selected performance indicators for the study are bootstrap

and supply line dynamics, drain line pressure losses and flow imbalance caused by asymmetric actuators.

Based on the simulation study presented in Chapter 5, proposals for aircraft hydraulic power supply system design guidelines are presented in Chapter 6. These guidelines provide practical instructions for systems designers in order to avoid unwanted behaviour and possible premature failures in fighter aircraft hydraulic pumps.

Chapter 7 contains discussion about results and objectives.

In Chapter 7 the research work of the thesis is concluded and suggestions for future research are presented.

2 LITERATURE STUDY

The focal points of this study are threefold. In a broad view, the study is about a specific type of hydraulic system used typically in fighter aircraft, but also in many other modern jet and turboprop aircraft. On the detailed level, the interest lies is in two key components which the operation of the hydraulic system affects: the hydraulic pump and bootstrap-type reservoir.

The literature study presented in this chapter concentrates on giving an overview of the state-of-the-art research on modelling axial piston swashplate-type hydraulic pumps. This approach is chosen because the pump is the focal point of this study and is also the most complex component of this system. Moreover, previous systematic research on the dynamics of bootstrap-type hydraulic reservoirs or semi-closed hydraulic systems incorporating them is non-existent.

Research related to aircraft hydraulic system in general is scattered many different fields of interest. Since 2010 topics such as landing gear (Pavan, et al., 2015) (Singh & Upendranath, 2013), flight control systems (Gheorghe, et al., 2013) (Gao, et al., 2013) and simulation methodologies (Staack & Krus, 2013) (Krus, et al., 2012) (Joshi & Jayan, 2002) have studied.

Advanced simulation methodologies such as CFD, co-simulation and hardware-in-the-loop simulation have also been studied in aerospace context (Xin & Shaoping, 2013) (Yin, et al., 2015) (Hietala, et al., 2009) (Hietala, et al., 2011) (Karpenko & Sepehri, 2006) (Alarotu, et al., 2013).

There has been plenty of research on aircraft hydraulic pump fault-finding, diagnostics and condition monitoring (Byington, et al., 2003) (Ruixiang, et al., 2002) (Skormin & Apone, 1995) (Gomes, et al., 2012). Pump and system dynamics are not the focal point of this research; it mainly concentrates on determining the remaining useful service life, predicting upcoming failures and isolating fault detection in the pump.

Condition monitoring and fault finding of hydraulic pumps in general service have also been studied widely (Poole, et al., 2013) (Du, et al., 2013).

Research in the field of modelling axial piston pumps can generally be divided into two main areas: modelling the exact behaviour of a certain pump detail and modelling the overall behaviour of the pump. Regardless of the approach chosen, three areas associated with the model must be acknowledged: friction, compressible flow, and equations of motion.

In the earliest approaches, mathematical analysis was carried out on piston pumps using a transfer function linearised at a certain operation condition. This type of analysis was typified by, for example, Merritt (Merritt, 1967). During this period, linearised models did not describe the internal operation of the pump. In the 1980s, interest in modelling internal operation grew and advances in computer simulation also made its simulation possible. Ikeya & Kato (Ikeya & Kato, 1985) examined slipper–swashplate friction at low speeds in the region. The slipper–swashplate pair was also examined by Iboshi & Yamaguchi (Iboshi & Yamaguchi, 1990) from the perspective of power losses. Zeiger & Akers (Zeiger & Akers, 1985), Kim, et al. (Kim, et al., 1987) and Manring & Johnson (Manring & Johnson, 1994) proposed pump models based on the equations of motion of the swashplate, cylinder barrel, pistons and control piston. These simple models had low accuracy at many operating points. Their importance, however, lies in generalising equations of motion for piston pumps. The first complete set of accurate analytical equations of motion describing the axial piston pump was presented by Ivantysyn & Ivantysynova (Ivantysyn & Ivantysynova, 1993).

Manring & Johnson (Manring & Johnson, 1994) improved friction modelling in their dynamic equation of a piston. Inoue & Nakasato (Inoue & Nakasato, 1994) left out the friction between the piston and the bore as an assumption. The same assumption was made by Zeiger & Akers (Zeiger & Akers, 1985). The work of Yi & Shirakashi (Yi & Shirakashi, 1995) and Ikeya & Kato (Ikeya & Kato, 1985) showed that piston bore friction cannot be left out when establishing piston equations of motion. A more modern two-part friction model was used by Harris (Harris, et al., 1993).

Dobchuk, et al. (Dobchuk, et al., 2000) established that friction on the swashplate affects the natural frequency of the system and the dynamic response. Slipper lubrication was further studied in the 1990s. A precise model of the piston–slipper relationship was developed in the work of Yi, et al. (Yi, et al., 1990). Harris (Harris, et

al., 1993) showed that the behaviour of the piston–slipper lubrication is affected by the operating conditions of the pump.

When modelling pump input torque, the interface between slipper and swashplate must be examined. According to Iboshi & Yamaguchi (Iboshi & Yamaguchi, 1982), this interface develops a significant portion of the losses in axial piston pumps. The second effect to be examined is the lubrication film between the barrel and the valve plate. Rui, et al. (Rui, et al., 1989) showed the dependence of film thickness on the supply pressure, viscosity and rotational velocity.

The torque balance on the swashplate is the most important factor in the control of the variable displacement axial piston pump. Zeiger & Akers (Zeiger & Akers, 1985) solved instantaneous swashplate torque numerically. Manring & Johnson (Manring & Johnson, 1994) took a simplified approach by assuming the transition happens linearly and then included a pressure transition angle to account for the torque imbalance.

The standard model of piston transition pressure was improved by Lin (Lin, et al., 1987) by including the entrapment region, where the piston chamber is open to neither the supply nor the pressure port of the valve plate. Edge & Darling (Edge & Darling, 1986) took into account the fluid inertia in the pressure–flow relationship and obtained an approximation of the overpressure transient that occurs in the transition from the suction to the discharge ports. The pressure–flow relationship was solved numerically by Wicke, et al. (Wicke, et al., 1998) and showed an overpressure due to compressibility and fluid inertia effects.

In the 2000s, development in the area of hydraulic pump modelling and simulation has been fast due to rapid general development in the area of modelling and simulation. Research done in the 2000s has mostly built on the foundation of earlier 1990s research, tackling the challenges of modelling the dynamics of the pump or the friction phenomena within it.

Equations for control and containment forces in the axial piston pump were thoroughly established by Manring (Manring, 2002) (Manring, 1999) (Manring, 2000). These studies also included completely generalised forms of equations of motion with two independent swashplate angles. The so-called secondary swashplate

angle was also studied by Johansson (Johansson, 2005) and Ma, et al. (Ma, et al., 2010).

General pump flow performance with traditional methods and computational fluid dynamics has also been studied during recent years. (Bergada, et al., 2012) (Zhang, et al., 2017). Performance has also been studied using thermal-hydraulic 1D modelling (Li, et al., 2015) (Li, et al., 2011). Also general pump control issues have been studied using traditional analytical methods (Jong-Hyeok, et al., 2015). Containment forces in terms of the tipping force between the valve plate and cylinder barrel were also studied and an equation for the forces derived by Bergada (Bergada, et al., 2008). New design features such as damping holes in portplate have also been studied (Johansson, 2005) (Guan, et al., 2014).

Other branches of research in the 2000s have been utilising more sophisticated computational engineering methodology such as CFD (Computational Fluid Dynamics) to study lubrication in the bearing surfaces of the pump (Xu, et al., 2015). Slipper–swashplate contact in water hydraulic axial piston pumps was studied using CFD by Rokala (Rokala, 2012). There has also been interest in utilising multibody simulation methodologies and software to simulate hydraulic pumps (Deeken, 2003) (Roccatello, et al., 2007).

Because modern model-based engineering design methodologies need rapidly generated yet accurate component models, interest in lumped parameter pump models has once again been growing. New lumped parameter models have been introduced by, for example Casoli & Anthony and Mare (Casoli & Anthony, 2013) (Mare, 2001) (Kauranne, et al., 2003).

3 SIMULATION MODEL OF THE HYDRAULIC POWER SUPPLY SYSTEM OF A FIGHTER AIRCRAFT

Modern fighter aircraft typically have a semi-closed type hydraulic system. The system's power supply consists of an engine-driven pump (EDP) driven through an airframe mounted auxiliary drive (AMAD) and bootstrap-type reservoir (Figure 3-1). Twin engine fighters have one separate hydraulic system per engine. The hydraulic systems are hermetically separated from each other in normal operations, but they can be connected to each other in emergency situations, such as power loss in another system. Hydraulic systems may also incorporate separable circuits, which in normal operation are fully connected to the system, but in emergencies can be hermetically separated from the power supply, for example to prevent fluid loss due to leakages.

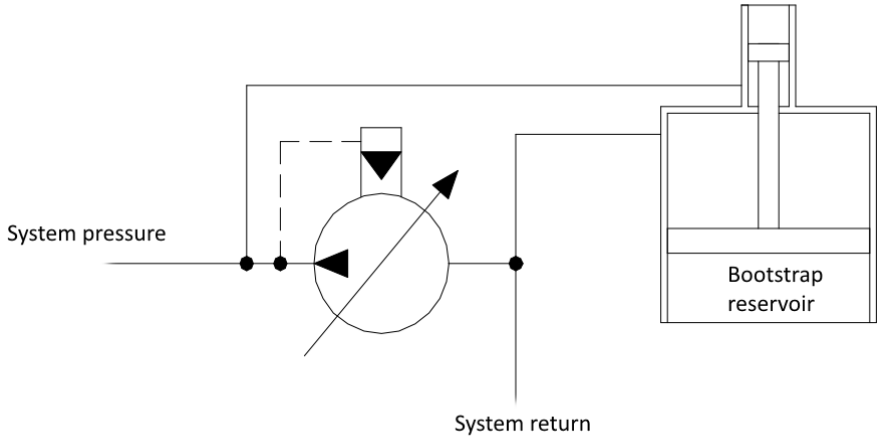

Figure 3-1 Hydraulic diagram of a typical power supply

This study concentrates on the normal operation of one single hydraulic system of a twin engine fighter. Therefore all auxiliary valves which are used only in emergencies to separate circuits from the system or to interconnect it to another system can be disregarded and omitted from the focus of study.

In this study the following limitations, simplifications and assumptions are made: internal loads are studied only in the x-z and x-y planes; swashplate friction is assumed to only consist of viscous friction; the angle between the portplate and cylinder barrel is assumed to be constant and thus the gap between them constant.

Flow-restricting auxiliary components, such as filters, are modelled as turbulent orifices with the flow–pressure drop characteristics of the specific component.

3.1 Modelling and Simulation Methodology

During the recent decades computer simulation has developed to every day engineering tool. This has happened mainly because the development in modelling and simulation methodologies has been fast and steps taken have been big. Also the development in available computing power has taken enormous leaps.

In general vast majority of the engineering problems are time-dependent, non-linear, dependent on spatial coordinates, and thus they can be mathematically described using non-linear partial differential equations (PDE). In some cases problems can also be described using non-linear ordinary differential equations (ODE). In very simple problems or when high level of abstraction is used also transfer functions are appropriate method for modelling. ODEs and PDEs are only numerically solvable, and because of computing power limitations, models usually need some level of simplifications in order to be solvable and manageable.

Common simulation methods range from spatially discrete methods to continuous field problem methods. On the hand they can also be classified according to temporal modelling to static, discrete and continuous. Generally static models in discrete space (for example: Engineering hand calculations etc.) are the simplest ones and the most advanced and most computationally expensive ones are time dependant continuous field problems (for example: Time dependant finite element analysis (FEA) and computational fluid dynamics (CFD).

Recently simulation tools based on methods, such as FEA, MBS and CFD, have become preferred choices in both industry and academia. Main reason for this is high fidelity of results achievable using them. Main enabler for their wide usage has been methodological developments making for example time-dependant field problems solvable even with PCs and also rapid increase of available computing power available in ordinary desktop PCs.

Analytical simulation using models based on analytical differential equations however still has its applications. Analytical models are kind of a “Swiss army knife” in the

world of modelling and simulation. Even though they generally lack fidelity in comparison to more advanced methods they have qualities other models do not have and offer possibilities not available with other models. Their main advantage is good interoperability – They can easily be connected to other models of same type as well as models based on other methodologies. Another advantage is ease of model reduction, i.e. its systematic simplification to allow faster solving in order, for example, to be able to simulate in real time. Together these qualities open possibility to hardware-in-the-loop simulations, where model is connected to real physical system, pilot-in-the-loop simulations, where human operator operates the simulation and software-in-the-loop simulations where real control software is used with the simulated system. Simulations, which combine models based on different methodologies running in different simulation tools, i.e. co-simulations, offer a possibility to compensate the low fidelity of analytical models. Analytical models can be simulated in connection to more advanced simulations, such as FEA or CFD, of certain critical system details of interest. This enables model structures which have high fidelity in points of deeper interest but are still efficient to solve. Even though computing power is cheap now-a-days and it is usually easily available it is nor unlimited neither free, therefore efficiency of solving is very important feature in system and system of systems level simulations especially if large amount of parameter combinations are to be studied.

In this research the modelling approach chosen is analytical modelling. The selection was based on efficient solving requirements and also requirements for model interoperability which however mostly relate to model uses outside the scope of this thesis. Requirements for efficient solving stem from foreseeable need to study effect of parameter variations. Furthermore as the system is relatively complex, stiff and level of detail needed is high it was seen that it is inevitable that the model will become computationally heavy to solve and thus it was justifiable to select the least computationally heavy method.

3.2 Hydraulic Pump Model

3.2.1 Structure and Operation Principle of the Swashplate-Type Axial Piston Pump

A swashplate-type variable displacement axial piston pump consists of five key components within its housing: the cylinder barrel, piston/slipper assembly, swashplate, valve plate, and swashplate control device, which is typically a hydraulic piston. These components and their relative positions are illustrated in the exploded view shown in Figure 3-2.

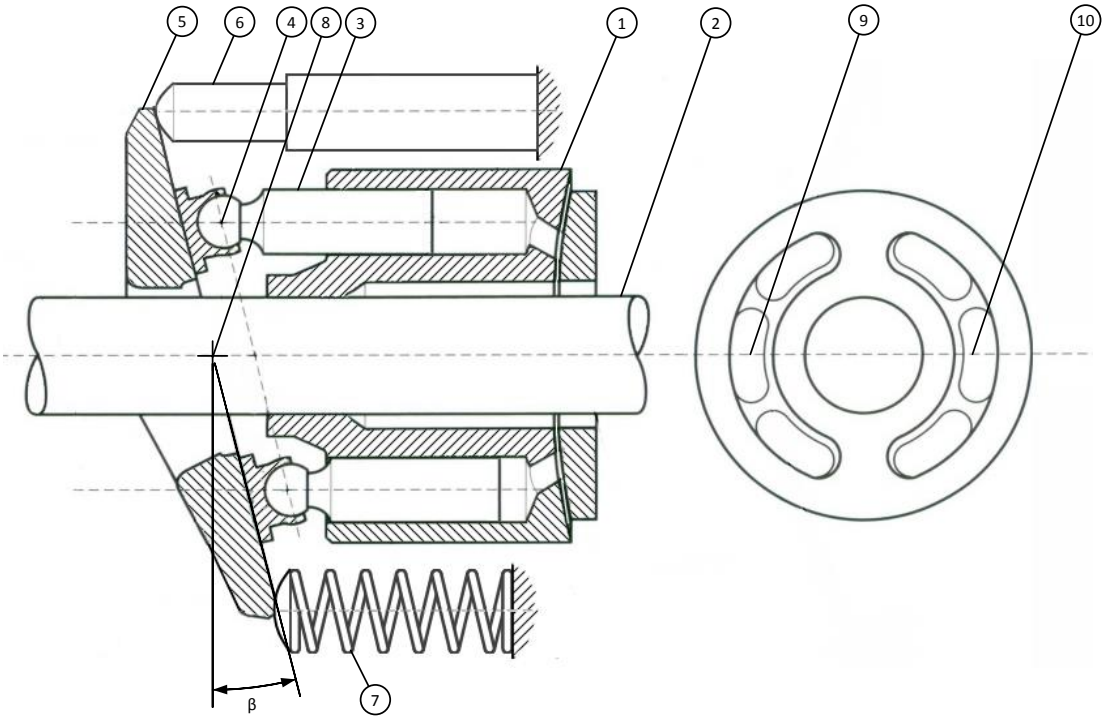

Figure 3-2 Key components of a variable displacement axial piston pump

The cylinder barrel (1) is attached rigidly to the pump input shaft (2). Motion applied to the shaft causes the cylinder barrel to rotate around its axis. The piston/slipper assemblies (3) inside the barrel are arrayed radially around the barrel axis. As a result of shaft and barrel rotation, the pistons also rotate around the same axis.

The piston/slipper assembly consists of two joined components. The pistons are fitted to the slippers by a ball joint (4). The ball joint allows the slippers to slide along the surface of the swashplate (5) regardless of the angle of the swashplate. The angle of the swashplate is controlled by a force applied by a swashplate control device, typically a hydraulic control piston (6). Control pressure applied to the control piston

counteracts the torque produced by the pumping pistons and swashplate return spring (7) in order to maintain the desired swashplate angle.

When the swashplate is displaced around the axis of its support bearings (8) to a certain angle, later denoted as β, a periodic linear motion, creating a pumping effect, occurs in the piston/slipper assemblies as the barrel rotates. The amplitude of the linear motion is defined by the swashplate angle as the piston/slipper assemblies slide on the swashplate surface. A swashplate-type axial piston pump can also incorporate a so-called secondary swashplate angle, later denoted as α. The secondary angle is not shown in Figure 3-2.

The cylinders are open to the discharge port of the valve plate (9) as the pistons move upwards and expel fluid from the cylinder to pump's pressure line. The fluid expelled from this port is referred as the pump's supply flow. As the pistons travel downwards, the cylinders are open to the suction port (10) of the valve plate and draw fluid in from the pump's suction line.

3.2.2 Piston Pressure Force

The first term considered is the piston pressure force term F_{Dki}. The pistons are modelled according to the schematic shown in Figure 3-3.

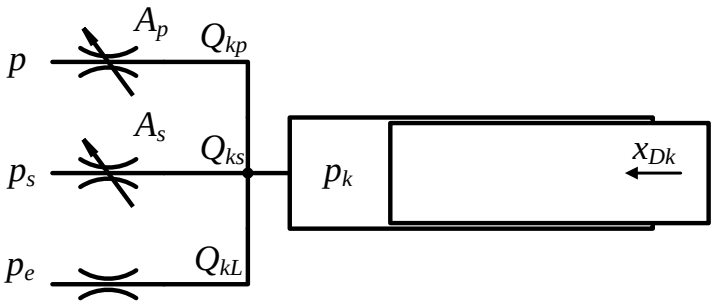

Figure 3-3 Schematic of the piston modelling principle

The pressure inside a single pumping piston (p_k) is the result of three time-dependent factors: speed of the piston (v_{Dk}); the port plate orifices (A_p, A_s) and flow through them (Q_{kp}, Q_{ks}); and leakage flow (Q_{kL}). All of these are related to the piston angular position, swashplate angle, portplate geometry and supply, pressure line and case pressures.

Cylinder volume is modelled using library submodel provided by Amesim. Because of the compressibility of the fluid, the pressure inside the piston chamber can be written as:

$$p_k = p_{k0} + \int_0^t \frac{dp_k}{dt} dt \qquad 3\text{-}1$$

The pressure change in the cylinder can be written as:

$$\frac{dp_k}{dt} = \frac{B}{V_c}\left[\frac{dV_c}{dt} - Q_{kp} - Q_{ks} - Q_{kL}\right] \qquad 3\text{-}2$$

The volume of each cylinder can be expressed as a function of the piston linear displacement:

$$V_c = V_{c0} - A_k x_{Dk} \qquad 3\text{-}3$$

The linear displacement of a piston as a function of the angular position defined by the pump geometry is described in later chapters.

Leakage in piston/barrel clearance has been modelled by (Blackburn, et al., 1960):

$$Q_{cL} = \pi v_k \frac{D_k}{2} h_{0k} + \frac{\pi D_k h_{0k}^3}{24\eta} \frac{(p_k - p_e)}{l_k}\left[1 + 1.5\left(\frac{e}{h_{0k}}\right)^2\right] \qquad 3\text{-}4$$

Leakage through the hydrodynamic bearing in the slipper has been estimated by (M., et al., 2010):

$$Q_{sL} = \frac{\pi h_G^3}{6\eta ln\left(\frac{R_G}{r_G}\right)} p_k \qquad 3\text{-}5$$

The third leakage term, having an effect of total leakage out of the cylinder volume, is $Q_{iL,}$ discussed in Section 3.2.5.

3.2.3 Swashplate

Each piston causes a torque to the swashplate which is relative to its position and the instantaneous force affecting it. Figure 3-4 shows the free-body diagram of the swashplate.

The torque caused by an individual piston to the swashplate around the x-axis is:

$$M_{Sxi} = \frac{R}{\cos^2 \beta} F_{Aki} \cos \varphi_i \qquad 3\text{-}6$$

The total torque around the x-axis caused by all pistons is thus:

$$M_{Sx} = \frac{R}{\cos^2 \beta} \sum_{i=1}^{z} F_{Aki} \cos \varphi_i \qquad 3\text{-}7$$

The model of swashplate is a simple rotational mass with inertia. The friction of the swashplate bearings is modelled as viscous friction. The torque arms of the control piston and return spring are modelled as changing length arms, as presented in the following. The spring is modelled as an ideal spring.

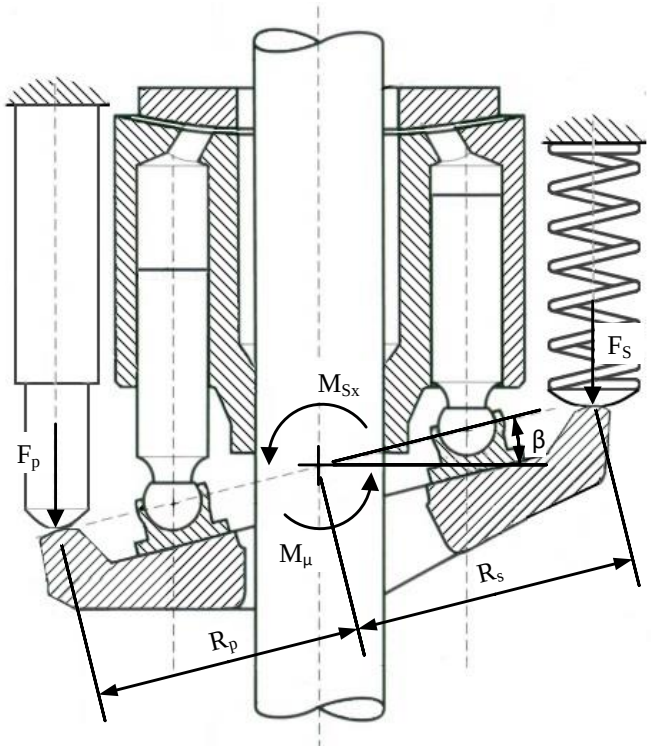

Figure 3-4 Free-body diagram of the swashplate

The ball joint of the pistons and slipper pads is travelling on the plane which runs through the origin and has an angle β related to the y-axis. The force caused by the pistons affect this plane and the axle of support is located in its origin. Forces caused by the control piston and return spring are perpendicular to the y-axis. Forces are always codirectional to the z-axis, and therefore the torque caused by them is a function of the primary swashplate angle β. Forces are not located on the z-y plane and therefore also cause tilting torque around the y-axis. This torque is, however, neglected in the simulation model.

The components perpendicular to the swashplate are:

$$F_p' = F_p \cos\beta \qquad 3\text{-}8$$

$$F_s' = F_s \cos -\beta \qquad 3\text{-}9$$

Therefore, the corresponding torques in relation to origin are:

$$M_p = F_p' R_p \qquad 3\text{-}10$$

$$M_s = F_s' R_s \qquad 3\text{-}11$$

The frictional torque is:

$$M_\mu = b_s \varpi_s sgn(\omega_s) \qquad 3\text{-}12$$

Defining the positive direction of rotation around x-axis towards the bottom dead centre, the torque equation for the swashplate is:

$$M_{Sx} + M_p - M_s - M_\mu sgn(\omega_s) \qquad 3\text{-}13$$

The angular speed of the swashplate relates to the speed of the return spring and control pistons:

$$\omega_s = \frac{v_p'}{R_p \cos\beta} = \frac{v_s'}{R_s \cos -\beta} \qquad 3\text{-}14$$

3.2.4 Rotating Group

The coordinate system for the pump rotating group is set as described in Figure 3-5. The direction of rotation is assumed to be clockwise. The secondary angle (cross-angle) is perpendicular to the primary swashplate angle.

The equations presented in this chapter are based on the single swashplate angle axial piston pump model presented by Ivantysyn & Ivantysynova (Ivantysyn & Ivantysynova, 1993). However, here the equations are formulated into a more generalised form by adding the effect of the secondary swashplate angle (α) to each equation.

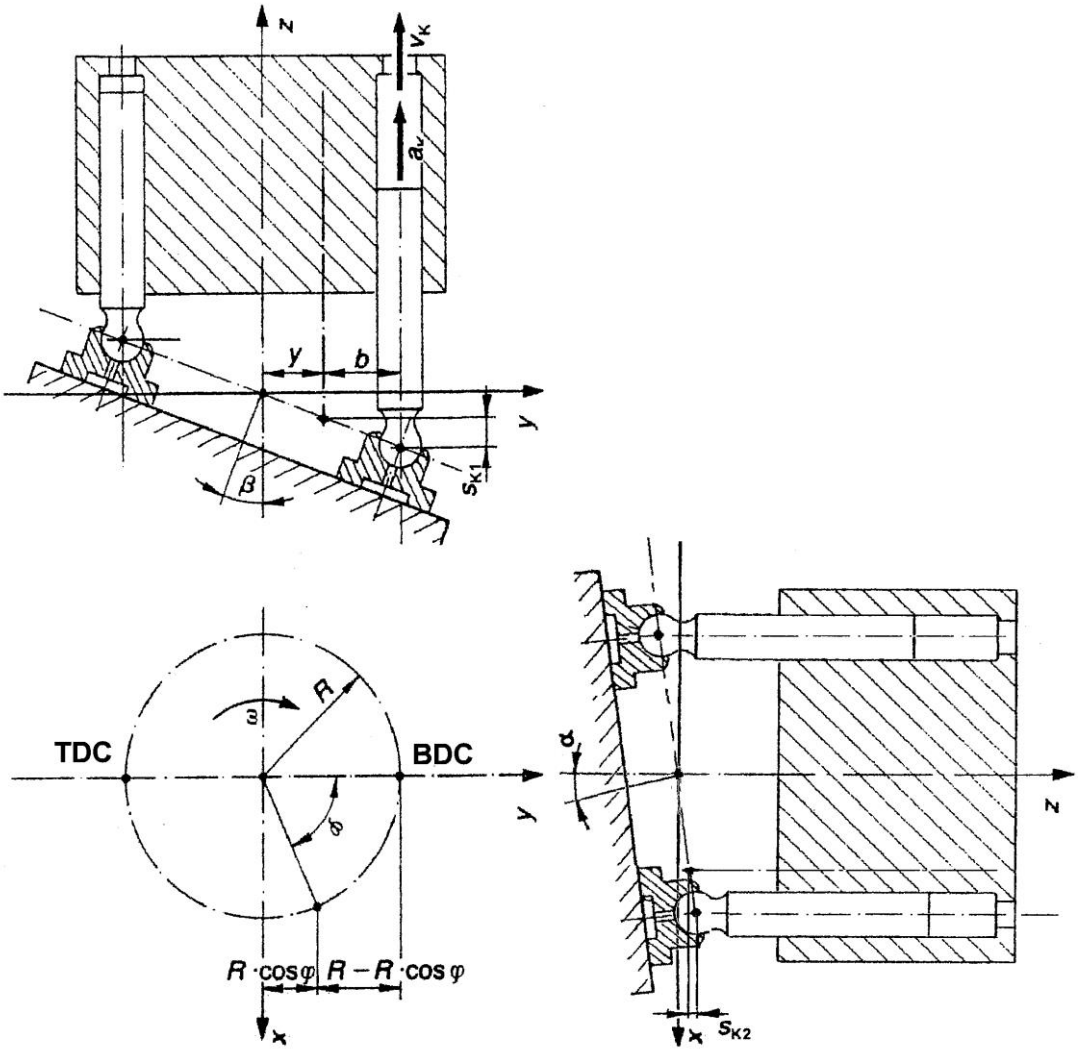

Figure 3-5 Coordinate system, adapted from Ivantysyn & Ivantysynova (Ivantysyn & Ivantysynova, 1993)

If the zero point in the direction of the z-axis is set to be bottom dead centre (BDC) on the z-y plane, the instantaneous piston position in the direction of the z-axis is:

$$s_k = s_{k1} - s_{k2} \qquad 3\text{-}15$$

The x-y plane projection of the piston position is:

$$z_1 = b_1 \tan\beta$$
$$b_1 = R - x_1$$
$$x_1 = R\cos\varphi$$
$$\Rightarrow s_{k1} = z_1 = R\tan\beta(1-\cos\varphi) \qquad 3\text{-}16$$

The z-y plane projection of the piston position is:

$$
\begin{aligned}
z_1 &= b_1 \tan\beta \\
b_1 &= R - x_1 \\
x_1 &= R\cos\varphi \\
\Rightarrow s_{k1} &= z_1 = R\tan\beta(1-\cos\varphi)
\end{aligned}
\qquad \textit{3-17}
$$

The z-x plane projection of the piston position is:

$$
\begin{aligned}
z_2 &= b_2 \tan\alpha \\
b_2 &= R - x_2 \\
x_2 &= R\sin\varphi \\
\Rightarrow s_{k2} &= z_2 = R\tan\alpha(1-\sin\varphi)
\end{aligned}
\qquad \textit{3-18}
$$

The piston lift yields from combining 3-8 and 3-9 are:

$$z_0 = s_k = R\left[\tan\beta(1-\cos\varphi) - \tan\alpha(1-\sin\varphi)\right] \qquad \textit{3-19}$$

The cross-angle in the swashplate causes the top dead centre and bottom dead centre to be functions of the swashplate angle (Figure 3-6). In Figure 3-6, the dashed red lines represent the movement of the top dead centre and bottom dead centre as the swashplate angle is varied. The actual dead centres move 90º as the swashplate main angle varies from zero to maximum.

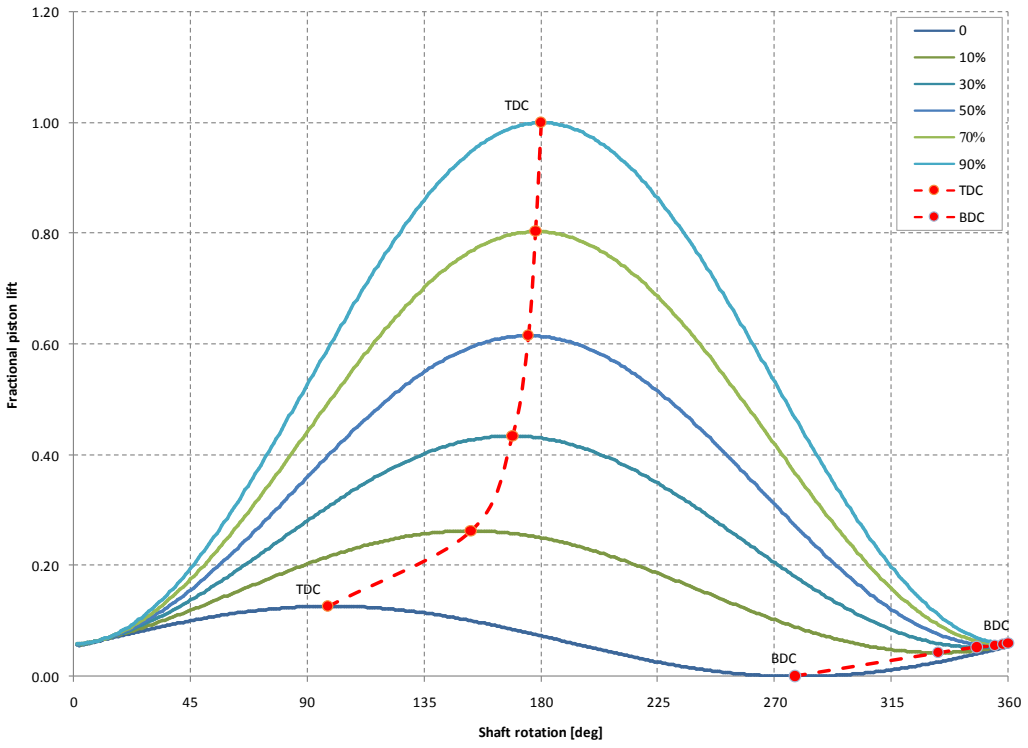

Figure 3-6 Fractional piston lift as a function of shaft rotational angle at various fractional swashplate angles

The x-coordinate of the piston position on the y-x plane is obtained from:

$$x_{Dk} = R\sin\varphi_i \qquad 3\text{-}20$$

The y-coordinate of the piston position on the y-x plane is obtained from:

$$y_{Dk} = R\cos\varphi_i \qquad 3\text{-}21$$

The piston velocity is obtained by derivation:

$$v_k = \frac{ds_k}{dt} = \frac{ds_k}{d\varphi}\frac{d\varphi}{dt} = \frac{ds_k}{d\varphi}\omega \qquad 3\text{-}22$$

Derivating once again gives the piston acceleration:

$$a_k = \frac{dv_k}{dt} = \frac{dv_k}{d\varphi}\frac{d\varphi}{dt} = \frac{dv_k}{d\varphi}\omega \qquad 3\text{-}23$$

Combining (4.5)… (4.7) yields:

$$\begin{aligned} a_{k1} &= \varpi^2 R\tan\beta\cos\varphi \\ a_{k2} &= \varpi^2 R\tan\beta\sin\varphi \\ \Rightarrow a_{ki} &= a_{k1} + a_{k2} = \varpi^2 R(\cos\varphi\tan\beta + \sin\varphi\tan\alpha) \end{aligned} \qquad 3\text{-}24$$

The free-body diagram in Figure 3-7 illustrates the forces acting on each piston. The total reaction force acting on the swashplate caused by each piston is:

$$F_{Aki} = F_{Dki} + F_{aki} + F_{Tki} \qquad 3\text{-}25$$

The inertial force in the direction of the z-axis is:

$$F_{aki} = m_k a_{ki} = m_k\left(a_{k1} + a_{k2}\right) = m_k\varpi^2 R(\cos\varphi\tan\beta + \sin\varphi\tan\alpha) \qquad 3\text{-}26$$

The friction force F_{Tki} is:

$$F_{Tki} = f_k F_{Rki}\,\mathrm{sgn}(-v_k) + b_k v_k \qquad 3\text{-}27$$

where the normal force between the piston and cylinder F_{Rki} is:

$$F_{Rki} = \sqrt{\left(F_{Sky} + F'_{\varpi ky} + F_{TGy}\right)^2 + \left(F'_{\varpi kx} + F_{TGx}\right)^2} \qquad 3\text{-}28$$

The y-component of the piston reaction force F_{Sky} is:

$$F_{Sky} = F_{Aki}\,\tan\beta \qquad 3\text{-}29$$

The centrifugal force affecting the centre of gravity of a piston $F_{\omega ki}$ is:

$$F_{\varpi ki} = m_k R \varpi^2 \qquad \textit{3-30}$$

The effect of the centrifugal force on the slipper ball joint is:

$$F'_{\varpi k} = F_{\varpi k} \frac{l_{s1} - l_{F/2}}{l_{KM}} \qquad \textit{3-31}$$

where the contact length L_F is:

$$l_F = l_{FA0} + s_K \qquad \textit{3-32}$$

The distance between the ball joint centre and contact midpoint is:

$$l_{KM} = l_K - l_{F/2} = l_k - l_{FA0} - s_K \qquad \textit{3-33}$$

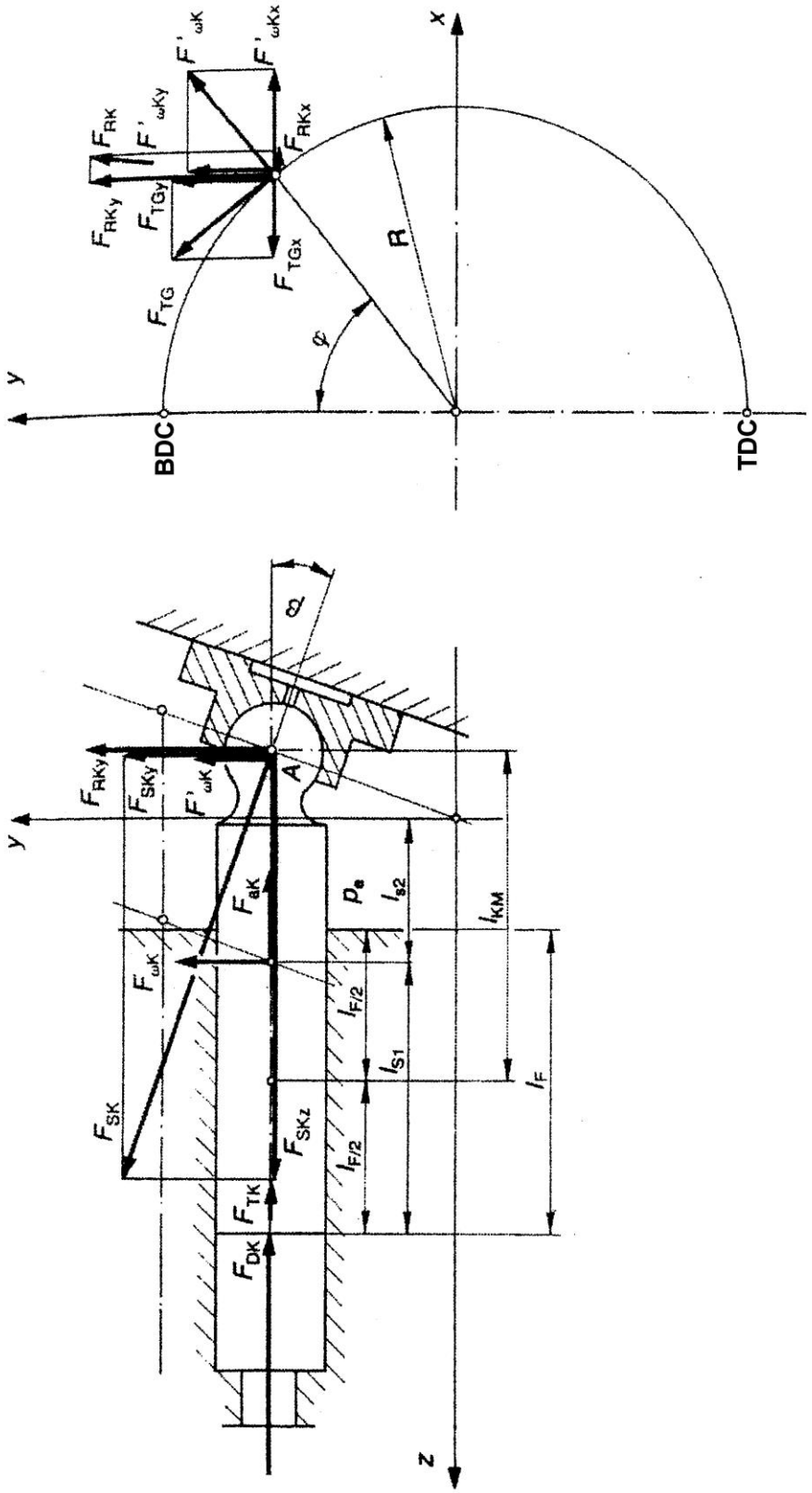

Figure 3-7 Free-body diagram of the piston, adapted from Ivantysyn & Ivantysynova (Ivantysyn & Ivantysynova, 1993)

The contact length in the bottom dead centre l_{FA0} and distance between the piston centre of gravity and piston head l_{s1} are a function of β and φ:

$$l_{s1} = \max(l_{s1}) - s_k \qquad \textit{3-34}$$

l_{s1} is at its maximum when $\beta = 0^o$ and $\varphi = 180^o$.

$$l_{FA0} = \max(l_{FA0}) - s_k \qquad \textit{3-35}$$

The maximum of l_{FA0} is reached when $\beta = 0^o$ and $\varphi = 180^o$.

The y-component of the centrifugal force is:

$$F'_{\varpi ky} = F'_{\varpi k} \cos\varphi \qquad \textit{3-36}$$

The x-component of the centrifugal force is:

$$F'_{\varpi kx} = F'_{\varpi k} \sin\varphi \qquad \textit{3-37}$$

The friction force between the slipper and the swashplate F_{TG} is:

$$F_{TG} = b_k \varpi R \qquad \textit{3-38}$$

The y-component of the friction force is:

$$F_{TGy} = F_{TG} \sin\varphi \qquad \textit{3-39}$$

The force caused by pressure in the cylinder F_{Dki} is:

$$F_{Dki} = A_k \left(p_k - p_e\right) \qquad \textit{3-40}$$

The x- and y-components of the radial force acting on the rotating group are:

$$F_{RByi} = F_{Skyi} + F'_{\varpi kyi} + F_{TGyi} \qquad \textit{3-41}$$

and

$$F_{RBxi} = F'_{\varpi kxi} + F_{TGxi} \qquad \textit{3-42}$$

The drive torque of the hydraulic pump is the sum of the torques caused by the resultant forces acting on each piston:

$$M_{Bz} = \sum_{i=1}^{z} x_{Ri} F_{RByi} - \sum_{i=1}^{z} y_{Ri} F_{RBxi} \qquad \textit{3-43}$$

3.2.5 The Portplate

The portplate controls the opening and closing of the piston chambers to the pressure and supply lines of the pump. The portplate throttles the flow of an individual cylinder

only in the areas near the top (TDC) and bottom dead centres (BDC). Figure 3-8 shows an example of portplate timing (relative openings of valve ports as a function of piston angular position). As seen in the figure, the flow is throttled only in limited areas (below 40°). During the time when the cylinders are connected to the pressure and supply lines through a completely open port, they are also connected to the cylinders next to them without restrictions.

Flow from and to the cylinder through the portplate is modelled as a turbulent orifice flow through an orifice with a cross-sectional area equivalent to the portplate opening. The orifice area is defined as the product of the nominal opening area (full opening) and fractional relative opening which is a function of the angular position (Figure 3-8).

$$A_p^{'} = r_p A_p \, , A_s^{'} = r_s A_s \qquad 3\text{-}44$$

Thus, flow through the portplate openings can, using Amesim library submodels, be pronounced as:

$$Q_{kp} = c_d A_p' \sqrt{\frac{2(p - p_k)}{\rho}} sgn(p - p_k)$$
$$Q_{ks} = c_d A_s' \sqrt{\frac{2(p_s - p_k)}{\rho}} sgn(p_s - p_k) \qquad 3\text{-}45$$

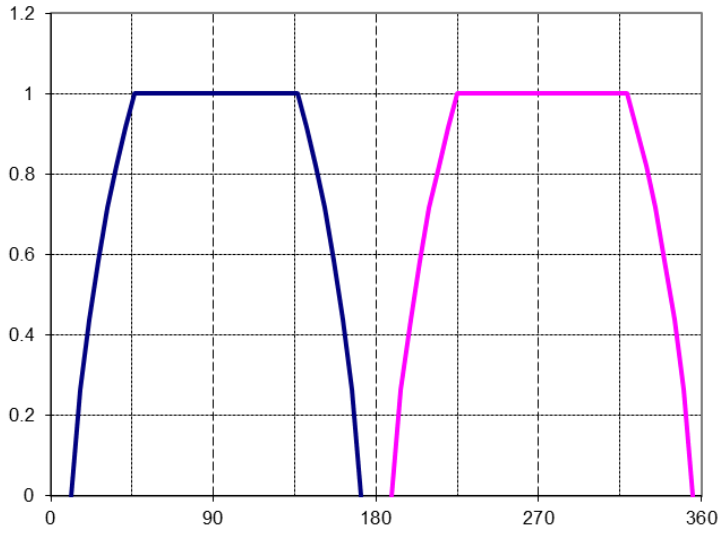

Figure 3-8 Relative opening of ports as a function of angular position (r_p, r_s)

There is a constant leakage flow through the gap between the portplate and cylinder barrel. In areas around TDC and BDC, where the portplate ports for individual piston

chambers are completely closed, leakage flow from an individual piston occurs in four directions (Figure 3-9).

The gap between the cylinder barrel and the portplate is not constant because of the pressure distribution between them (Ivantysyn & Ivantysynova, 1993) (Manring, 2000). However, in this study, the gap is assumed to be at a constant angle (ψ) and a constant maximum height.

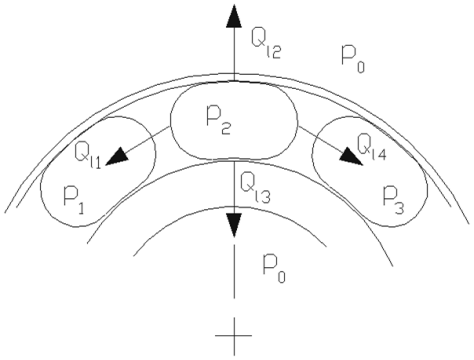

Figure 3-9 Leakage flow from an individual piston ($p_1<p_2$ and $p_2>p_3$)

The leakage flow model can thus be divided into four separate components without too severe modelling inaccuracies.

Considering leakage flow in the direction of the movement between the moving and stationary plate, it has been defined by (Blackburn, et al., 1960):

$$Q_{iL} = w\left(\frac{h^3}{12\mu}\frac{dp}{dx} + \frac{vh}{2}\right) = \frac{wh^3}{12\mu}\frac{dp}{dx} + w\frac{vh}{2} \qquad 3\text{-}46$$

$$\frac{dp}{dx} = \frac{\Delta p}{L}$$

If there is no movement, the equation is simplified to (Blackburn, et al., 1960):

$$Q_{iL} = \frac{wh^3}{12\mu}\frac{dp}{dx} \qquad 3\text{-}47$$

Considering that the leakage component caused by movement is at a constant speed only, which is a function of the gap, it can be disregarded and included in the gap height. Thus the leakage equation of an individual piston can be simplified as:

$$Q_{iL} = \frac{wh^3}{12\mu}\frac{dp}{dx} = \frac{w_i\left(h_0 - r_i\tan\psi\cos\varphi_i\right)^3}{12\mu}\frac{dp}{dx} \qquad 3\text{-}48$$

3.2.6 Pressure Compensator

The pump compensator consists of a control valve and control piston (Figure 3-10). Compensator is modelled completely using library submodels provided by Amesim, equations are given to give reader an insight of model structure.

Flow through control valve is modelled as turbulent orifice flow:

$$Q_p = \frac{x}{x_{TOT}} c_d \pi A_v \sqrt{\frac{2(p-p_c)}{\rho}} sgn(p - p_c) \qquad 3\text{-}49$$

Assuming control spool control pressure is equal to system pressure (holes in the spool control end gland do not restrict the flow), the control valve spool displacement is governed by a force equation:

$$kx_v = (p - p_e)A_{SP} - m_{sp}\ddot{x}_v + sgn(\dot{x}_v)F_\mu - p_{SP}A_{SP} \qquad 3\text{-}50$$

where spring chamber pressure is modelled as a function of spool displacement speed, pressure loss in the chamber exhaust orifice (Equation 3-49) and compressibility of the chamber volume.

Spool friction force F_μ is modelled as:

$$|F_\mu| = F_C + (F_S - F_C)e^{-\left|\frac{v}{v_s}\right|^{\delta_s}} + b_c v \qquad 3\text{-}51$$

Leakage flows in the spool and control piston are modelled as a flow in eccentric annular passage using Equation 3-4

Control piston movement is governed by:

$$F_p = (p_c - p_e)A_{CP} - m_p\ddot{x}_p + sgn(\dot{x}_p)F_\mu \qquad 3\text{-}52$$

Control pressure is defined by:

$$\frac{dp_c}{dt} = \frac{B}{x_p A_{CP}}\left(Q_p - \frac{dx_p}{dt}A_{CP} - Q_{LCP}\right) \qquad 3\text{-}53$$

Control piston leakage is modelled using Equation 3-4.

$$Q_{cL} = \pi v_k \frac{D_k}{2} h_{0k} + \frac{\pi D_k h_{0k}^3}{24\eta}\frac{(p_k - p_e)}{l_k}\left[1 + 1.5\left(\frac{e}{h_{0k}}\right)^2\right] \qquad 3\text{-}4$$

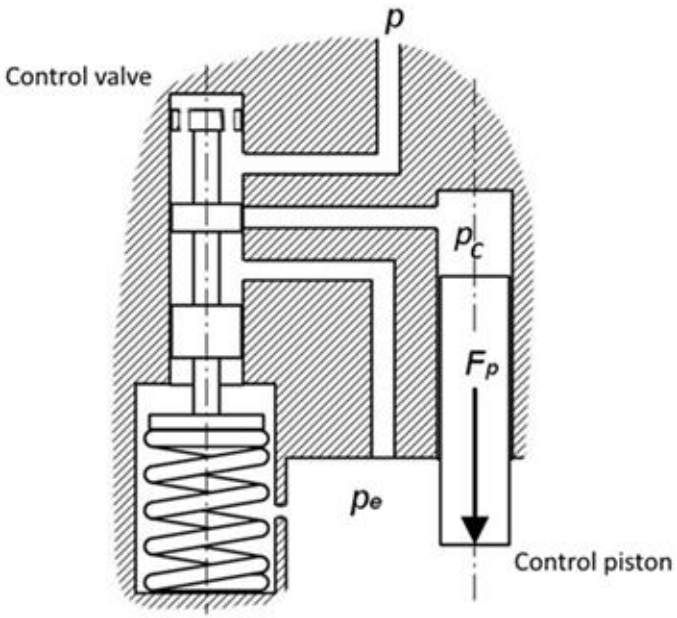

Figure 3-10 Operation principle of the pressure compensator

Case pressure is modelled as a variable volume using a compressibility equation (for example Equation 3-53), which volume changes as control piston moves. Flow into the case comes from the pump leakages (Sections 3.2.2 and 3.2.5) and compensator operation explained in this chapter. Case outflow is modelled using the pipe model and turbulent orifice models as the heat exchanger and filter (further explained in Chapter 3.5).

3.3 Bootstrap Reservoir Model

A bootstrap reservoir assembly contains numerous valves and other devices which are used for auxiliary and emergency functions such as maintenance for system bleeding and filling or preventing fluid loss in leakage damage. These valves and devices are omitted from the model, but their effect on the total friction of the assembly is included. The only valve included in the model is the check valve on the reservoir energising piston side. The reservoir is mounted transversely very near to the longitudinal axis and behind the centre of gravity of the aircraft. Due to the mounting, it is also necessary to include the force caused by lateral acceleration into the model.

The bootstrap reservoir model essentially consists of two connected hydraulic cylinder models. Reservoir is modelled completely using library submodels provided by Amesim, equations are given to give reader an insight of model structure. Figure 3-11 shows the free-body diagram of the reservoir.

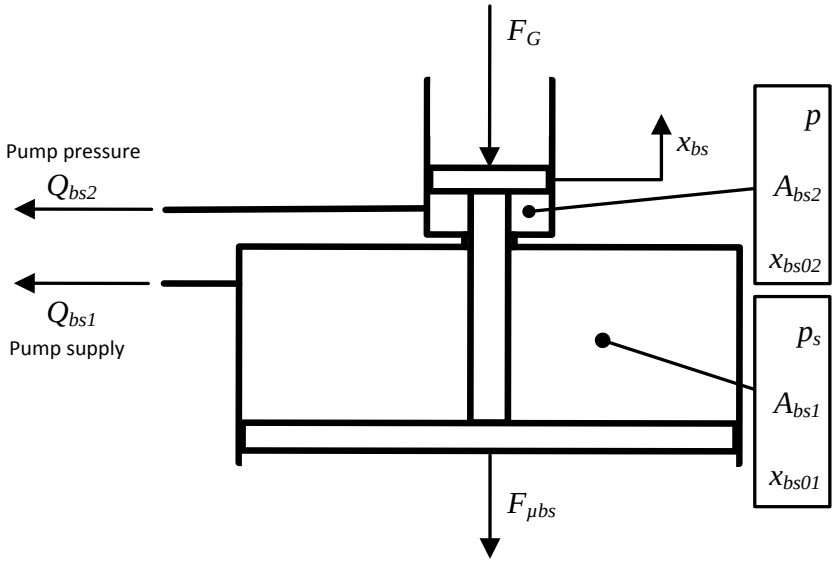

Figure 3-11 Free-body diagram of the bootstrap reservoir model

Reservoir piston assembly displacement is governed by:

$$m_{bsTOT}\ddot{x_{bs}} = pA_{bs2} - p_sA_{bs1} - sgn(\dot{x}_{bs})F_{\mu bs} - F_G \qquad 3\text{-}54$$

Pressures in the chambers are defined by:

$$\frac{dp}{dt} = \frac{B}{A_{bs2}(x_{bs02}+x_{bs})}\left[Q_{bs2} - \frac{dx_{bs}}{dt}A_{bs2}\right] \qquad 3\text{-}55$$

$$\frac{dp_s}{dt} = \frac{B}{A_{bs1}(x_{bs01}+x_{bs})}\left[Q_{bs1} - \frac{dx_{bs}}{dt}A_{bs1}\right] \qquad 3\text{-}56$$

Friction force is modelled using Equation 3-51.

3.4 Hydraulic Load Model

The hydraulic system has both symmetric and asymmetric actuators which cause there to be operating points where the system return flow is almost equal to the pump supply flow and operating points where there is high imbalance between these two flows. The flow from the reservoir to the pump supply is equal to the drain flow of the pump when only symmetric actuators are in use, but when asymmetric actuators are used, flow from or to the reservoir can be instantaneously very high because asymmetric actuators return a different flow rate to their intake.

Figure 3-12 shows the AMESim block diagram of the model used to incorporate this phenomenon into the system model. The model consists of four main submodels: system pressure side volume (1), load throttle (2), system return side volume (3), and flow variation throttle (4). The pressure and return side volumes model the hydraulic

capacitance of the system. Calculation of the capacitance is based on the effective bulk modulus and chamber volume (LMS Imagine.Lab Amesim® User's Guides, 2014). The load throttle is set by the control input (C1) and gives pump delivery demand which equals the total flow demand of the system in the current operating point. Flow through the flow variation throttle can be in both directions, depending on the current system pressure and pressure in the other side of the throttle. The pressure and throttle settings are set by control (C2) input to match the flow variation of the current operating point.

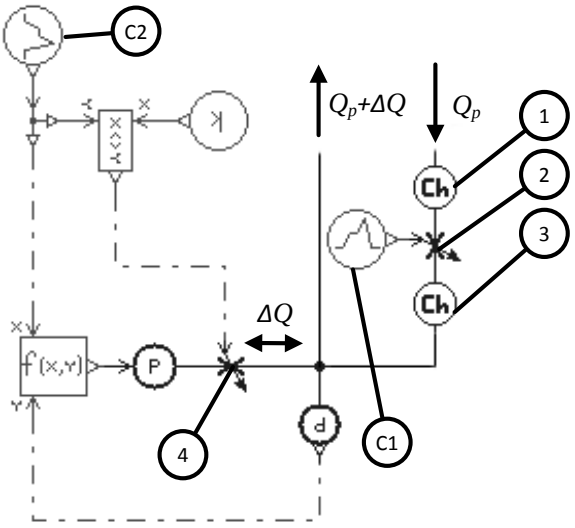

Figure 3-12 Block diagram presentation of the load model

3.5 Integrated Hydraulic Pump and System Model

The integrated system model was built using AMESim software. Figure 3-13 shows a block diagram presentation of the integrated pump and system model. The integrated model consists of eight main submodels: (1) rotating group and portplate model (Chapters 3.2.2, 3.2.3 and 3.2.5); (2) swashplate and compensator model (Chapters 3.2.3 and 3.2.6); (3) bootstrap reservoir model (Chapter 3.3); (4) turbine and AMAD modelled as a simple rotational speed source; (5) hydraulic load model (Chapter 3.4); (6) pump case modelled as a simple compressible hydraulic volume (LMS Imagine.Lab Amesim® User's Guides, 2014); (7) case drain filter and heat exchanger combined and modelled as a throttle (Equation 3-49); and (8) return line filter modelled as a throttle (Equation 3-49).

The integrated model also includes three pipe models: return line, return line pump branch and drain line. These lines are modelled using pipe models to incorporate pressure losses in each line and to enable the effect of the dimensioning of these lines to be studied. The pipe submodels used are lumped parameter models with compressibility of fluid, expansion of pipe walls, air release and cavitation, gravitational effects and pipe friction provided by AMESim (LMS Imagine.Lab Amesim® User's Guides, 2015).

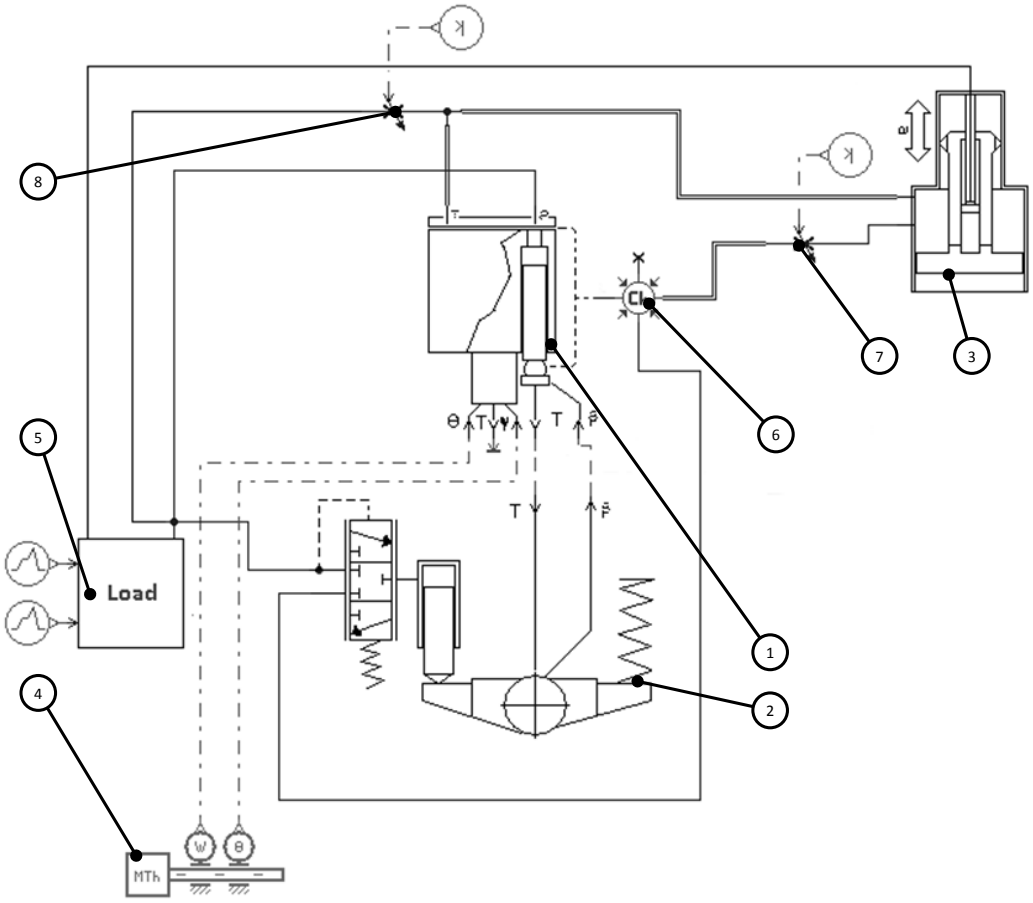

Figure 3-13 Block diagram presentation of the integrated hydraulic pump and system model

The fluid model is provided by AMESim and includes: density, bulk modulus, absolute viscosity, saturation pressure for dissolved air/gas, air/gas content, temperature, polytropic index for air/gas/vapour content and absolute viscosity of air/gas. It makes the following assumptions: the bulk modulus of the liquid with zero air/gas content is constant, which means the corresponding density varies exponentially with pressure; and the viscosity of the liquid with zero air/gas content is

constant. The model includes an air release and cavitation model (LMS Imagine.Lab Amesim® User's Guides, 2015).

3.6 Initial Setting of Model Parameters

Majority of model parameters are based on real physical dimensions of parts and components of the system and they can therefore easily be taken from the documentation or measured directly. Possible variation of these parameters can usually also be found from the technical documentation (tolerances, allowable wear limits etc.).

Most problematic parameters, which include the biggest uncertainties, are parameters of empirical and semiempirical submodels, such as parameters of friction models or discharge coefficient orifice submodel. For initial setting of these parameters there are various rules of thumb. For example initial friction parameters can be estimated on the basis rough estimate dry friction coefficient derived from the shear strength and the hardness of the weaker material in contact (Pope, 1996). These equations play an essential role in the dynamic behaviour of the model and they no right and wrong values, but only typical ranges in certain types of applications. Therefore they among the key parameters used in tuning the model to match verification measurements. In this case these parameters are not directly connected to any parameters which can be directly measured in either the laboratory or field tests. Therefore tuning them is based on minimising difference between measurement and simulation at the operating points studied. In practice this procedure usually leads to a need to make decision whether good fidelity is needed quantitatively or qualitatively, i.e. whether the phenomena in themselves or their magnitude is the most important thing. Parameter tuning can be done manually on basis of trial and error and utilising features simulation tools offer, such as batch simulations. Process can also be done using optimization tools provided as a feature in some simulation tools. In this research the first approach was taken.

4 VERIFICATION OF THE SIMULATION MODEL

Model verification in this case is a multifold problem. On one hand, there is a question of system-level model verification, but on the other hand the question is about pump model verification. Pump model verification has two levels: firstly it has to verify that the model's performance and response characteristics match its real-world counterpart, secondly, since the pump model is not a lumped parameter black box model, the inner workings of the model also have to be verified.

Pump model performance and response characteristics are verified against component data found in aircraft maintenance manuals, typical maintenance testing records and laboratory measurements. The inner workings of the model cannot be verified on the basis of direct measurements because there are no applicable ways to measure phenomena occurring inside the pump. Therefore, verification has to be based on sanity-checking the behaviour of the model's inner parts.

The main challenge in system-level verification lies in determining the operating points at which the verification is done. The load spectrum, and thus also the instantaneous operating points, under which the hydraulic system operates depend heavily on the type of mission and theatre of operations. In general, the majority of the load is generated by primary flight controls. Secondary controls and auxiliary systems play only a minor role in the overall load because they are only used at certain points of a mission and only for short times, even though they still may have relatively high instantaneous power requirements. Therefore the load on the system is at its maximum during aerobatic manoeuvres typical of dogfights or other high-intensity operations, and at its minimum during cruising. However, the load on the hydraulic system in aerodynamically instable aircraft such as most modern is still considerable even during cruising.

The primary flight control system in a modern fly-by-wire aircraft is controlled by flight control computers which can perform under multiple flight control laws (modes) depending on the current flight state. There are no such simplistic relations between pilot commands and flight control surface deflections as there are in traditional analogue control systems, but deflections depend on multiple factors, from air speed and acceleration to altitude and attitude. It is complicated to study flight control laws

to analytically find relations because laws are incorporated into the flight control software, which is proprietary closed source software. Thus, determination of peak loads and other points of interest in system operation is not a straightforward task.

The most thorough way to study the hydraulic system load spectrum is to combine flight simulation which includes simplified flight control laws with a simple hydraulic system simulation model and to extract the load spectrum from the simulation results. This approach has been studied extensively during the last decade (Hietala, et al., 2011) (Alarotu, et al., 2013) (Hietala, et al., 2009) (Öström, 2007) (Öström, et al., 2008). Certain operating points which are likely to induce adverse system-level effects can be identified on the basis of these studies. From these operating points which are possible on the ground, tests with real aircraft were selected to be used as verification points.

4.1 Laboratory Tests for Pump Model Verification

4.1.1 Test System

The test system built for the laboratory tests is shown in Figure 4-1. The power source of the test system is a 110 kW variable frequency drive (3). An electric motor drives the hydraulic pump (1) by a belt drive. The load for pump testing is generated by a throttle valve (4) in a pressure line. Parallel to the throttle valve are two fast response 2/2-valves (6) and a throttle valve (5) regulating flow through one of them; these valves can be used for generating fast flow changes of various magnitudes. Supply pressure is generated by an electric motor-driven centrifugal pump (2); supply pressure is controlled by controlling the centrifugal pump drive speed. Back pressure in a drain line is generated by a pressure relief valve (7) in the drain line. The test rig has filters in the return and drain lines (9, 11). The hydraulic fluid reservoir (10) capacity is 250 litres and it is equipped with a breather filter. The test bench has a heat exchanger (8) with a cooling power of 100 kW in the return line. The volume is matched between the pump and load throttles to test the requirements set by maintenance manuals. The fluid used in the system is MIL-PRF-83282. The test temperature was kept constant at 90ºC. The drain and supply pressures were kept constant.

The test rig is equipped with a PC-based data acquisition system. The DAQ system consists of a National Instruments 16-bit DAQ-card and PC running DasyLab. The maximum number of sensors simultaneously in use is 16 analogue sensors (pressure, flow, force, torque, etc.), 8 temperature sensors and 16 digital sensors (rotational speed, etc.).

The sampling frequency used for analogue inputs was to 10 kHz/ch. The following sensors and transducer were used: a DC-drive torque sensor (D) (HBM); pressure, drain and supply line pressure transducers (A) (Kulite); drain and pressure line flow sensors (B) (Kracht); drive rotational speed sensor (E) (Honeywell); reservoir temperature sensor (C) (generic PT100).

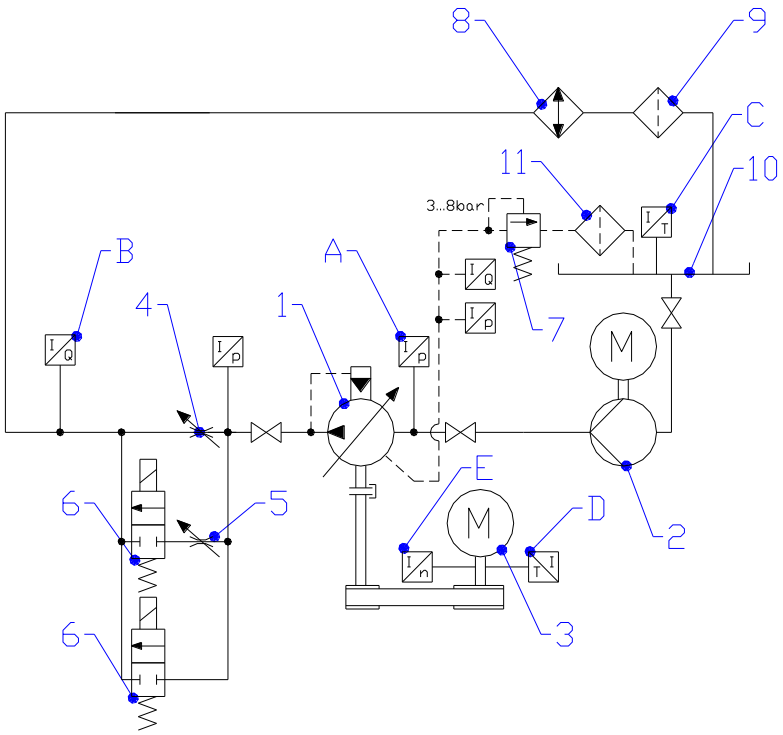

Figure 4-1 Laboratory test system

4.1.2 Test measurements

Figure 4-2 shows the situation where the delivery demand for the pump changes from 180 l/min to 75 l/min in 50 ms.

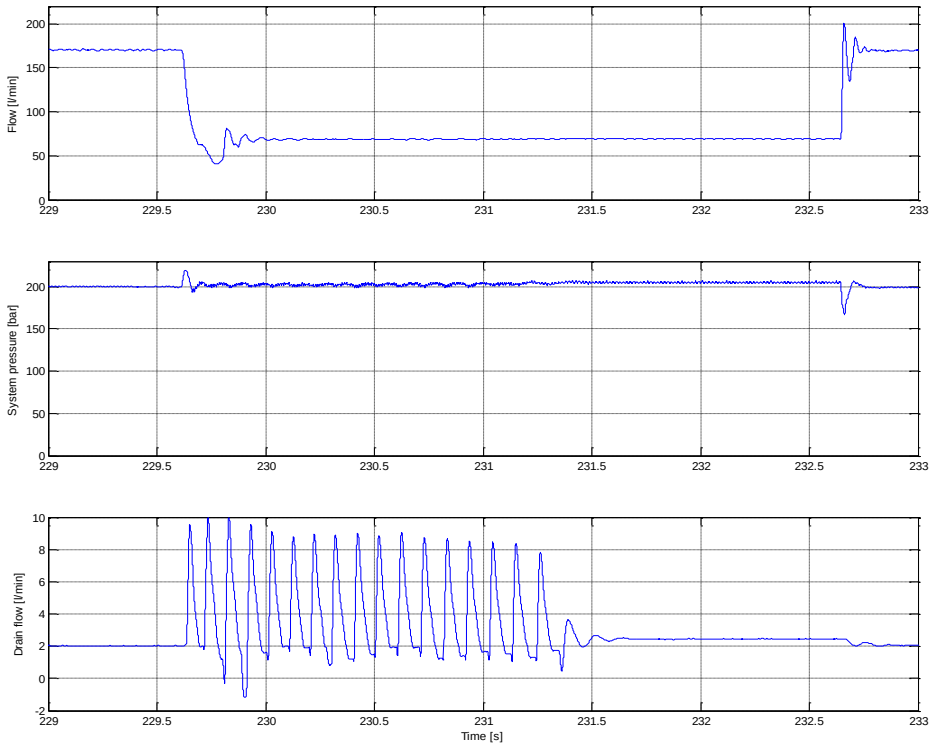

Figure 4-2 Flow change 180 -> 75 -> 180 l/min

As can be seen in all of the curves, a slight pressure regulator vibration occurs after the flow change. The amplitude of flow peaks in the drain line is relatively high, even though the vibration seen in the system pressure and flow curves has a small amplitude.

Figure 4-3 shows the situation where delivery demand changes from 180 l/min to 0 in 50 ms. In this situation, the vibration is not dampening but a steady state vibration occurs. It can also be seen that the system pressure in this case rises well above the nominal pressure, but is well within the maximum set by both the maintenance manuals and SAE-AS5440 and MIL-H-5440H (SAE International, 2011) (US Department of Defence, 1999).

The third test case shown in Figure 4-4 shows the situation where delivery demand for the pump changes from 180 l/min to 20 l/min in 50 ms. In this case, too, the vibration is not dampening but a steady state vibration occurs. Comparing Figure 4-3 and Figure 4-4, it can be seen that significant pressure rise in the system pressure occurs only in zero output flow situations, which are practically impossible in real aircraft.

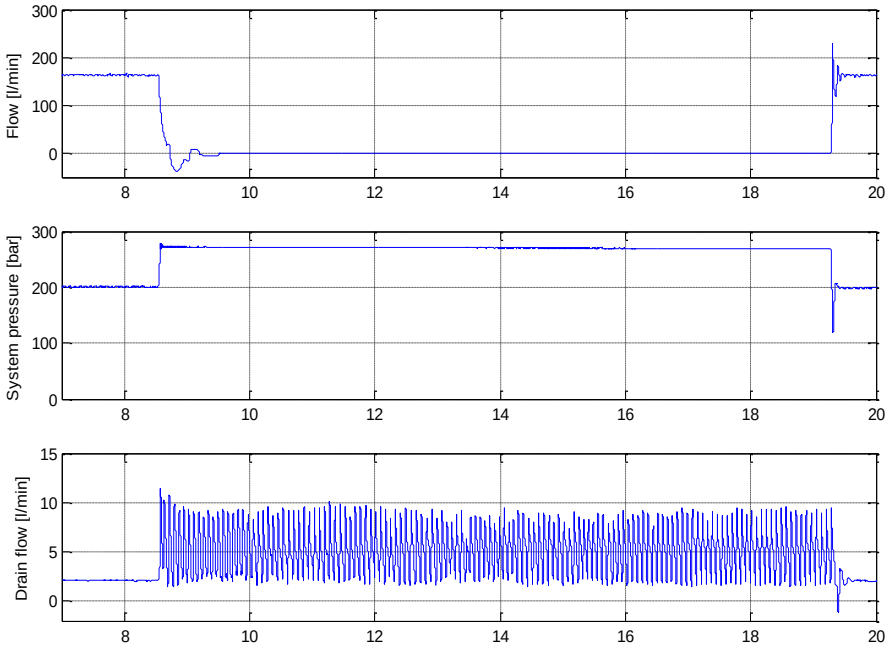

Figure 4-3 Flow change 180 -> 0 -> 180 l/min

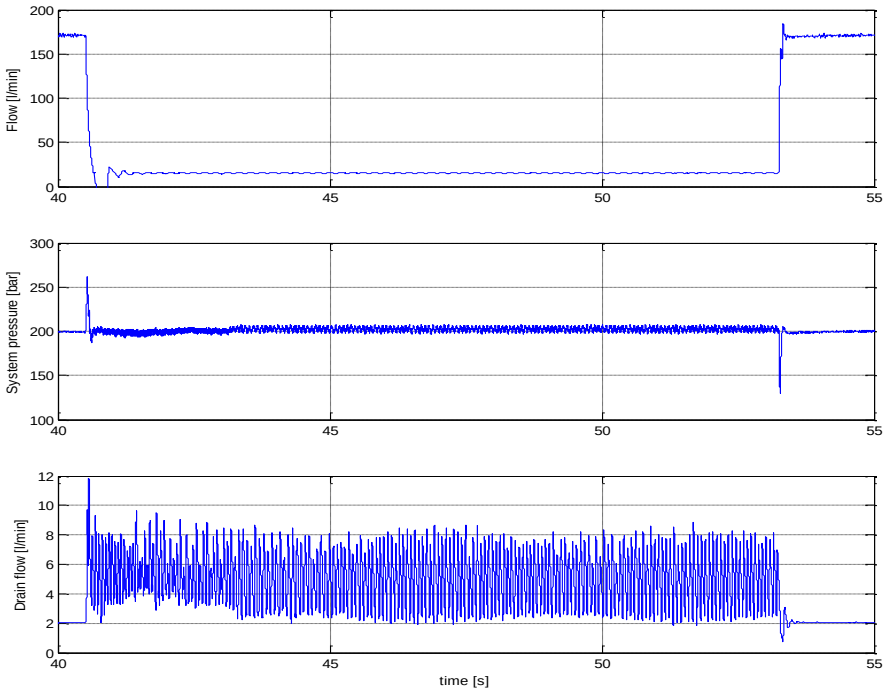

Figure 4-4 Flow change 180 -> 20 -> 180 l/min

4.1.3 Discussion

Pressure control vibrations are dependent on the system capacitance, i.e. its volume and effective bulk modulus, as well as on the pressure control device itself. The laboratory test system does not replicate the actual aircraft system and thus the exact amplitude and frequency of the vibrations detected in laboratory tests are not the same

as those occurring in the aircraft. Nor is the operating point where vibrations occur. However on the basis of the laboratory test findings, some pressure control vibrations are likely to occur in the aircraft as well.

The tests done showed that steady state vibrations tend to occur when there is a fast change from high delivery to zero or low delivery. In real aircraft, a zero delivery operating point is not possible due to leakages of the system. In addition, a sudden demand for very low delivery is unlikely to occur during normal operation. Even though steady state vibration is therefore very unlikely to occur in aircraft, short-term vibrations can occur there. In the field measurements, it is important to discover if these vibrations occur, in order to be able to match the hydraulic capacitance of the model to the actual system in system-level model verification.

As can be expected on basis of the pump construction, the pump pressure regulator induces flow peaks to the drain line. The flow peaks measured in the tests were five to six times higher than the nominal drain flow of the pump being studied. On the test bench, the drain pressure is controlled by the pressure relief valve, which makes the drain pressure relatively constant with minimal flow dependence. This, however, is not the case in the aircraft, where the drain pressure is determined by the pressure in the reservoir, which depends on the current system pressure and pressure losses in the drain line. Drain line pressure losses are the sum of pipeline losses and losses in flow through the heat exchanger and filter.

The main challenge in verifying and validating the model through comparison of the measurements and simulation results lies in the very nature of the model. The model is targeted to giving an insight into phenomena occurring inside the hydraulic pump during normal operation, i.e. in-flight operating points, and the effect of system-level phenomena on them. However, measuring the phenomena inside this particular hydraulic pump is technically not a feasible alternative.

The model targets mostly qualitative results and thus the model verification and validation process does not concentrate on the exact magnitude of phenomena but rather on the phenomena themselves. On the other hand, the model is a detailed analytical model based on actual dimensions, properties and physical equations, which make most of its parameters not freely variable, but very tightly tied to the actual

physical dimensions and their possible variation due to wear, tear and manufacturing tolerances. The number of more freely variable parameters is limited to abstract parameters such as friction parameters, flow coefficients, etc.

Laboratory test results were used to set and tune the pump model parameters. For this purpose, simulations were done using the pump model alone with constant pressure supplies as the supply and drain line pressure sources and a single orifice as the load. The simulations replicated the same operating points that were tested in the laboratory. Parameter setting and tuning was done by varying one single parameter at a certain operating point and within certain limits. As soon as a good match was found, the parameter value was also tested at other operating points. The selected parameter values for the final pump model are those giving a satisfying match at all operating points studied.

4.2 Field Tests for System Model Verification

4.2.1 Test Setup

System field tests were done with real aircraft in a test hangar (Figure 4-5). The measurement setup was done according to the instrumentation schematics presented in Figure 4-6. In total five pressure transducers, two hall sensors and eight temperature sensors were installed into the aircraft. System, drain line and supply line pressures and temperatures were measured from the hydraulic pump manifold. Leading Edge Flap Hydraulic Drive Unit (LEF HDU) operating pressures were measured between the remote control valve and the drive unit. The temperature of the hydraulic fluid inlet to the remote control valve was measured from the supply line. The remote control valve command output was also logged. In addition, the rotation speed was measured with two hall-effect sensors on the hydraulic drive unit output shaft. Additional temperature measurements were taken from the horizontal stabilator servo actuator return line, hydraulic fluid reservoir and hydraulic fluid–fuel heat exchanger in and out ports.

Figure 4-5 Fighter aircraft during instrumentation in test hangar

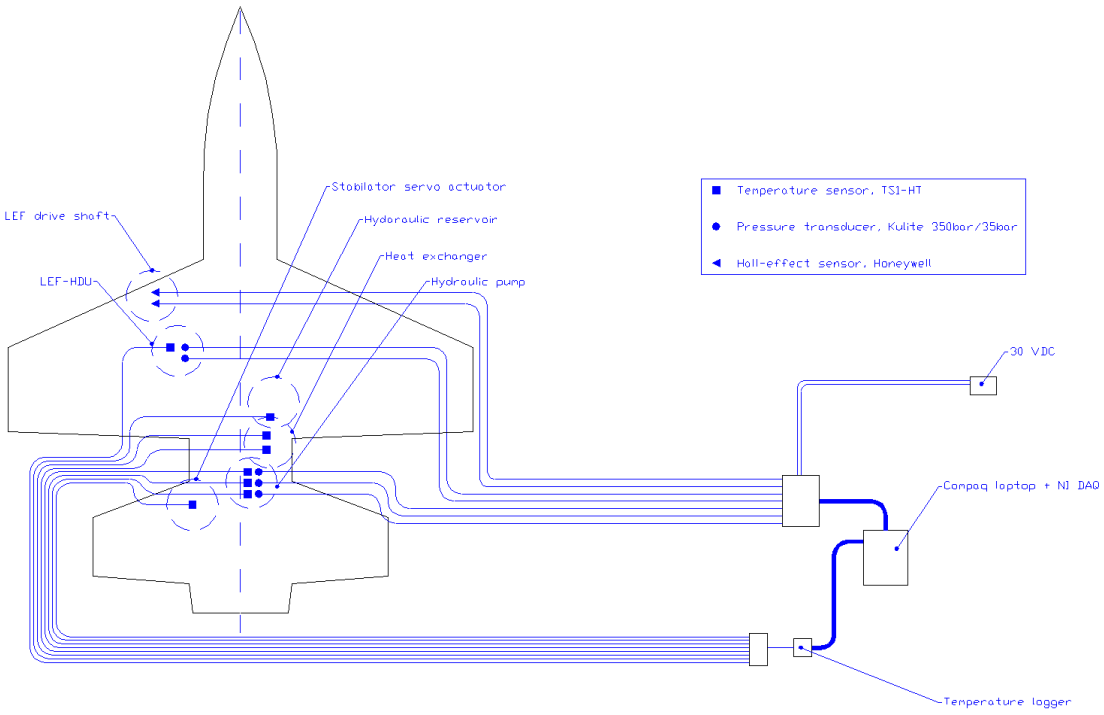

Figure 4-6 Schematic of the field measurement setup

Data acquisition was carried out using a 16-bit DAQ-card with a laptop computer. The software used was DasyLab. The sampling frequency was 2000 Hz/ch. All sensors, except the hall sensors in the LEF HDU output shaft, were analogue. The temperatures

were logged using an 8-channel temperature logger which was connected to the computer to visually monitor temperature readings and synchronise logging.

4.2.2 Test Operating Points

Operating points to be tested and measured were chosen according to the findings from the preliminary system simulations (Aaltonen, et al., 2007). The preliminary simulations showed that there is a possibility that a flow imbalance between the system pressure and supply lines caused by asymmetric actuators can cause very high supply pressure oscillations in the system. Furthermore, they also indicated that rapid pump delivery demand variations can cause high pressure oscillations in the drain line, which was also indicated by the drain flow measurements made in the laboratory tests. Therefore, test operating points were chosen to give a wide variety of different operating points of the hydraulic systems and to include the problematic operating points mentioned before. Because the tests were ground tests and not test flights, there were a number of limitations and restrictions which affected the test programme. Most of these limitations are caused by the flight control system control laws, which, for example, limit the speed of actuators in ground testing, but there are also restrictions caused by the test hangar and occupational safety. It is worth noting that the aircraft's flight control system does not provide the possibility to move only a single flight control surface; nearly always, several surfaces are moved simultaneously. It should also be noted that in most cases there is no external load on the actuators during ground operation because of the lack of aerodynamic loads. Table 4-1 shows the aircraft test programme which was carried out in the field tests. The programme included a warm-up sequence in which the system was operated using an exerciser programme until a steady state idling temperature was reached (80°C). The test programme was initiated after the warm-up sequence and was repeated twice on two different power settings (engine rotational speeds): 80% and 100%.

Table 4-1 Test programme

1.	Gun, 10 s
2.	Horizontal stabilator up and down, MECH-mode, 10 s
3.	Leading edge flaps and landing flaps, FLAP-switch, 10 s
4.	Stick moved in rectangular track, FLAP-switch occasionally, gun occasionally
5.	Air brake three times open–closed
6.	Leading edge flaps and trailing edge flaps, FLAP-switch (0 to 12deg), 4 times
7.	Control stick moved back and forth to move horizontal stabilators, 2 to 5 min

Besides the technical limitations and restrictions, the ambient temperature is also far from what it is in airborne operation. Thus the test results cannot be seen as representing any real in-flight operating points, but only serve the purpose of model verification and validation.

Test Point 1 – Gun Response

The hydraulic motor driving the gun barrel assembly has high flow demand and is accelerated and decelerated very rapidly, which makes it a perfectly suited actuator for testing system-level effects caused by symmetric actuators.

Figure 4-7 and Figure 4-8 show the system response when the trigger is released and then pressed again once, the engine power setting being 80% and 100%. These operating points loosely represent the same situations as were tested in the laboratory. It can be seen that both increasing and decreasing flow in the system induces pressure transients to the supply and drain lines. The hydraulic motor being a symmetric actuator does not however cause an imbalance to the system return flow and actual pump delivery, which makes the transients relatively small. Comparing the system pressure to the supply and drain pressures also shows the dependence of the supply and drain pressures on the system pressure. This is caused by the design of the reservoir. The engine power setting and maximum available pump flow have no effect on the phenomena.

The system temperature varied between 80 and 100°C during this phase.

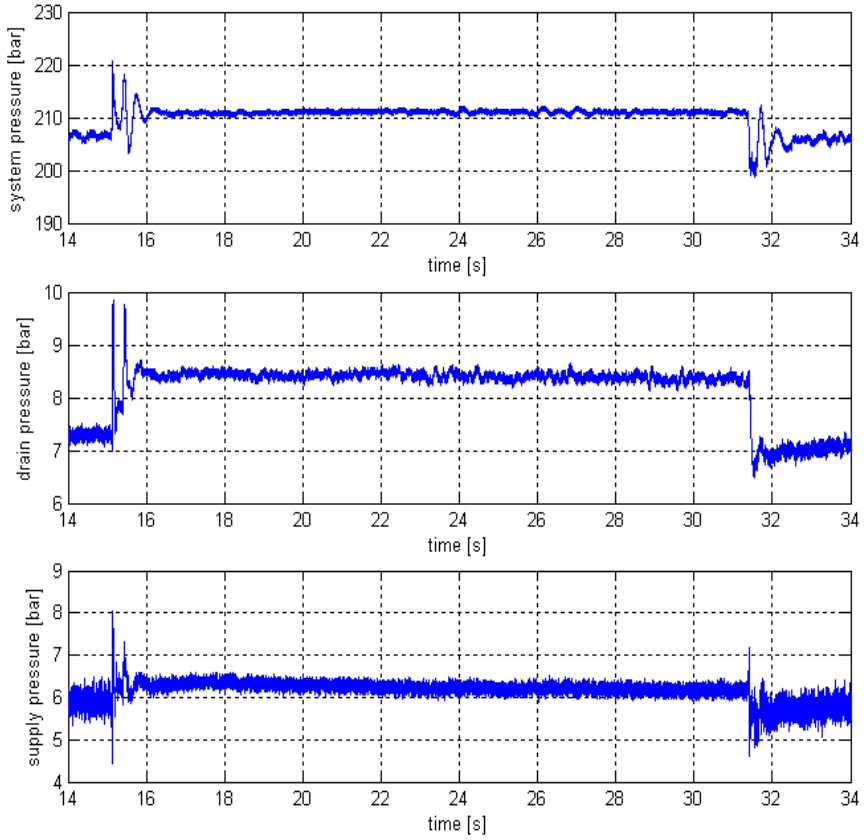

Figure 4-7 Gun firing response, 80% power

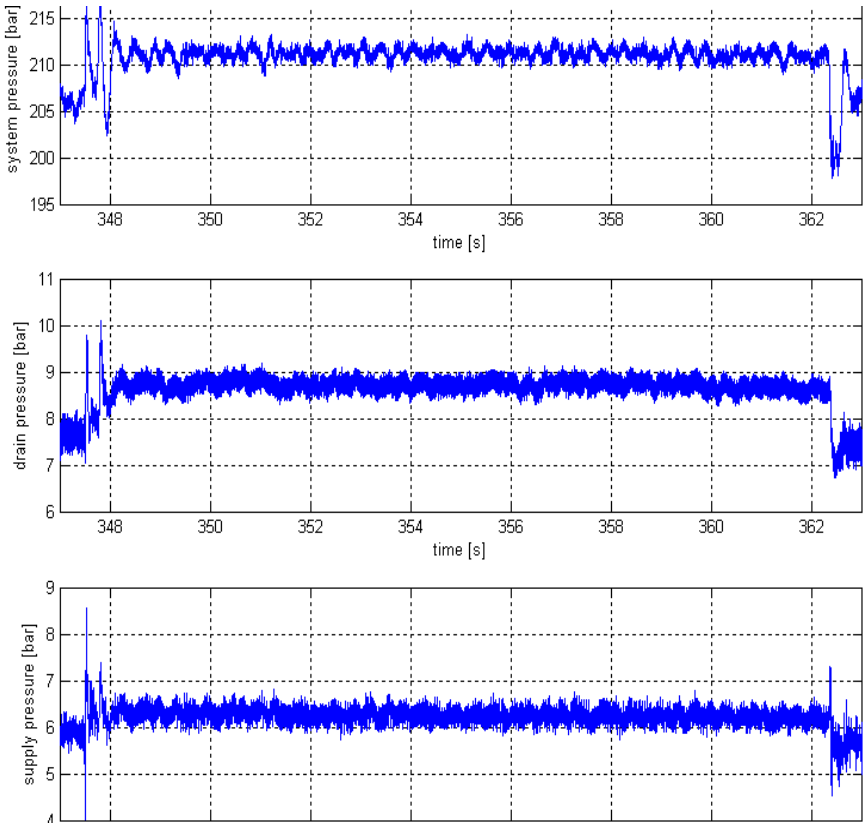

Figure 4-8 Gun firing response, 100% power

Test Point 2 – Horizontal Stabilator Response in MECH-mode

The hydraulic servo actuator of the stabilator has very high instantaneous power and due to the position control loop, its flow demand can vary greatly during movement. The response of a servo valve is much faster than the response of a pump's pressure compensator, as is a typical situation, which causes pressure in the servo valves supply line to oscillate. Figure 4-9 and Figure 4-10 show the system response when horizontal stabilators are actuated in so-called MECH-mode. MECH-mode is an emergency operation mode, where the stabilators alone are controlled directly by the control stick. Pressure oscillation caused by the difference between the pump's and servo valve's response can be clearly seen in both Figure 4-9 and Figure 4-10.

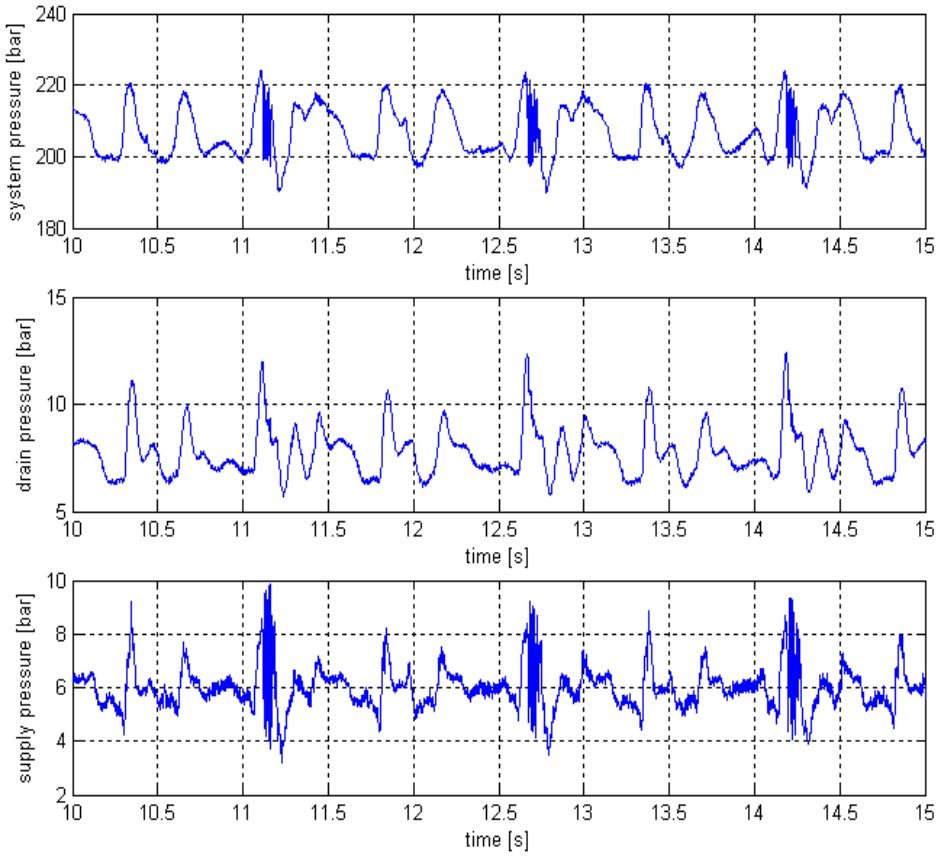

Figure 4-9 Horizontal stabilator in MECH-mode, 80% power

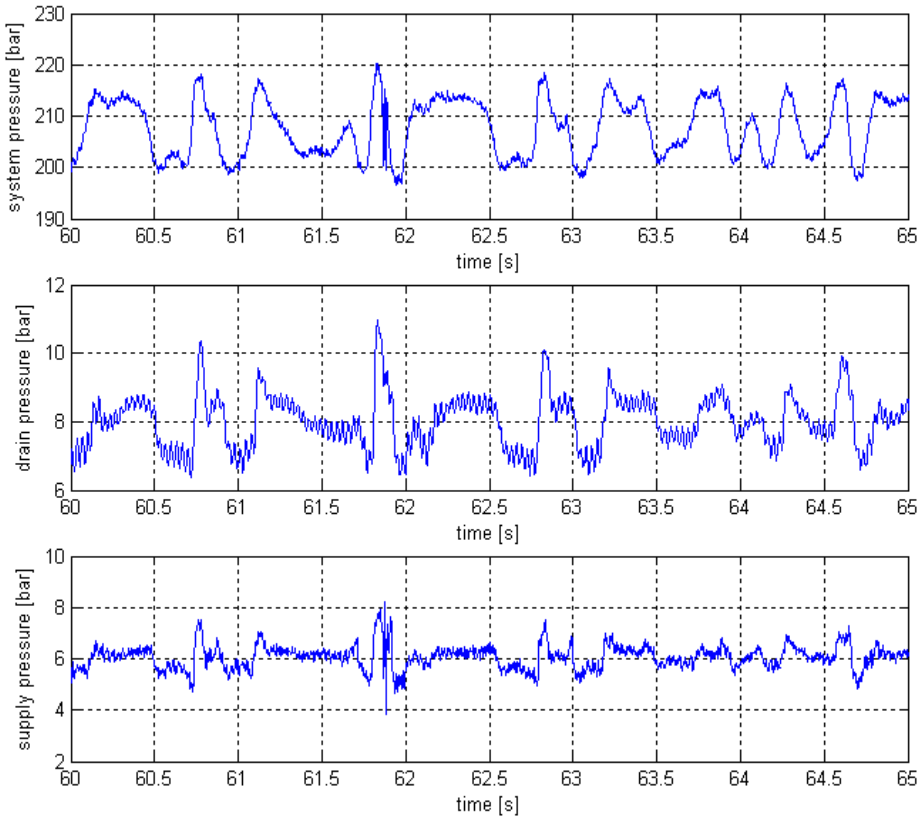

Figure 4-10 Horizontal stabilator in MECH-mode, 100% power

Figure 4-9 shows short vibrations in the pump's supply and pressure line pressure. These vibrations are most likely induced by the stabilator servo valve when the stabilator reaches the end point of its movement and is stopped momentarily. In the same figure can also be seen a clear repetition of the pressure patterns, which shows that movement in both directions happens very similarly. The notable difference between Figure 4-9 and Figure 4-10 is a small constant oscillation of the drain line pressure in the right-hand plot. The same oscillation can also be seen in the pressure and supply line pressures, but on a smaller scale, which can be an indication of it being induced by the pump pressure compensator.

The system temperature varied between 80 and 100°C during this phase.

Test Point 3 – Leading Edge Flap Response

The LEF HDU is a motor-driven actuator, thus also a symmetric one. LEF HDU motors, however, are smaller flow consumers than the previously tested gun drive. They also have a closed loop control which makes higher instantaneous flow rate variations likely to occur.

Figure 4-11 shows the LEF movement in one direction. The two uppermost plots show the pressures in the pump lines and lines between the HDU and remote control valve. The pressure plots show that the pressure difference needed to move LEF is quite small in ground operation. During ground operation, both the maximum speed and maximum angle of LEF are limited to approx. one quarter of the maximums in airborne operation, which causes a large difference in the operational parameters in comparison to airborne operation, especially when combined with the effect of aerodynamic load on the LEF.

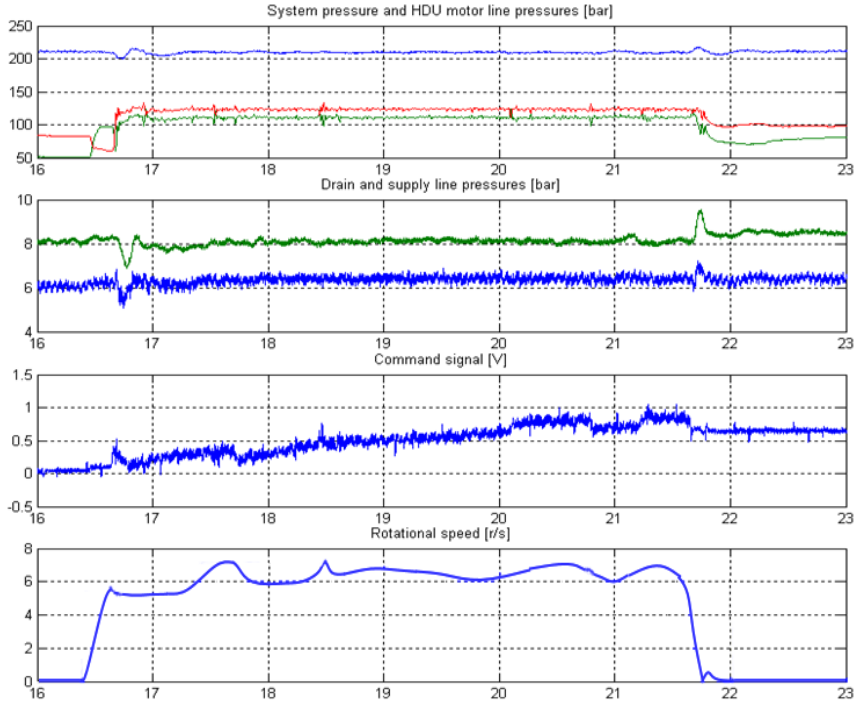

Figure 4-11 LEF HDU pressures, LEF control command value, LEF drive shaft speed and pump line pressures, power setting 80%

As an expected result, it can be seen that the low power symmetric actuator has a smaller effect on the system level than the higher power one.

The system temperature varied between 80 and 100°C during this phase.

Test Point 4 – Response of all Flight Control Surfaces and Gun

Figure 4-12 shows the same parameters as Figure 4-11. At this operating point, as well as the LEF, all other flight control surfaces and the gun were also actuated. The system, drain and supply pressures in Figure 4-12 show considerably higher oscillations than in Figure 4-11.

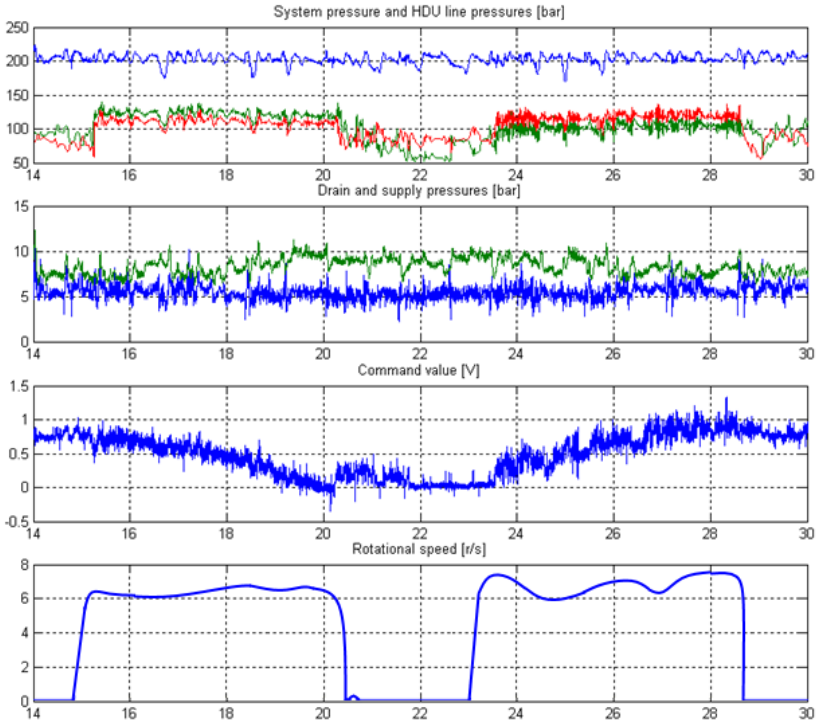

Figure 4-12 All flight control surfaces and gun actuated, power setting 100%

Further comparing Figure 4-11 and Figure 4-12 shows that these higher oscillations and variations do not have any visible effect on the actuator performance.

The system temperature reached its peak during this phase and varied between 100 and 130°C.

Test Point 5 – Air Brake Response

The air brake actuator is an asymmetric hydraulic cylinder. Preliminary simulations suggested that asymmetric actuators could cause the most severe pressure oscillations in the pump's supply and drain lines because they cause flow imbalance in the system pressure and return lines. To test the assumption, measurements were made in the situation where air brake alone was actuated. Figure 4-13 and Figure 4-14 show one air brake operation cycle: the air brake is actuated open and soon after that is actuated back into the closed position.

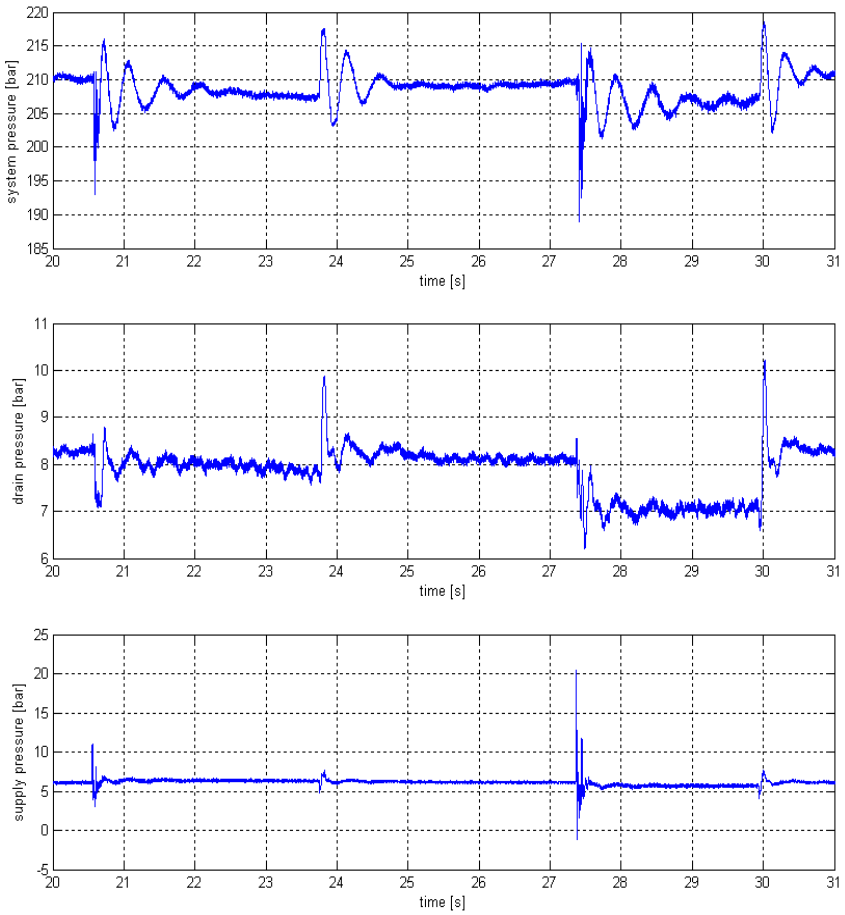

Figure 4-13 Air brake operation, 80% power setting

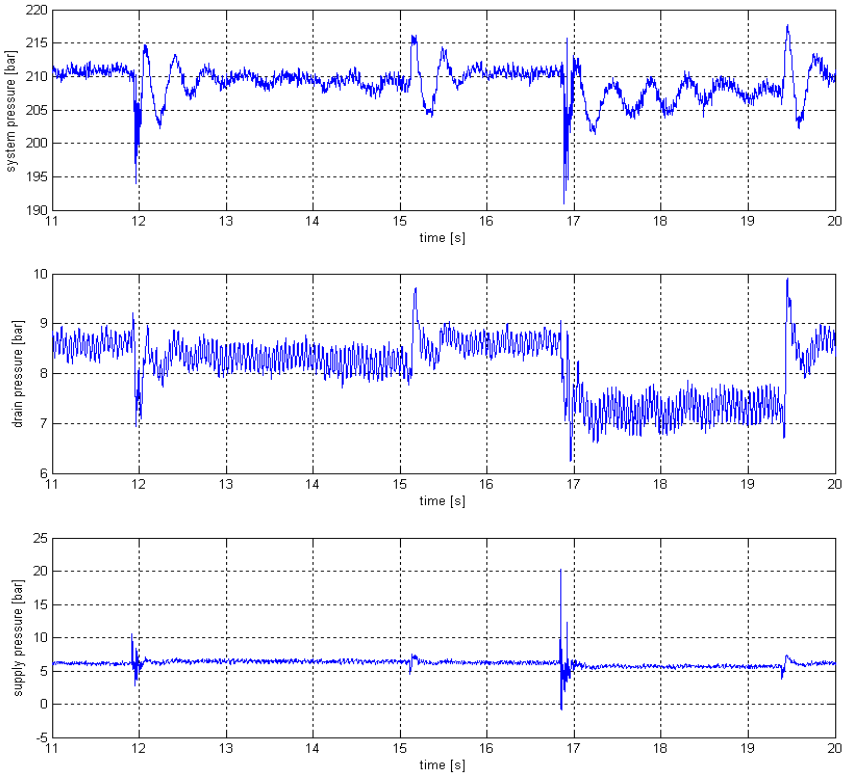

Figure 4-14 Air brake operation, 100% power setting

Both Figure 4-13 and Figure 4-14 show significant pressure transients at the beginning of both movements. In the beginning, on the return movement of the air brake actuator, the supply pressure drops momentarily to zero. There are significant differences in the magnitude of the drain and supply line pressure transients between this operating point and other tested operating points.

The system temperature varied between 80 and 100°C during this phase.

4.2.3 Discussion

The field tests give good verification points for the system-level phenomena found in the preliminary simulations. It should however be noted that ground tests have many limitations, as explained in earlier sections, and thus their results cannot be reliably generalised.

The most important findings were that the supply line pressure has very high magnitude oscillations and can even drop to zero in some cases. An important finding was also that the magnitude of pressure transients and oscillations in the drain line are very high. These findings in themselves and alone give an explanation for the rapid pump wear experienced.

The level of asymmetricity and also flow demand seem to have an effect on the pressure oscillations and transients found in supply line. The stabilator actuator has very low asymmetricity and does not cause high oscillations, but the air brake, with only slightly higher asymmetricity, causes significant oscillations.

The temperature measurements give an understanding of the system temperature variation in ground operations and thus give a baseline to the operating viscosity range of the system, which has a great effect on leakage and orifice flow rates as well as friction.

The field test results were used to set and tune the system model parameters. For this purpose, simulations were done with the system model introduced in Section 3.5. The simulations replicated the same operating points that were tested in the field tests as closely as possible. As explained earlier, the flight control system does not allow single actuators to be actuated, and there is no exact knowledge available on the

operation of most of the actuators at the tested operating points, thus it is impossible to replicate operating points exactly in the simulation model. Parameter setting and tuning was done by varying one single parameter at a certain operating point and within certain limits. As soon as a good match was found, the parameter value was also tested at other operating points. The selected parameter values for the final system model are those giving a satisfying match at all of the operating points studied.

4.3 Comparison of Simulated and Measured Operation of the System

The main challenge in verifying and validating the model through comparison of the measurement and simulation results lies in the very nature of the model. The model is targeted to giving an insight into phenomena occurring inside the hydraulic pump during normal operation, i.e. in-flight operating points, and the effect of system-level phenomena on them. However, it is technically not a feasible alternative to measure phenomena inside this particular hydraulic pump, and the ability to experimentally measure in-flight operating points is seriously limited, as explained earlier.

The model targets mostly qualitative results and thus the model verification and validation process does not concentrate on the exact magnitude of phenomena but rather on the phenomena themselves. On the other hand, the model is a detailed analytical model based on actual dimensions, properties and physical equations, which make most of its parameters not freely variable, but very tightly tied to actual physical dimensions and their possible variation due to wear, tear and manufacturing tolerances. The number of more freely variable parameters is limited to abstract parameters such as friction parameters, flow coefficients, etc.

The level of reliability and accuracy of the pump model was established on the basis of laboratory measurements and simulations done at the same operating points with a pump model alone with constant pressure supplies as the supply and drain line pressure sources and a single orifice as the load. Figure 4-15 and Figure 4-16 show both simulated and measured responses to flow changes 180 -> 20 -> 180 l/min and 170 -> 70 -> 170 l/min. At both operating points, the match between the simulated and measured response is relatively good. At both operating points, the magnitude of vibrations is the same in the simulations and measurements, but they are damped faster than happens in real life.

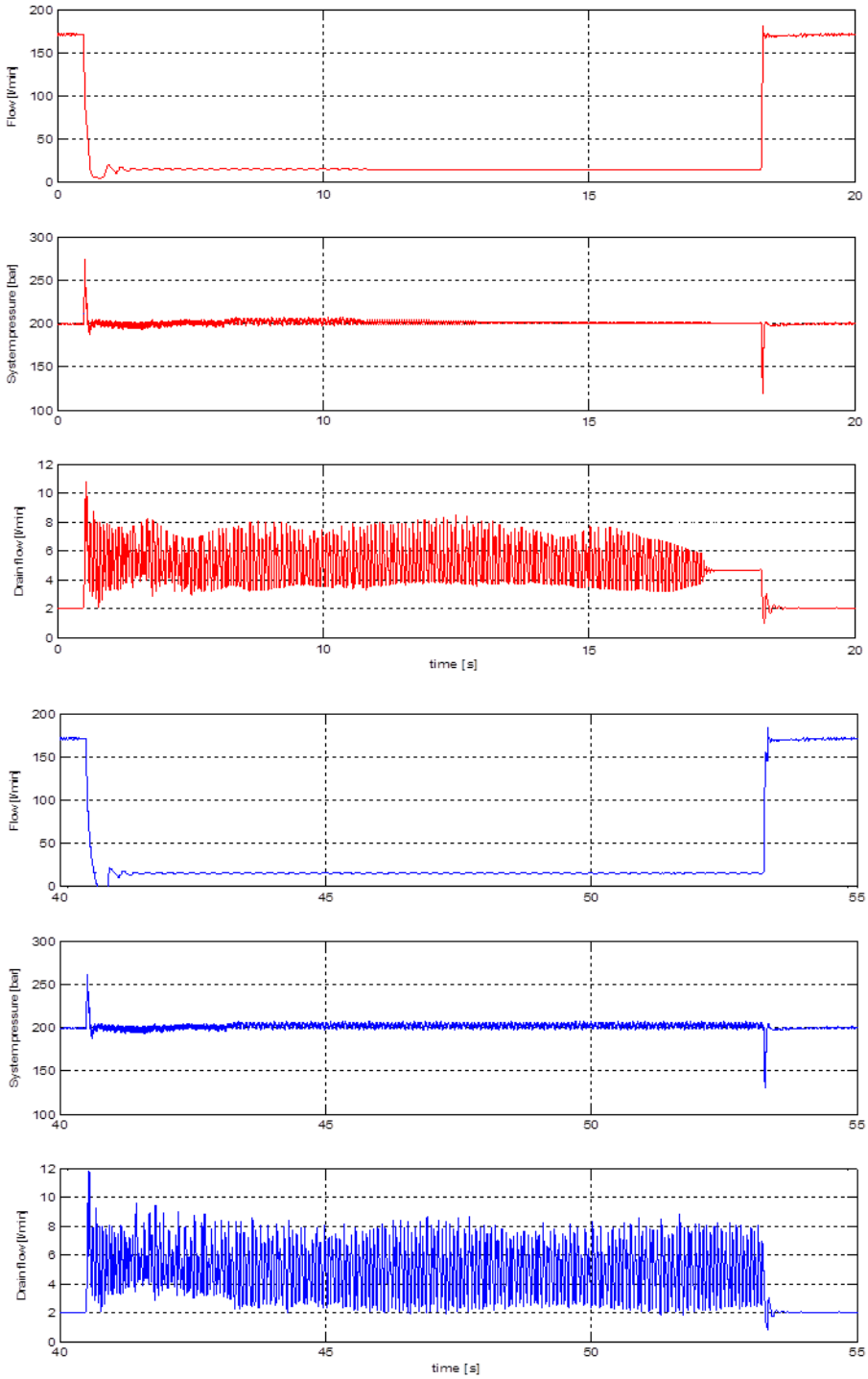

Figure 4-15 Response to flow change 180 -> 20 -> 180 l/min – above simulated (red), below measured (blue)

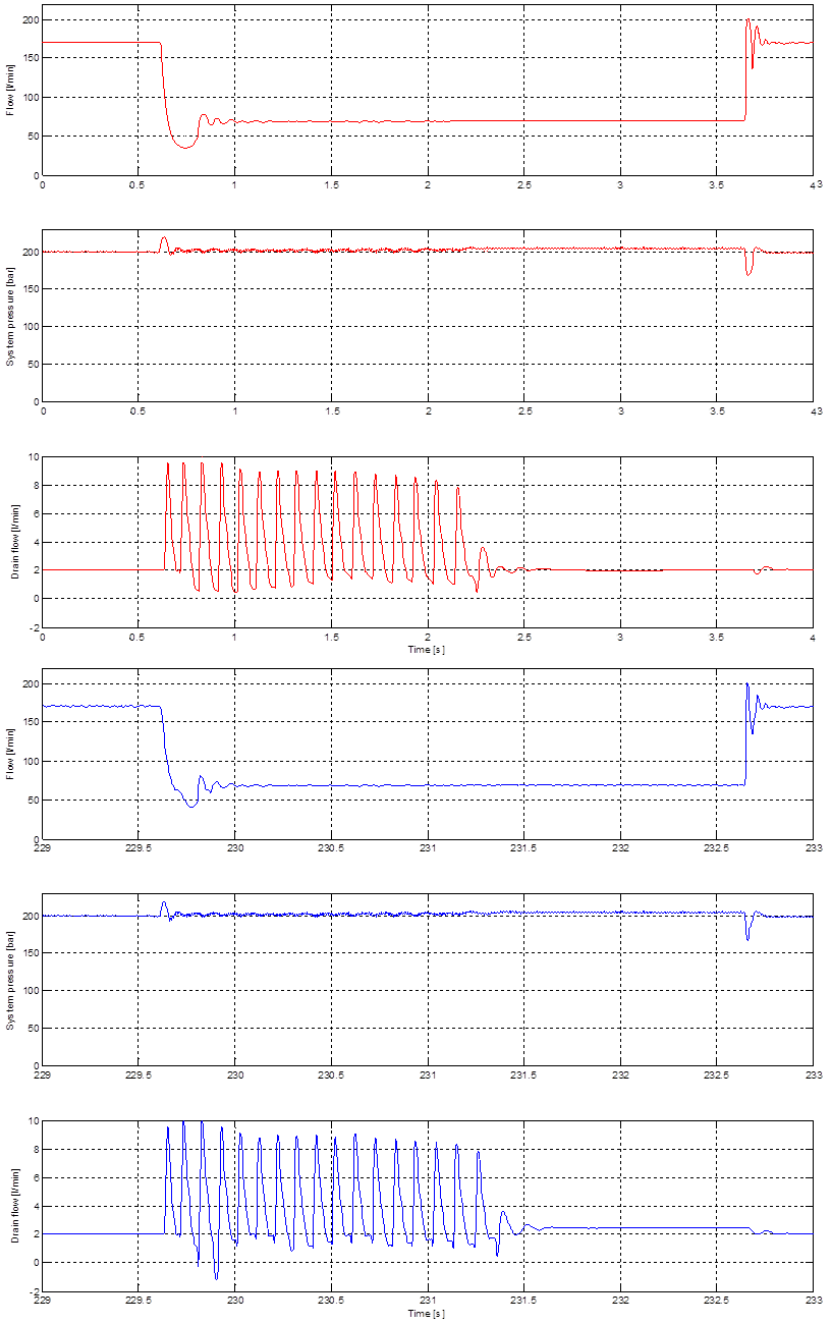

Figure 4-16 Response to flow change 170 -> 70 -> 170 l/min – above simulated (red), below measured (blue)

Damping relates to both friction and leakages in pump control. However, because of the pump construction, the friction forces are relatively small in comparison to the control force, and thus the most important factor affecting damping is the leakage control piston and control valve damping. In particular, the control piston leakage varies greatly because of wear and manufacturing tolerances.

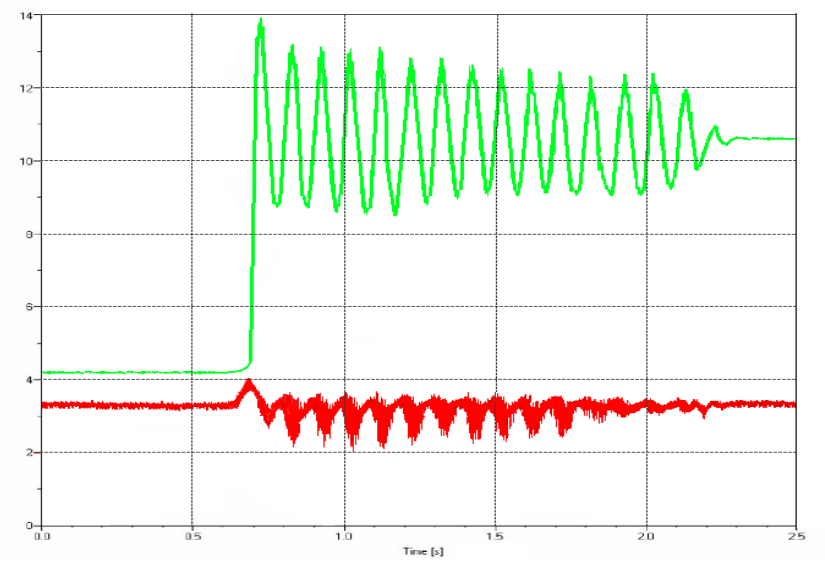

Figure 4-17 Simulated control piston and control valve spool displacements 170 -> 70 l/min flow change

Figure 4-17 shows simulated control piston and control valve spool displacements during the first 2.5 seconds in the simulation also presented in Figure 4-16. It can be seen that flow oscillations in the drain line correspond nicely to the control piston movements which naturally follow the movement of the control valve spool. The phenomenon is caused by the volume of the pump case changing as the control piston moves.

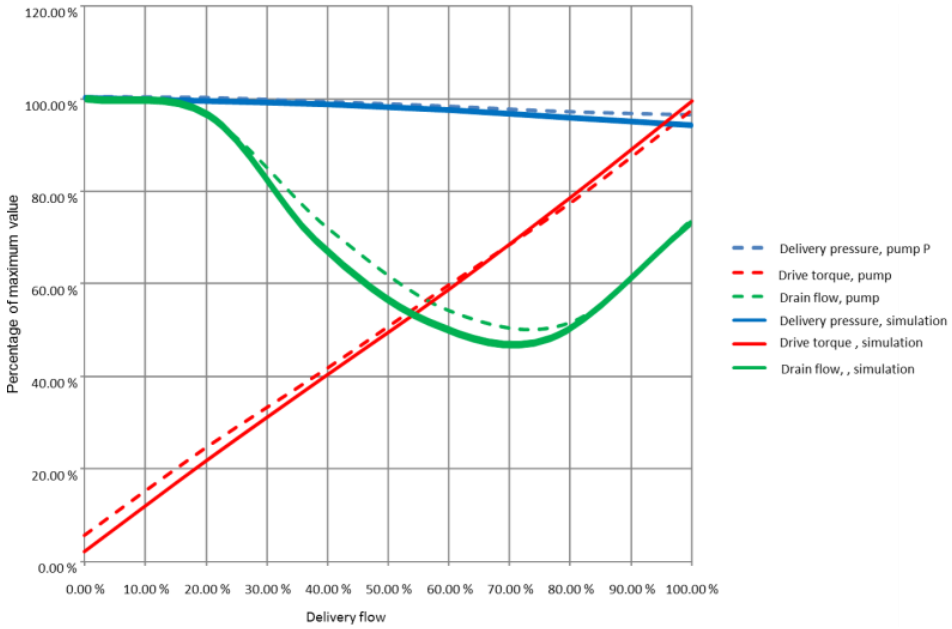

Figure 4-18 Measured and simulated delivery pressure, drive torque and drain flow as percentages of maximum value

A comparison of the measured and simulated static performance characteristics of the pump is shown in Figure 4-18. The figure shows the measured and simulated delivery pressure, drive torque and drain flow as percentages of the maximum value with the function delivery flow given as a percentage of maximum delivery. The difference between the measured and simulated performance is small, and the overall behaviour of the model in the simulations is similar to that of the real pump.

In the case of the system, the simulated and measured operation is best compared at most simple test points where the system flow demand is set unambiguously by only one single actuator. Such test points were Test Points one and five (Section 4.2.2).

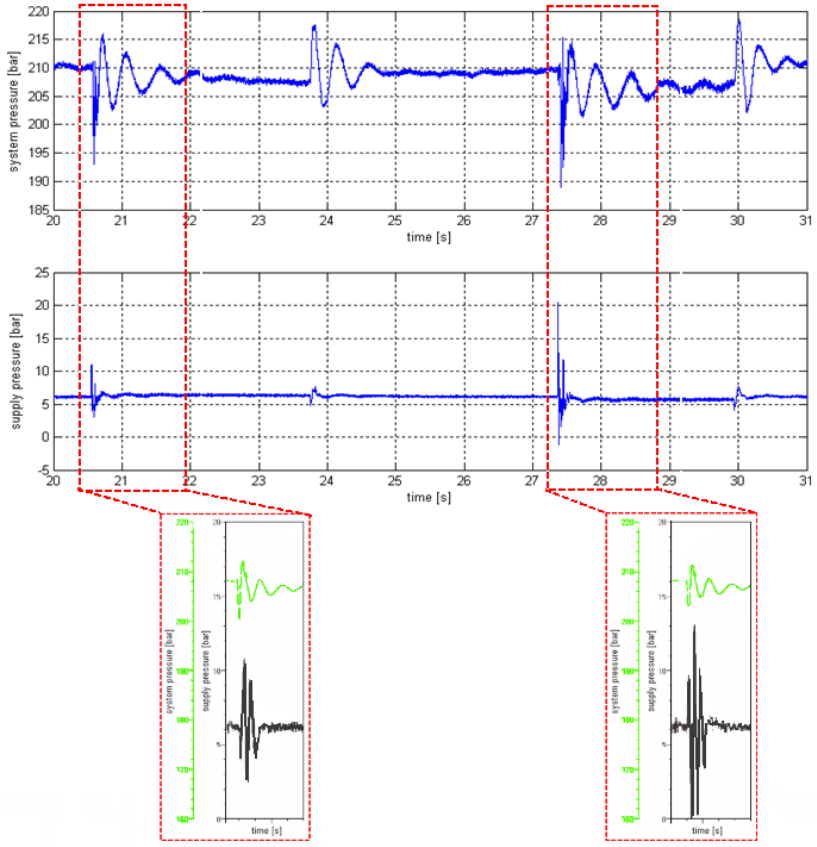

Figure 4-19Measured and simulated (inserts) system and supply pressures when airbrake is actuated at 80% engine power.

Figure 4-19 shows the measured and simulated system and supply pressures at the airbrake actuation test point. Both the simulation and measurement show similar supply pressure oscillations in both opening and closing the airbrake. Figure 4-20 shows the measured and simulated system, drain and supply pressures at the gun firing test point. Both cases show a good match between the simulated and measured

operation. There are differences, but in general terms the behaviour is the same in the model as it is in the model's real-life counterpart.

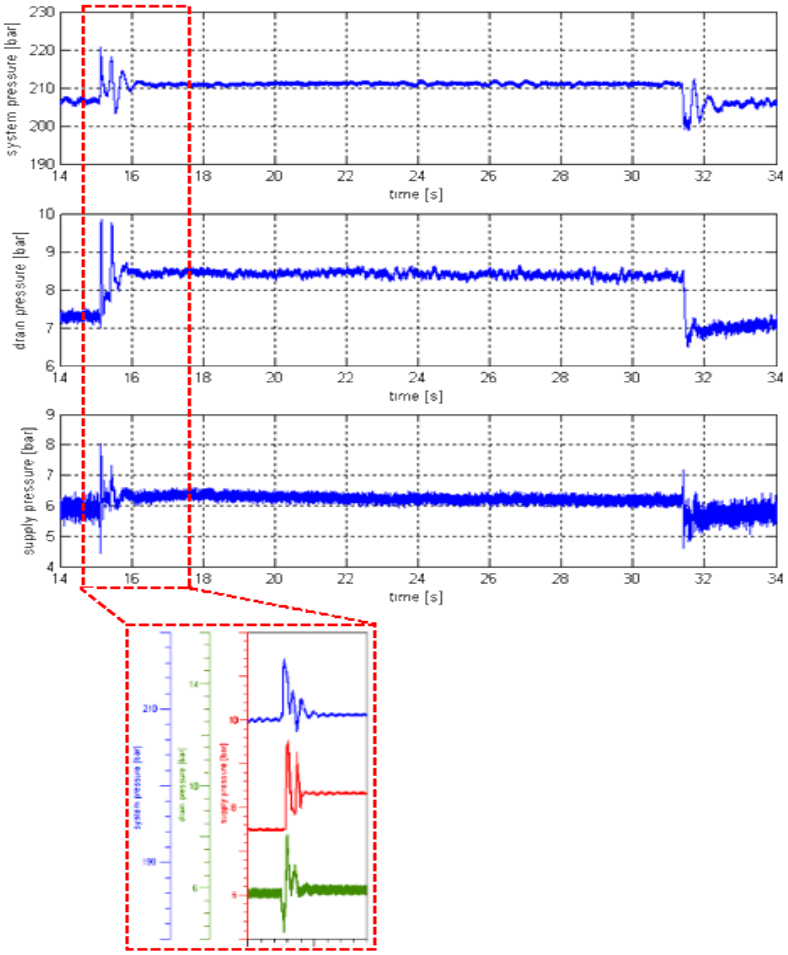

Figure 4-20 Measured and simulated (insert) system, drain and supply pressures when gun is fired at 80% engine power.

4.4 Discussion

The model includes certain inaccuracies, as any other analytical model does. Modelling inaccuracies are clearly visible when the simulations and measurements are compared, but it is not possible to determine the exact level of accuracy or boundaries of reliability universally.

The inaccuracies are to some extent related to the limitations of the analytical equations used and the variation possibilities of their parameters. The parameters of the analytical equations ate tightly tied to real-world dimensions and properties and can vary only within their natural variation limits caused by manufacturing tolerances, wear and tear and natural variation in material properties. In most cases, the allowable

parameter variation can be found in the component documentation, is otherwise known from experience or can be found from the literature; however, because of the vast number of parameters, it is was impossible to thoroughly verify all of the combinations of variations. Thus only the most essential parameters, the dimensions or properties of which are known to vary by experience, were varied in the model verification and tuning.

The model also incorporates a number of semi-empirical and empirical equations, such as friction equations, orifice flow equations, leakage flow equations, etc. These equations typically play an essential role in the behaviour of dynamic models and therefore great care and also freedoms are taken in selecting the parameters for these models. However, in this case these semi-empirical and empirical parameters are buried deep inside the model and are not directly connected to any of the parameters measured in either the laboratory or field tests. Therefore they are kept within values that experience and the literature show are good and which give a decent match at the operating points studied, even though this practice does not necessary provide the best match at all operating points.

5 INFLUENCE OF SYSTEM OPERATION ON PUMP INTERNAL LOADS

The field tests of the aircraft hydraulic system (Chapter 4.2) showed some features in the operation, such as high magnitude oscillations in the pump's supply and drain lines, which can be linked to the rapid wear encountered in the pump (Casey, 2014).

Even though aircraft hydraulic pumps, unlike hydraulic pumps in general, are designed to operate with high case pressure, and, more distinctively, a case pressure higher than the supply pressure, high pressure peaks and high differences between case and supply pressures cause additional stresses on the pump's components. Furthermore, as supply pressure in some occasions can drop below atmospheric pressure, cavitation in the pump is an inevitable phenomenon.

On the basis of findings in field tests and earlier simulations certain cases which were found to be distinctive for system or which contain untypical or distinctly violent phenomena were isolated and studied further using simulations with analytical model presented in previous chapters. Cases studied were:

1. Step-like pump delivery flow change without flow imbalance
   a. Delivery change 87 – 70 – 87 %
   b. Delivery change 80 – 30 – 80 %
   c. Delivery change 40 – 20 – 40 %

2. Step-like pump delivery flow change with flow imbalance between pump delivery and system return
   a. Delivery change 87 – 70 – 87 % with 10 % imbalance
   b. Delivery change 80 – 30 – 80 % with 20 % imbalance
   c. Delivery change 40 – 20 – 40 % with 4 % imbalance

Imbalance is expressed as a percentage of the delivery change, not the maximum flow. Flow imbalances chosen in cases 2 a – b represent worst case scenarios and 2 c represent more common scenario. Cases 1 a – c are studied also as references to cases 2 a – c to validate effects of flow imbalance. In all cases the rotational speed was constant 90 % and system temperature 90°C. All cases were first studied with original system parameters. In later stage the effects of parameter variations related to

reservoir were studied in cases 2 a – c and the effect of drain line parameter variations were studied in cases 1 a – c.

Figure 5-1 shows a simulated system response in the case 2 b in the system return and pump delivery flows.

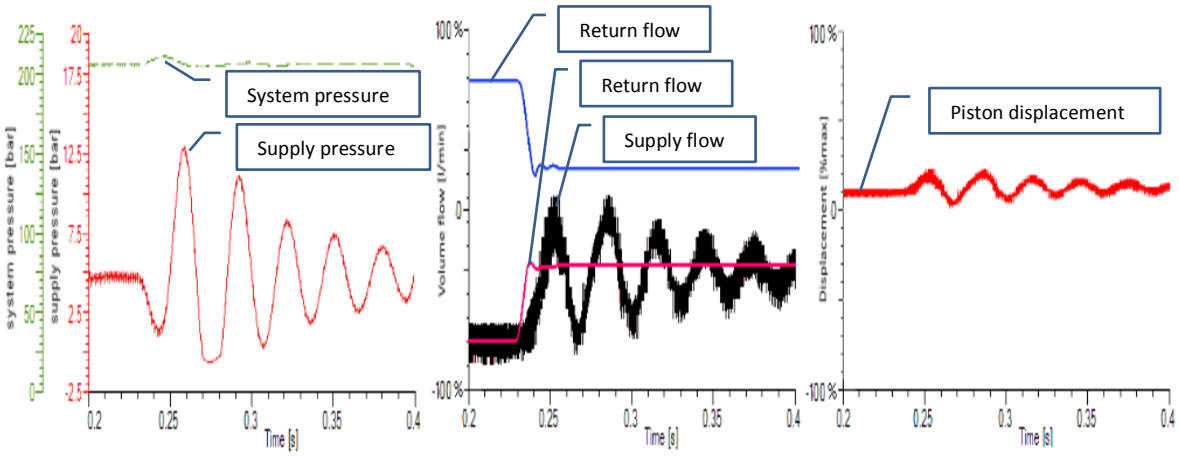

Figure 5-1 Simulated system response to high and fast pump delivery change accompanied by an imbalance in the system return and pump supply flows (case 2b). Left: system pressure and supply pressure. Middle: blue – system return flow, crimson – pump delivery, black – pump supply flow (percentage of maximum). Right: Displacement of the reservoir piston (percentage of maximum).

Heavy supply pressure oscillations are encountered at this operating point. As was also seen in the field tests, these oscillations are also reflected in the pump's case pressure, which on the other hand is also affected by the operation of the pump's compensator.

The most significant effect these oscillations have is on the pump's suction conditions. As oscillations cause the supply pressure to momentarily drop below atmospheric pressure, cavitation is an inevitable consequence. In terms of the pump's internal loads, oscillations naturally have an effect on forces affecting the pistons, but they also have some effects on the operation of the compensator, because the control piston operates against the case pressure and the control valve discharges fluid into the case. The effect on the formation of hydrostatic and dynamic bearings in the slippers and portplate should also be noted, even though it is not included in the model.

Figure 5-2 shows Piston force during suction stroke with two different case pressures. The pump does not have a retainer spring keeping the pistons against the swashplate, but there is only a retainer plate assembly which prevents the slippers from rising

further than the preset gap from the swashplate. The case pressure generally is higher than the supply pressure because of flow restrictions in both the drain line and supply line. Because of this, slippers are lifted against the retainer plate during the suction stroke, especially at high rotational speeds. Figure 5-2 shows the contact force between the swashplate and slipper during the suction stroke in four different case and supply pressure combinations taken from pressure fluctuations in simulation case 2 a.

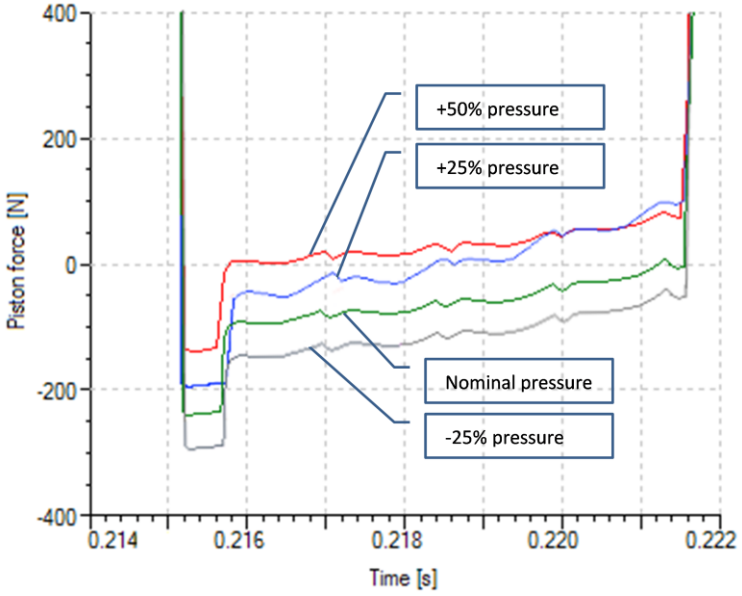

Figure 5-2 Slipper contact force during suction stroke with three different case pressures in case 2 a (green – nominal case and supply pressure, grey - supply pressure 25% below case pressure, blue – supply pressure 25% over case pressure, red – supply pressure 50% over case pressure)

The variation of the balance between the case and supply pressures cause the contact force between the slipper and swashplate to vary greatly. In cases where the supply pressure rises above the case pressure (blue and red curves) the operation of the piston changes because the direction of force changes and the slipper no longer rests against the retainer plate during the suction stroke. In this situation, the slipper however cannot bear high loads because pressure in the hydrostatic bearing is low and thus there is a high risk of metallic contact between the surfaces.

At the operating point where the supply and case pressures are in their nominal range (Figure 5-2 green curve), the contact force approaches zero at the bottom dead centre, which ensures that the slipper can drop back into contact with the swashplate quickly and a lubrication film can begin to form. At the bottom dead centre, the direction of its motion changes but both ports in the portplate are closed (Figure 3-8), which causes a

pressure peak in the cylinder pressure (Figure 5-3). This pressure peak causes a peak in the slipper contact force. The formation of a load-bearing hydrostatic lubrication film in the slipper is not instantaneous, and initial conditions such as contact force affect its formation, therefore it is very likely that the slipper and swashplate will meet in full metallic contact at the bottom dead centre at operating points that are outside the nominal case and supply pressure ranges.

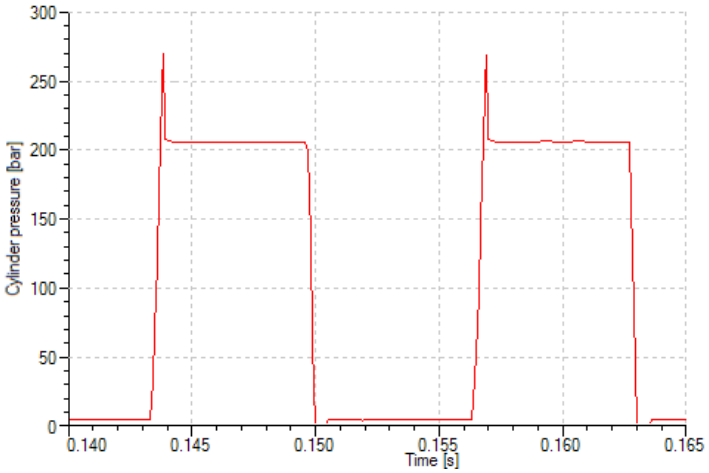

Figure 5-3 Cylinder pressure (case 2 a)

The operation of the pump's compensator also causes oscillations in case pressure. Figure 5-4 shows the case drain flow and the angle of the swashplate in a 17% delivery change. Because of the drain line filter and heat exchanger and pressure losses in the drain pipe line, these flow transients cause oscillations in the case pressure.

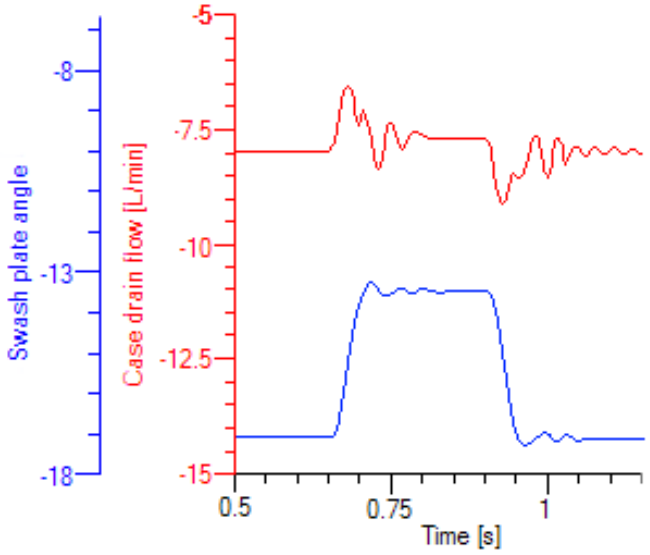

Figure 5-4 Case drain flow and swashplate angle

Case pressure peaks and fluctuations also cause higher surface pressures on the sliding surfaces of the pump shaft seal and thus increase its wear.

5.1 Effect of the Bootstrap Reservoir and Supply Line

The simulation results show that supply pressure oscillation relates to vibration of the reservoir piston. There are several factors which can have an effect on this vibration. Figure 5-5 shows oscillations in the pump supply flow in the situation where pump's delivery demand changes and there is a 4% imbalance with the system return flow. It can be seen that there is no significant delay in operation of the reservoir, but its response is very fast.

If simplified as a second order system, the response of the reservoir depends on two parameters: the natural frequency and damping ratio. The natural frequency depends on the capacitance of the system, i.e. its effective bulk modulus, volume and mass. Damping depends on the resistance of the system, i.e. factors such as the friction of the reservoir piston and flow resistances. Parameters such as mass (reservoir piston mass and moving fluid column mass) have an effect on supply pressure oscillations. In addition, the reservoir piston areas have an effect on the oscillations because they affect the forces acting on the piston.

The high pressure side of the reservoir has an effect on the dynamics of the reservoir because it is pressurised by the system pressure. However, this effect is minimal because the volume of the high pressure side is very small in comparison to the low pressure side, which drives its natural frequency into a higher region than phenomena on the supply side.

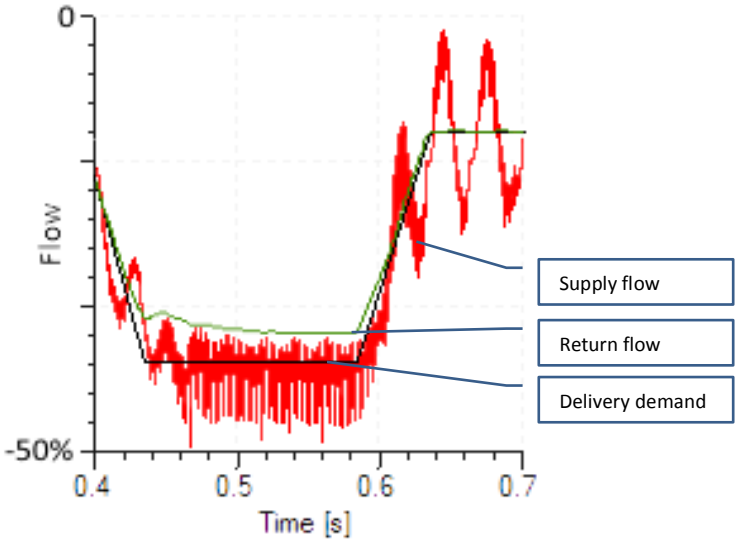

Figure 5-5 Supply pressure oscillations in case 2 c. Pump's delivery demand (black), system return flow (green) and pump supply flow (red)

The effect of the design parameters of the reservoir and pump supply line can be evaluated in terms of the characteristics of the supply system's step response. The input step is the flow demand from the reservoir, i.e. the flow imbalance between the pump supply and delivery, and the output is the supply flow from the reservoir. The characteristics of the step response used for the evaluation are shown in Figure 5-6.

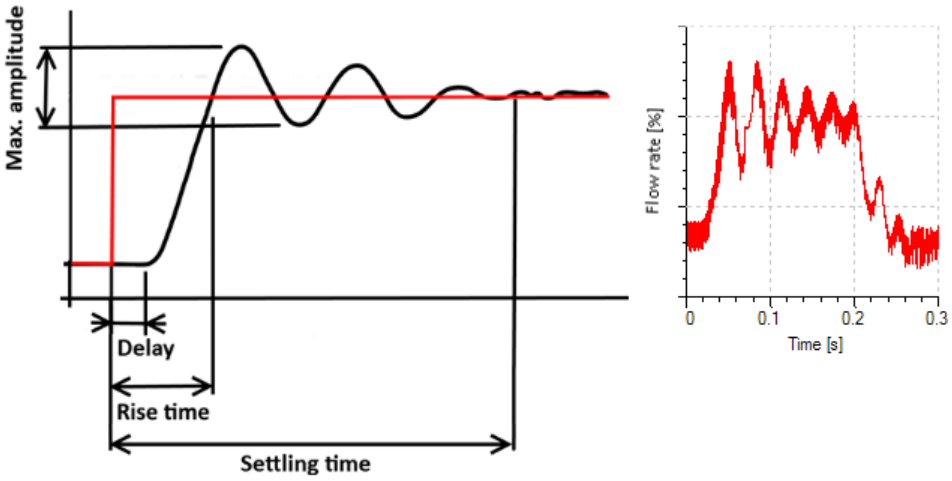

Figure 5-6 Step response of the supply system (red – flow demand from the reservoir, black –supply flow from the reservoir). Left – principle of determining characteristic values, right – example of simulated step response

Only certain system and component design parameters can be considered freely selectable for an individual system. For example, the aircraft layout sets the location of components and thus also the length and maximum diameters of pipelines. The reservoir volume is set by the properties of the hydraulic system and survivability,

maintainability and reliability requirements. Design specifications and standards set certain requirements, such as minimum pipe diameters, filtration and cooling. In addition, general requirements and limitations related to aircraft service limit freely selectable parameters and range of parameter selection.

Three design parameters which can be considered freely selectable within certain limits are: reservoir low pressure piston diameter (the reservoir pressure ratio was kept constant and thus the high pressure piston was also changed accordingly), supply line diameter and reservoir piston seal friction. The piston diameter has an effect on the force acting on the piston, but it also has an effect on the piston travel needed. The supply line diameter affects damping by increasing or decreasing flow resistances. Seal friction is not a freely selectable parameter per se, but seal type can be selected and different types of seals have differences in friction.

The effect of the above-mentioned three design parameters on step response characteristics in cases 2 a – c is shown in Figure 5-7. The figure shows how each step response characteristic changes as one design parameter is varied within $\pm$30% of its original value. Friction is varied by varying the parameters of a friction model (Equation 3-51) so that total friction in the velocity range studied varies $\pm$30%. The change in response characteristics is given as ratio relative to the original value, which is an arithmetic mean of response characteristics in three cases studied.

Changing the piston diameter changes the piston travel because the reservoir volume is kept constant. It also changes the forces affecting the piston. Varying the piston diameter does not have a major effect on the delay, because the delay mostly depends on the volume, which remains unchanged, and its effect on the force is insignificant. The rise time, however, also depends on the piston travel and is thus affected more by the change in piston diameter. The maximum amplitude decreases as the diameter is increased because the piston travel gets smaller and the reservoir's ability to react faster increases. The piston diameter however has no effect on piston damping, which causes the settling time to increase when the amplitude decreases.

The supply line diameter has an effect through the pressure drop in the line. The smaller the pipe diameter, the higher the pressure drop or the smaller the flow rate. Because of this, decreasing the diameter increases the delay and rise time. The

maximum amplitude of vibrations also increases and the settling time decreases when the pipe diameter decreases. This is caused by the fact that the vibration energy dissipated in the pipe flow pressure drop is small and thus the line does not have a major damping effect.

Varying the piston seal friction has a minimal effect on the step response. This is mostly caused by the fact that friction caused by the piston, i.e. piston seal friction, is only one part of all of the resisting forces affecting the piston assembly. Other forces resisting the motion are caused by the set of auxiliary valves actuated by the reservoir and other equipment connected to the reservoir. Friction has a very small effect on the delay because it changes only as a function of static friction. The rise time is affected by the friction force because it resists piston movement and thus causes acceleration to decrease. Friction also has a damping effect by consuming vibration energy and thus decreasing the amplitude and settling time.

There is no unambiguous optimal range for any of the three parameters studied. The maximum level of vibration amplitude directly affects the case pressure, but on the other hand, the delay and rise time directly affect how low the minimum supply pressure is. Thus in all cases parameter selection includes a trade-off and it should thus be carefully considered.

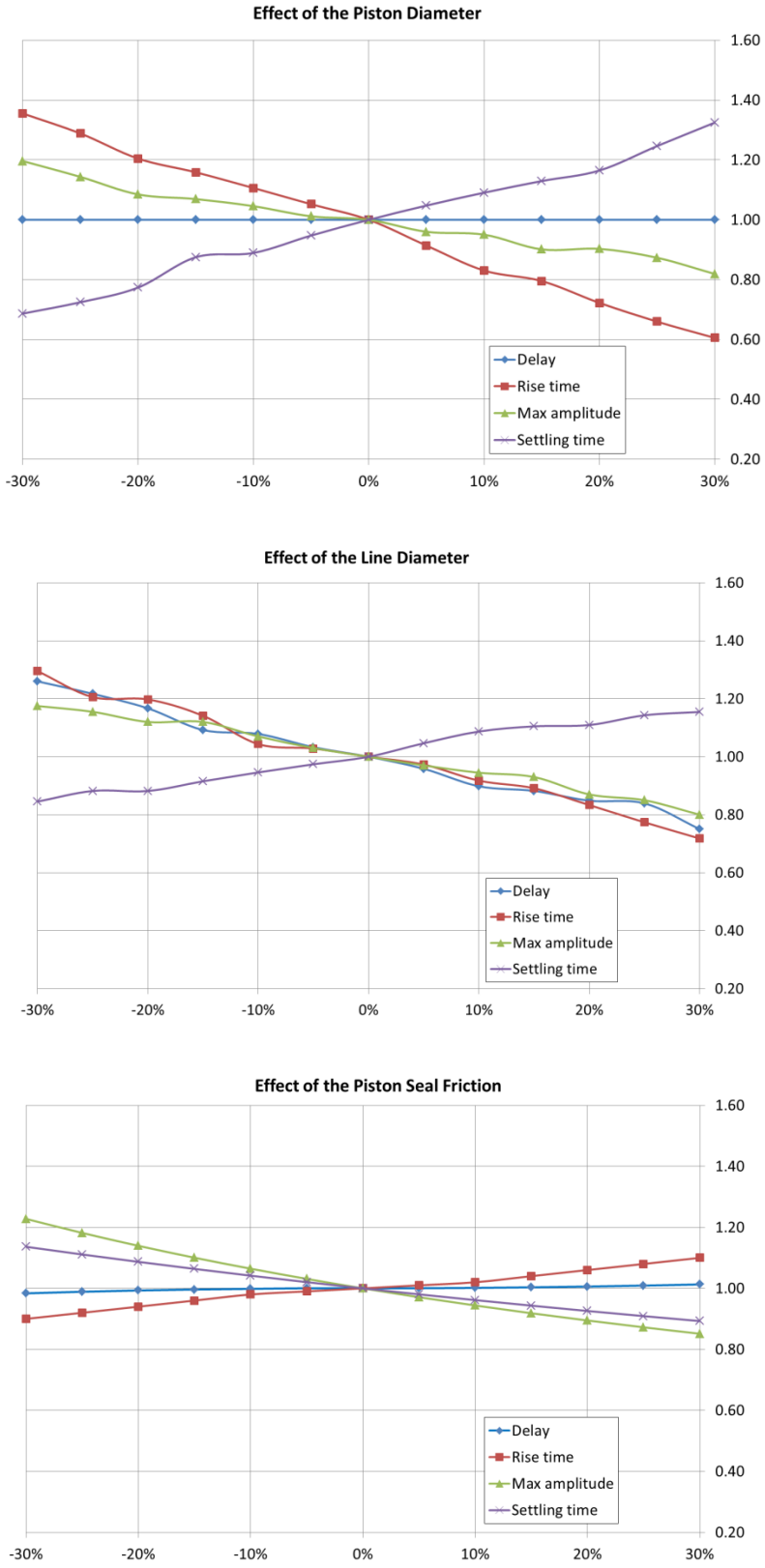

Figure 5-7 Effect of piston diameter (top chart), line diameter (middle chart) and piston seal friction (bottom chart) on step response characteristics. The vertical axis is the step response characteristic value relative to the original value. The horizontal axis is the design parameter value relative to the original value.

5.2 Effect of Drain Line Pressure Losses

Pressure losses in the drain line together with the flow rate define the case pressure, which has an effect on various loads inside the pump as discussed earlier in this chapter. Case drain line pressure losses consist of three main parts: pipeline losses, losses in the drain line filter and losses in the heat exchanger. All of these can be seen as design parameters or design selections. Pipeline losses are mainly defined by the pipe diameter, which can vary within certain limits. Losses in the filter depend on filter design parameters such as filtration rate, filter area, etc. These cannot be varied with the same ease, but there are some alternative filter designs available. The same applies to the heat exchanger: its pressure loss is more a question of component selection than parameter tuning.

The drain flow rate is also a design parameter to some extent, with a strong interdependency with the design issues mentioned earlier. A certain minimum drain flow is needed to ensure the cooling of the entire system. The lubrication and cooling of the pump itself require a certain drain flow in those rare situations where the pump has to idle. This base level of drain flow has an effect on the drain line diameter and filter and heat exchanger selection. Ultimately it defines both the heat balance of the system and the steady state case pressure of the hydraulic pump. On the other hand, the operation of the pump's pressure compensator produces flow in the drain line and has very high transients, as earlier described. In the sense of drain line dimensioning and component selection, these transients play a more important role than the base level drain flow.

Figure 5-8 shows how drain line total pressure losses change with different drain flow rates as the pipe diameter is varied from nominal to 150% and the heat exchanger and filter are kept unchanged.

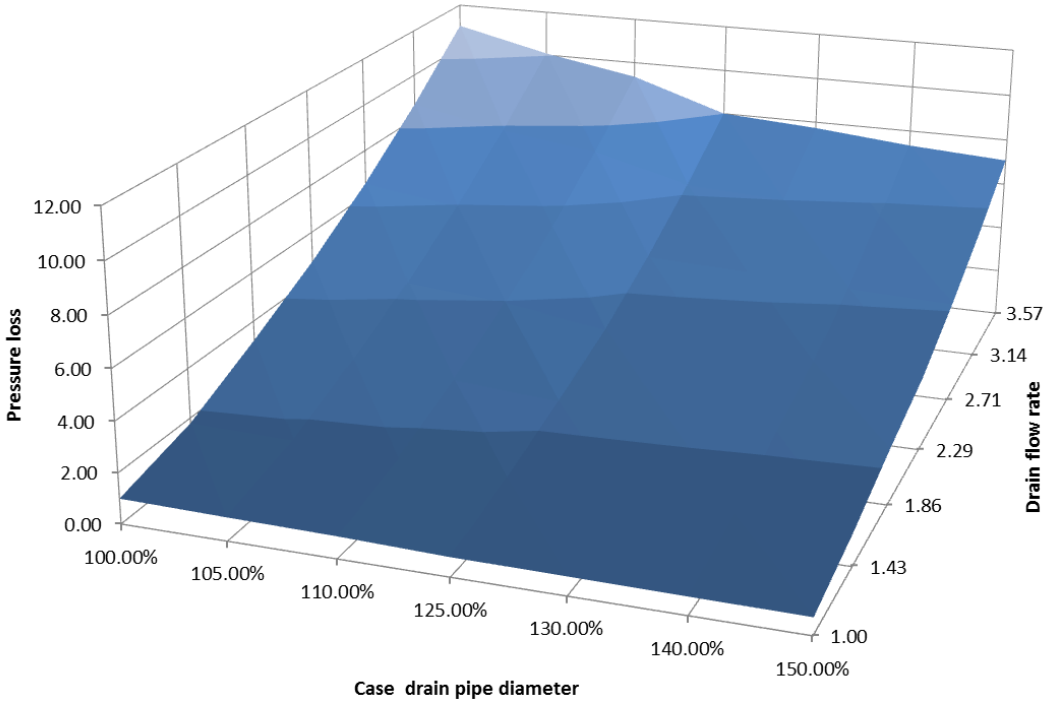

Figure 5-8 Drain line total pressure losses in cases 1 a – c as function of flow rate (relative to nominal) and pipe diameter (relative to original)

From Figure 5-8 it can be seen that even though increasing the line diameter would have definite benefits for the pump's case pressure, the flow variation has more influence on it. Because of the nature of pressure losses caused by flow restrictions, changes in the filter and heat exchanger would also have similar effects on the total pressure loss as the pipe diameter.

As described earlier, the drain flow has two components: base level drain flow from pump leakages and flow caused by compensator operation. The base level drain flow can be affected by design and parameter choices. However, as these also affect lubrication and idle cooling, there is only a limited tolerance available. In compensator flow, the tolerance is even more limited, since parameter and design choices also have an effect on the response of the controller.

To some extent, the drain flow issue is contradictory: cooling and lubrication would benefit from higher drain flow, which would require larger diameter pipes and larger filters and heat exchangers to keep pressure losses within tolerable limits. A faster response compensator would also increase the transients in the drain flow. This would all lead to a heavier but faster response, and a better lubricated and cooler running system. However, increasing the drain flow leads to decreased efficiency, which

increases the heat load to be dissipated by the heat exchanger. Furthermore, the filter's performance in the drain line is heavily affected by flow transients and would benefit from a steady flow (Multanen, 2002) (Multanen, 2000). It is, however, an unambiguous fact that the smaller the pressure loss in the drain, the lower the case pressure, and thus unwanted stresses and other adverse effects inside the pump are also smaller.

5.3 Effect of the Decreased Bulk Modulus Caused by Free Air in the Reservoir

Free air in hydraulic fluid decreases its bulk modulus, thus making the system more flexible. Even though aircraft systems are usually hermetically separated from their environment, some air can be introduced into the system. Air is introduced mainly during maintenance and overhauls in which components are removed and reconnected. Adding new fluid also usually introduces some air in the system, due to fluid becoming aerated in storage containers and handling. Furthermore, commonly used hydraulic test stands can also be sources of aeration in the fluid.

Aircraft hydraulic systems, as with hydraulic systems in general, are usually designed such that air released from the fluid as solubility changes accumulates in the reservoir. Hydraulic systems other than in aircraft can usually breathe through a reservoir breather, and thus air accumulating there is released from the reservoir. However aircraft systems, being typically hermetically sealed from the environment, do not breathe via a breather, but rather the air released from the fluid accumulates in the reservoir and forms a gas bubble there until it is bled manually.

The hydraulic systems of fighter aircraft generally require considerably more maintenance, and overhaul periods are also considerable shorter, than other hydraulic systems, thus the amount of air introduced into the system through maintenance and overhaul activities is very high. Fighter aircraft hydraulic systems are also notoriously hard to bleed thoroughly because of their complex layout, therefore there are always some amounts of free air in certain points of the system.

The most important drawback caused by free air in the system is reduced system stiffness, but besides this, free air also causes other drawbacks such as the possibility of pseudocavitation in the pump and valves. Free air also increases the rate of

oxidation of the fluid and thus ages it prematurely. The effects of air in aircraft hydraulic systems and the ways in which air is introduced into systems are thoroughly discussed in SAE Aerospace Information Report AIR5829 (SAE International, 2008).

Figure 5-9 shows how changes in the amount of free air affect the step response characteristics of the supply system. The simulations show that as the amount of air is reduced and the system becomes stiffer, the delay, rise time and settling time are reduced and the amplitude of the vibrations is decreased. Therefore it is clear that in order for the system to perform as well as possible, the free air content must be minimised.

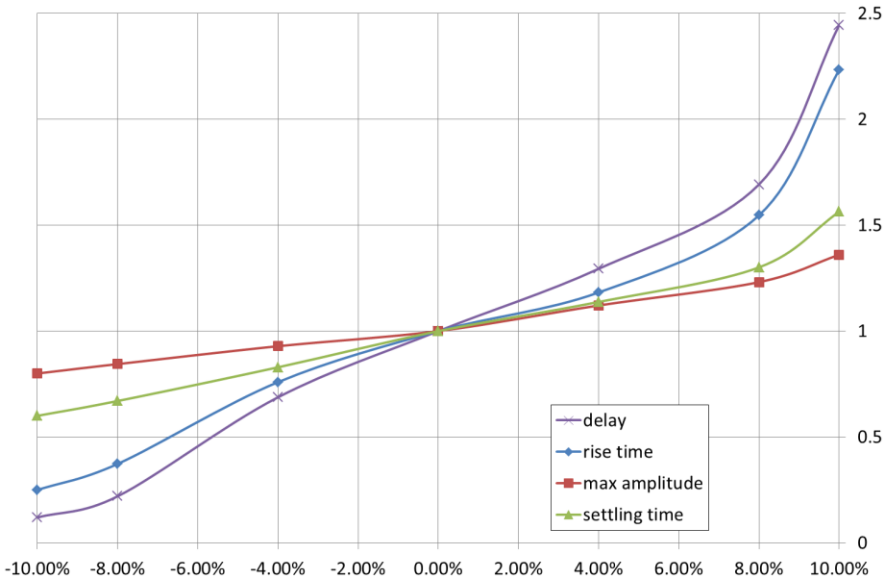

Figure 5-9 Effect of free air in the reservoir in cases 2 a – c. The vertical axis is the step response characteristic value relative to the original value. The horizontal axis is the amount of free air relative to the original amount.

It should be noted that here the absolute magnitude of these results is affected by the selection of the fluid model and its parameters (discussed in Chapter 3.5). However, the fluid model used does not change the phenomena themselves, only their magnitudes (LMS Imagine.Lab Amesim® User's Guides, 2015) (Nykänen, et al., 2000). Furthermore, the exact amount of free and dissolved air at any operating point cannot be known, and the system stiffness can have dynamics if considerable air release occurs at the operating point. Therefore this result should merely be taken as a guide to target as low an air content as possible.

5.4 Discussion

Each of the step response characteristics studied have different significances to the internal loads of the pump and thus also to its lifetime. Delay and rise time have their highest significance in the amplitude of the pressure peaks in the supply line and the reservoir. In layman's terms, they can be seen as sluggishness of the reservoir. Amplitude and settling time are closely connected to each other and the excitation energy of vibration. If the excitation energy of vibration stays constant and nothing damping the vibration is added to the system, the settling time increases as amplitude decreases and vice versa. However, if factors dissipating vibration energy or the stiffness of the system are changed, both the amplitude and settling time can change. These two characteristics define how violent and long the pressure vibrations are after each change of operating point. Considering the fast pace at which operating points may change during flight operations, the settling time can be seen as the least important of these four characteristics, as the system does not have time to reach a steady state operating point anyhow. Therefore, attention can be paid only to minimising the amplitude, delay and rise time.

As shown in the previous sections, there is no single set of design parameters studied which would offer a combination with no trade-offs. This is mostly caused by the fact that the excitation energy of the vibration is constant in all studied cases. As damping does not change, the settling time and amplitude are then connected to each other. The only studied parameter which has a significant effect on damping is piston friction. This cannot be freely selected, but itis a feature of piston seals. Furthermore, in real-life application, the available variation is even smaller than studied here. Another parameter with an effect on damping is supply line diameter, but its effect is only minor, due to the small amount of energy dissipated in it.

The design parameters studied are all interconnected, and their cooperative actions are not studied. Changing one design parameter changes the magnitude of effect of the other design parameters. It must also be noted that the absolute level of the drain line and case pressures depend on the reservoir and supply pressure, as the drain line leads to the reservoir, thus the supply side's dynamic response also affects the case pressure.

6 PROPOSALS FOR FIGHTER AIRCRAFT HYDRAULIC POWER SUPPLY SYSTEM DESIGN GUIDELINES AND MAINTENANCE PRACTICES

6.1 Improving the Dynamic Response of the Reservoir and the Supply Line

The reservoir's main functions in aircraft hydraulic systems are to be a fluid reserve and to enable volume changes due to thermal expansion and asymmetric actuators. Unlike in most general hydraulic systems, it is neither an effective part of the cooling system nor part of fluid condition control.

The main design requirements for the reservoir are the volume of fluid needed as a reserve, and the system volume changes because of asymmetric actuators and thermal expansion. The design constraints which define the location and dimensions of the reservoir are set by the aircraft layout. The layout also sets constraints on the supply line by defining its routing, length and maximum diameter. Secondary design requirements stem from the system operation and relate to the dynamic response of the pump supply side during system operation.

Table 6-1 Design recommendations for the reservoir and supply line

Design parameter	**Affects**	**Recommendation**
Reservoir piston diameter	Amplitude Delay Rise time	Increasing low pressure piston diameter decreases the piston travel and improves amplitude, delay and rise time
Reservoir piston seal friction	Amplitude Settling time Delay Rise time	Low friction seals improve delay and rise time
Supply line diameter	Amplitude Settling time Delay Rise time	Large supply line diameter improves amplitude, delay and rise time

The key design parameters of the pump supply side (discussed in Chapter 5.1) each have different importance and effects on the dynamic response of the supply side. Table 6-1 lists the studied design parameters, their effects and recommendations for them.

Piston diameter and supply line diameter are also tightly tied to the aircraft's layout requirements and can be only be altered within the limits set by them. The reservoir piston seal friction, on the other hand, can only be varied within the limits of available seal types and also within the limits set by seal compatibility and lifetime issues. On the basis of these findings, a general rule of thumb can be set: the reservoir piston diameter and supply line diameter must both be as large as possible.

6.2 Minimising Pressure Losses in the Case Drain Line

The case drain flow rate is defined by the characteristics of the pump itself and those of its controller. The steady state base level of the case drain flow is created by various leakage flows inside the pump. Leakage flow rates are functions of pressure difference over the leakage gap, and therefore the flow rate in the drain line is a function of the reservoir pressure and drain line pressure loss. However, higher flow peaks which result in high case pressure peaks are generated by the pump's controller and are not affected by case pressure variations. The pump's case drain leads to the reservoir, and thus the dynamic behaviour of the pump's supply side pressure is a factor in the pump's case pressure. Case drain line pressure loss is however an equally important factor. Pressure loss in the case drain line comes from three sources: pressure loss in the pipeline, filter and heat exchanger.

Heat exchanger dimensioning is based on the system heat balance: a certain amount of heat energy carried by a certain flow rate must be dissipated through it to the jet fuel. The object to maximise heat transfer capacity generally also leads to high surface area and low flow velocity, which naturally lead to a low pressure drop in the heat exchanger.

Filter dimensioning is based on the filtering result required in terms of both filtering efficiency and particle size, and also on the filter element lifetime requirement. Generally, the filter is dimensioned so that it satisfies these requirements with minimal weight and size. Filtering efficiency and lifetime requirements drive towards a high filtration area and low flow velocity, which also give a low pressure loss in the filter.

The only design parameter which can be set with higher level of freedom is the case drain line tube diameter. The usable tube diameter is limited by the routing of the line

and available space along the route. The higher the line diameter, the lower the pressure loss in the line. Using as high a diameter pipe as possible is worthwhile, even though the pipe line causes only one part of the total pressure loss in the case drain line.

6.3 Minimising the Free Air Content of the Reservoir

Of the studied parameters, the free air content of the reservoir has the biggest impact on the dynamic response of the pump's supply side. The higher the free air content, the more flexible the system. Increased flexibility leads to all of the studied step response characteristics degenerating. The supply's side response is better as the free air content becomes smaller.

The level of free air content in the aircraft hydraulic system is a question of both system design and maintenance. Air is introduced into the system as free air in the form of air bubbles or pockets in replaced components, or as dissolved air in new fluid added to the system. The system must be designed so that air from pockets and bubbles and air released from the fluid travels to a certain spot in the system, usually the reservoir, where it can be bled out either manually or automatically.

The latest releases of SAE AS 5440 require military aircraft to have an automatic air bleed valve permanently installed in the hydraulic system. Earlier releases also already required a manual bleed valve in the reservoir. A requirement for a method to indicate the amount of free air in the reservoir has also been added to SAE AS 5440. These two inclusions can offer a definite improvement to the free air content of the reservoir, provided that their function and placement in the system are correct (SAE International, 2011).

Portable hydraulic test stands used with aircraft usually have a larger-volume reservoir which breathes to the outside air. A large volume reservoir with free breathing offers the fluid the same possibility to deaerate as it would have in a generic hydraulic system. Some test stands also employ a bleed system which collects free air bubbles from the fluid and releases them to air. Test stands may also be able to vacuum-treat the fluid to remove air from it. The efficiency of these measures depends on their design and how often they are employed.

Besides the technical measures to remove free air or reduce its amount, maintenance practices can also be improved. The most important matter to acknowledge is that all maintenance actions which include removing or replacing system components will introduce air into the system. Therefore, practices for bleeding the system thoroughly should be developed for all individual maintenance actions which can introduce air into the system. In addition, fluid handling when topping up the aircraft system or test stand should be developed such that fluid aeration is kept to a minimum.

7 DISCUSSION

The objectives of this research were to identify the phenomena causing premature failures of axial piston hydraulic pumps encountered in some fighter aircraft and to study these phenomena and interactions related to them. Main research methodology selected was mathematical modelling and computer simulation accompanied by laboratory and field testing.

System and component models are based on common analytical, empirical and semiempirical equations. Selecting system modelling approach which is mostly based on analytical equations was a compromise, as choice of modelling methodology always is. Analytical modelling approach enables flexible and relatively simple models with limited number of easily variable parameters which are mostly based on real physical dimensions. Simulation of the model can be done with only moderate computing power which enables very efficient batch simulations of parameter variations.

It is undeniable fact that analytical modelling does not give such a high fidelity results that are available more advanced methods such as FEA or CFD. However in this research correct results as absolute numeric values and high fidelity results were not the objective but it was merely indicating and isolating root causes for failures and finding phenomena and interactions behind them. Therefore lack of fidelity can be accepted as a trade-off for efficient simulations. In future if the need for higher fidelity results arises it is possible to include FEA or CFD using co-simulation methods to the details of interest. By co-simulation methods it is also possible to utilise MBS tools which enable more accurate modelling of mechanisms, such as swashplate and its control system.

Laboratory measurements were carried out using specific test rig developed for studying pump operation. Field tests with real fighter aircraft were carried out in a test hangar, which enables operating aircraft with full thrust. Both of these test methods have short comings which have to be taken into account in analysing the results. Firstly, operating points achievable in tests are different from in-flight operating points. Secondly, in laboratory tests the test rig is completely different from aircraft system. For both tests the test scenarios were designed on basis of experiences from

simulations the way that operating points of interest can be found. Therefore these tests only give information for model verification and validation purposes, no conclusions about system operation in flight situations can be made on basis of them.

Pump model verification was done in two levels: firstly it was verified that the model's performance and response characteristics match its real-world counterpart, secondly the inner workings of the model were verified also. The key issue is verification of the inner workings. As inner workings cannot be verified on the basis of direct measurements verification has to be done on basis of sanity-checking the behaviour. Thus verification relies extremely heavily on the experience of the person performing it and also available prior research knowledge and literary sources. In the system level it should be noted that models tend not to be universally accurate, but their fidelity is usually the best in operating points where they are verified. Thus the main challenge in system-level verification is determining the operating points at which the verification is done. In this study verification was done seemingly in relatively wide range of operating points, but it should also be noted that verification points only cover very narrow range of all possible operating points. Because objectives of the research are mainly qualitative the verification methods used offer adequate accuracy for the purpose. However if the model would be used to model based design the verification process should be rethought, especially if inside parts of the pump would be of interest.

The first and third research questions were proven by studying step response characteristics of the supply side of the system. Step response characteristics were studied in terms of delay, rise time, settling time and maximum amplitude. In cases studied the excitation energy of vibration is constant in each case and therefore effect of the design parameters on the natural frequency and damping of the system can be studied and specified. It should however be noted that parameters are all interconnected and their co-operative actions and interactions are not studied in this research. Direction of individual effects of each variable is known on basis of this research and it also gives an indication of their co-operative actions and interactions, however magnitude of co-operative actions and interactions is not known. No single set of design parameters studied was found to offer a combination with no trade-offs.

The second research question was proven by studying effect of the case drain line pressure losses. Drain line flow depends on the pump leakage flow and the flow caused by the pump's controller. The higher the flow is the higher is also the case pressure which has an effect on various components inside the pump. The variable studied was drain line pipe diameter. However pressure loss in the pipe is only one of the three components from which the total pressure loss is formed. Other two components are hydraulic fluid – fuel heat exchanger and drain line filter which are not included in this research. Another component not included in this research is controller which has a significant effect on drain line pressure dynamics. In the scope of this research only the most obvious answer of increasing the pipe diameter could be provided. However in order fully address drain line issue also controller, drain line filter and heat exchanger should be studied.

Pressure control vibrations, which emphasize the need to study also the controller, were found in laboratory tests,and simulations done with models replicating the system of the aircraft, but in field tests they were not encountered. The tests showed that steady state vibrations tend to occur when there is a fast change from high delivery to zero or very low delivery. In real aircraft this is very unlikely to occur in normal operation. However short-term vibrations can still occur there. Pressure control vibrations are directly linked to the flow variations in the drain line and thus also to case pressure which is one of the factors having an effect on pump failures.

Free air in hydraulic fluid is addressed by studying effects of decreased bulk modulus it causes. Free air in the system is both a system design and maintenance issue. Design issue is designing system easy to bleed free from air. Maintenance issue is that air is introduced mainly during maintenance and overhauls. Aircraft hydraulic systems are usually designed so that air accumulates in the reservoir from where it has to be bled manually. Fighters generally require considerable amount of maintenance and overhaul periods are short. Therefore there are always some amounts of free air in the reservoir and some other points. Free air has several drawbacks in hydraulic systems. This research however concentrates only in decreased bulk modulus even though other drawbacks, such as increased risk of cavitation, pseudocavitation etc, are also related to pump failures encountered in fighter aircrafts. The effects of air in aircraft hydraulic systems thoroughly discussed in SAE Aerospace Information Report AIR5829 (SAE

International, 2008). In the model free air is only considered through the fluid bulk modulus even though its solubility is modelled as pressure dependant phenomenon. If free air would be the detail of interest in the model it should be modelled differently by using for example 1 D two phase flow models or CFD as a cosimulations.

8 CONCLUSION

The focus of this research is on studying system- and component-level phenomena and interactions in fighter aircraft hydraulic power supply systems in detail. The objective was to discover system-level root causes for the premature failures of hydraulic pumps encountered in many modern fighter aircraft and to study phenomena related to them. The hydraulic pump and bootstrap reservoir were studied using computer simulations to find out how system-level interactions influence the internal loads of the pump. For the simulations, a hydraulic pump and bootstrap-type reservoir with pipework connecting them were modelled as analytical physical models. Other parts of the hydraulic system were modelled using empirical black box-type models. The models were verified in the laboratory using laboratory and field measurements.

The **research hypothesis** of the thesis was proven by identifying root causes for failures and phenomena triggering them through the computer simulations. The sensitivity of the system and component design variables which have an effect on these phenomena was studied. The results of the study show that premature failures of hydraulic pumps encountered in certain types of high-performance fighter aircraft are related to pressure and flow fluctuations occurring in the pump's drain and supply lines. These fluctuations originate in system-level interactions between components. The selection of design parameters and maintenance practices both have an effect on the magnitude and thus effect of these interactions.

The **research questions** were studied by examining the system's sensitivity to the variation of four design parameters.

1. **The effect of the bootstrap-type reservoir's dynamics** was studied by varying the reservoir's low pressure piston diameter and reservoir piston seal friction. It was found that piston diameter mainly affects the response time of the supply side and is the single most important parameter in the supply side dynamics. The piston seal friction has the biggest effect on settling time, as it affects system damping.

2. **Drain line pressure loss** was studied by varying the drain line diameter. The system's sensitivity to it can be compared to the other parameters because it is

not evaluated in terms of the characteristics of the supply side dynamics, but in terms of the steady state pressure drop, which has a crucial effect on the phenomena behind the root causes found. It was found that drain line pressure loss should be minimised to keep the level of unwanted stresses in the pump as low as possible.

3. **The system's sensitivity to free air in the reservoir** was evaluated in terms of the characteristics of the supply side dynamics, and was found to be considerably more significant than any of the design parameters studied. Thus, reducing the amount of free air in the reservoir through maintenance activities is the most efficient way to improve the dynamic response of the supply side.

Design and maintenance recommendations were given on the basis of the results. Their applicability depends on the phase of the lifecycle of the aircraft. During the design phase, attention can be paid to details of system operation without compromising the big picture. During the early design phases, the possibilities to change the system design are still almost endless. However, fully utilising this possibility requires the availability of relatively high fidelity system modelling in the early design stages. After the design has been completed and the aircraft is entering prototype production and test flights, making modifications at the level of changing the design parameters discussed here becomes considerably more difficult, and the related costs become harder to justify. As the aircraft moves ahead through its lifecycle, modifications become constantly harder and related costs become more difficult to justify. In the early operational phase, modifications improving reliability, availability and operational costs can be economically justifiable when they are viewed in terms of lifecycle costs. The closer we come to mid-life and end-life, the more likely it is that modifications need other than economic justification, such as an improvement in operational capabilities, or an extension of lifetime.

8.1 Suggestions for Further Research

The inclusion of requirements for free air detection capabilities and automatic bleeding in SAE AS 5440 and the availability of automatic bleed valves in the OEM (Original Equipment Manufacturer) market indicate that future military aircraft will have automatic detection of free air and automatic bleeding (Parker Hannifin

Corporation, Parker Aerospace, Hydraulic Systems Division, 2016). Automatic bleeding and detection is, however, more a case of removing a symptom than removing the actual cause. The cause of air being introduced to the system in the first place lies in the maintenance practices and equipment used. Furthermore, the cause of difficulties in bleeding is usually shortcomings in the system design and ineffective bleeding practices. However, if system design and maintenance practices and also maintenance equipment could be developed such that the introduction of air into the system could be minimised, and manual bleeding made more efficient and effective, the addition of new component functionalities into hydraulic systems could be avoided. To achieve this, systematic research on hydraulic systems technology and the maintenance procedures of hydraulic systems is required.

This research left numerous scientific and technical questions related to the system and its components. The most important question is finding universal quantitative relations design parameters system performance characteristics. Other important questions can be found from design of drain line components, i.e. drain line filter and heat exchanger, and also from the design of pump's controller.

9 REFERENCES

Aaltonen, J., Koskinen, K. & Vilenius, M., 2007. Pump supply pressure fluctuations in the semi-closed hydraulic circuit with bootstrap type reservoir. *The Tenth Scandinavian International Conference on Fluid Power, May 21-23, 2007, Tampere, Finland, SICFP'07*, pp. 117-133.

Alarotu, V., Aaltonen, J., Koskinen, K. & Siitonen, M., 2013. *Combined Virtual Iron Bird and Hardware-in-the-Loop Simulation Research Environment for Jet Fighter Hydraulic Systems.* Linköping, 4th CEAS International Conference of the European Aerospace Societies.

Alarotu, V., Aaltonen, J., Koskinen, K. T. & Siitonen, M., 2013. Combined Virtual Iron Bird and Hardware-in-the-Loop Simulation Research Environment for Jet Fighter Hydraulic Systems. *Proceedings of the 4th CEAS Conference in Linköping, 2013*, pp. 196-202.

Bajpai, G., Chang, B. & Lau, A., 2001. Reconfiguration of Flight Control System for Actuator Failures. *IEEE Aerospace and Electronic Systems Magazine,* 16(9), pp. 29 - 33.

Bergada, J., Kumar, S., Davies, D. & Watton, J., 2012. A complete analysis of axial piston pump leakage and output flow ripples. *Applied Mathematical Modelling,* 36(4), pp. 1731-1751.

Bergada, J. M., Watton, J. & Kumar, S., 2008. Pressure, Flow, Force, and Torque Between the Barrel and Port Plate in an Axial Piston Pump. *Journal of Dynamic Systems, Measurement, and Control,* Osa/vuosikerta 130.

Blackburn, J. F., Shearor, J. L. & Reethof, G., 1960. *Fluid power control.* Cambridge, MA: MIT Press.

Busch, D. A. & Aldana, J. F., 1993. *An Approach to Aircraft Subsystem Design and Integration.* Fort Worth, TX , USA, Institute of Electronics and Electrical Engineers, pp. 469 - 474.

Byington, C. S., Watson, M., Edwards, D. & Dunkin, B., 2003. *In-Line Health Monitoring System for Hydraulic Pumps and Motors.* s.l., s.n., pp. 3279 - 3287.

Casey, B., 2007. *'Inside Hydraulics' Newsletter, Issue 61*. [Online] Available at: http://www.insidersecretstohydraulics.com/newsletters/issue61.html [Haettu 5 September 2016].

Casey, B., 2014. *The Hydraulic Troubleshooting Handbook: And how to Troubleshoot Everything Else!*. Perth: HydraulicSupermarket.com Pty Limited.

Casoli, P. & Anthony, A., 2013. Gray box modeling of an excavator's variable displacement hydraulic pump for fast simulation of excavation cycles. *Control Engineering Practice,* 21(4), pp. 483-494.

Deeken, M., 2003. Simulation of tribological Contacts in an Axial Piston Machine. *Ölhydraulik unf Pneumatik,* 47(11-12).

Dobchuk, J. W., Burton, R. T., Nikiforuk, P. N. & Ukrainetz, P. R., 2000. Effects of Internal Pump Dynamics on Control Piston Pressure Ripple. *Proceedings of FLUCOME 2000*.

Du, J., Wang, S. & Zhang, H., 2013. Layered clustering multi-fault diagnosis for hydraulic piston pump. *Mechanical Systems and Signal Processing,* 36(2), pp. 487-504.

Edge, K. A. & Darling, J., 1986. Cylinder Pressure Transients in Oil Hydraulic Pumps With Sliding Valve Plates. *Proceedings of the Institution of Mechanical Engineers,* Osa/vuosikerta 200, p. 45.

Gao, F., Ouyang, X., Yang, H. & Xu, X., 2013. A novel pulsation attenuator for aircraft piston pump. *Mechatronics,* 23(6), pp. 566-572.

Gheorghe, ym., 2013. Model-Based Approaches for Fast and Robust Fault Detection in an Aircraft Control Surface Servo Loop: From Theory to Flight Tests [Applications of Control]. *IEEE Control Systems,* 33(3), pp. 20-84.

Gomes, J. P. P. ym., 2012. *Failure Prognostics of a Hydraulic Pump Using Kalman Filter.* Minneapolis, Annual Conference of the Prognostics and Health Management Society 2012.

Guan, C., Jiao, Z. & He, S., 2014. Theoretical study of flow ripple for an aviation axial-piston pump with damping holes in the valve plate. *Chinese Journal of Aeronautics*, 27(1), pp. 169-181.

Harris, R. M., Edge, K. A. & Tilley, D. G., 1993. The Spin Motion of Pistons In a Swashplate-Type Axial Piston Pump. *The Third Scandinavian International Conference on Fluid Power SICFP 1993*, p. 95.

Hietala, J.-P., Aaltonen, J., Koskinen, K. T. & Vilenius, M., 2009. Modelling and simulation of the aircraft rudder hydraulic servo actuator with dynamic interconnections to flight dynamics and flight control system models. *SICFP'09 Proceedings, the 11th Scandinavian International Conference on Fluid Power, Linköping, Sweden, June 2-4 2009*, p. 12.

Hietala, J.-P., Aaltonen, J., Koskinen, K. T. & Vilenius, M., 2011. Aircraft hydraulic system model integration to fligh simulation model. *The Twelfth Scandinavian International Conference on Fluid Power SICFP; Vol. 12, No. 1*, pp. 271-280.

Hietala, J.-P., Aaltonen, J., Koskinen, K. & Vilenius, M., 2009. *Modelling and simulation of the aircraft rudder hydraulic servo actuator with dynamic interconnections to flight dynamics and flight control system models.* Linköping, the11th Scandinavian International Conference on Fluid Power.

Hietala, J.-P., Aaltonen, J., Koskinen, K. & Vilenius, M., 2011. *Aircraft hydraulic system model integration to fligh simulation model. julkaisussa The Twelfth Scandinavian.* Tampere, International Conference on Fluid Power, SICFP'11.

Iboshi, N. & Yamaguchi, A., 1982. Characteristics of a Slipper Bearing for Swash Plate Type Axial Piston Pumps and Motors (1st Report, Theoretical Analysis). *Bulletin of the Japanese Society of Mechanical Engineers*, p. 1921.

Iboshi, N. & Yamaguchi, A., 1990. Effects of Swash Plate Angle, Fluid Viscosity and Operating Conditions on Characteristics of a Slipper Bearing For Swash Plate Type

Axial Piston Pumps and Motors. *Fluid Power Control and Robotics - Proceedings of Chengdu 90 ICFPCR*, p. 274.

Ikeya, M. & Kato, H., 1985. Leakage Characteristics of the Hydraulic Slipper Bearing in Swashplate Type Axial Piston Motor at Starting and Low Speed. *Proceedings of the International Conference on Fluid Power Transmission and Control*, p. 695.

Inoue, K. & Nakasato, M., 1994. Study of the Operating Moment of a Swash Plate Type Axial Piston Pump Second Report. *Journal of Fluid Control*, 22(1), p. 30.

Ivantysyn, J. & Ivantysynova, M., 1993. *Hydrostatische Pumpen und Motoren: Konstruktion und Berechnung.* Würzburg: Vogel Business Media.

Johansson, A., 2005. *Design Principles for Noise Reduction in Hydraulic Piston Pumps.* Linköping: Linköpings universitet.

Jong-Hyeok, K., Chang-Sooand, J., Hong & Yeh-Sun, 2015. Constant pressure control of a swash plate type axial piston pump by varying both volumetric displacement and shaft speed. *International Journal of Precision Engineering and Manufacturing,* 16(11), pp. 2395-2401.

Joshi, A. & Jayan, P., 2002. *Modeling and Simulation of Aircraft Hydraulic System.* s.l., AIAA Modeling and Simulation Technologies Conference and Exhibit.

Karpenko, M. & Sepehri, N., 2006. *Hardware-in-the-loop simulator for research on fault tolerant control of electrohydraulic flight control systems.* Minneapolis, 2006 American Control Conference.

Kauranne, H., Kajaste, J., Ellman, A. & Pietola, M., 2003. *Applicability of Pump Models for Varying Operational Conditions.* Washington, D.C, Proceedings of the ASME Conference, November 16-21, 2003.

Kim, S. D., Cho, H. S. & Lee, C. O., 1987. A Parameter Sensitivity Analysis for the Dynamic Model of a Variable Displacement Axial Piston Pump. *Proceedings of the Institution of Mechanical Engineers* , Osa/vuosikerta 201, p. 235.

Krus, P., Braun, R., Nordin, P. & Eriksson, B., 2012. *Aircraft System Simulation For Preliminary Design.* Brisbane, ICAS 2012, 28th International Congress of the Aeronautical Sciences.

Li, J., Zhang, X., Yin, Y. & Zhang, J., 2011. *Dynamic temperature simulation of an accumulator in aircraft hydraulic systems.* Beijing, 2011 International Conference on Fluid Power and Mechatronics (FPM).

Li, K., Lv, Z., Lu, K. & Yu, P., 2015. *Thermal-hydraulic modeling and simulation of piston pump in electro-hydrostatic actuator system.* Harbin, 2015 International Conference on Fluid Power and Mechatronics (FPM).

Lin, S. J., Aker, A. & Zeiger, G., 1987. Oil Entrapment in an Axial Piston Pump and its Effect Upon Pressures and Swashplate Torques. *42nd National Conference on Fluid Power,* p. 113.

LMS Imagine.Lab Amesim® User's Guides, 2014. *LMS Imagine.Lab Amesim Hydraulic Component Design Library, User's Guide.* Roanne: Siemens Industry Software NV.

LMS Imagine.Lab Amesim® User's Guides, 2015. *LMS Imagine.Lab Amesim Hydraulic Library, User's Guide.* Roanne: Siemens Industry Software S.A.S..

Locheed Martin Corporation, 1994. *T.O.1F-16A-1, Flight Manual, F-16A/B, Blocks 10 and 15.* 036802 toim. s.l.:US Air Force.

M., B. J., J., W., M., H. J. & L., D. D., 2010. The hydrostatic/hydrodynamic behaviour of an axial piston pump slipper with multiple lands. *Meccanica,* 45(4), p. 585–602.

Ma, J.-e., Fang, Y.-t., Xu, B. & Yang, H.-y., 2010. Optimization of Cross Angle Based on the Pumping Dynamics Model. *Journal of Zhejiang University-SCIENCE A,* 11(3).

Manring, N., 2000. Tipping the Cylinder Block of an Axial-Piston Swash-Plate Type Hydrostatic Machine. *Journal of Dynamic Systems, Measurement, and Control,* pp. 216-221.

Manring, N. D., 1999. The Control and Containment Forces on the Swash Plate of an Axial-Piston Pump. *ASME Journal of Dynamic Systems, Measurement, and Control* , Osa/vuosikerta 121.

Manring, N. D., 2000. Tipping the Cylinder Block of an Axial-Piston Swash-Plate Type Hydrostatic Machine. *ASME Journal of Dynamic Systems, Measurement, and Control,* Osa/vuosikerta 122.

Manring, N. D., 2002. The Control and Containment Forces on the Swash Plate of an Axial Piston Pump Utilizing a Secondary Swash-Plate Angle. *Proceedings of the American Control Conference*.

Manring, N. D. & Johnson, R. E., 1994. Swivel Torque Within a Variable-Displacement Pump. *46th National Conference on Fluid Power*.

Mare, J. C., 2001. *Simplified Model of Pressure Regulated, Variable Displacement Pumps for the Sizing of Complex Hydraulic Systems.* s.l., International Academic Publishers World Publishing Corporation, pp. 151-156.

Merritt, H. E., 1967. *Hydraulic Control Systems.* London: John Wiley & Sons.

Multanen, P., 2000. Testing and development of hydraulic filter performance under variable flow conditions - new filter solution -. *Proceedings of the 1st FPNI-PhD Symposium Hamburg 2000, September 20-22, Germany*.

Multanen, P., 2002. *Hydraulic Filter Performance under Variable Flow Conditions.* Tampere: Tampere University of Technology, 2002. 131 p. (Acta Polytehcnica Scandinavica, Mechanical Engineering Series; No. Me 162).

Nykänen, T., Esque, S. & Ellman, A., 2000. *Comparison of different fluid models.* Bath, Bath Workshop on Power Transmission and Motion Control (PTMC 2000).

Öström, J., 2007. Enhanced inverse flight simulation for a fatigue life management system. *Collection of Technical Papers – 2007 AIAA Modeling and Simulation Technologies Conference,* Osa/vuosikerta 1, pp. 60 - 68.

Österöm, J., Lähteenmäki, J. & Viitanen, T., 2008. F-18 Hornet Landing Simulations Using Adams and Simulink Co-Simulation. *AIAA Modeling and Simulation Technologies Conference*.

Parker Aerospace, 2016. *Aerospace Systems and Technologies.* [Online] Available at: http://www.parker.com/Literature/Hydraulic%20Systems%20Division/HSD%20literature%20files/HSD[1].product.spec.sheet_BootstrapReservior.pdf

Parker Hannifin Corporation, Parker Aerospace, Hydraulic Systems Division, 2016. *Hydraulic Innovations - Systems, Subsystems, and Components.* Kalamazoo, MI: Parker Hannifin Corporation.

Pavan, M. S., Vyas, J. J. & Balamurugan, G., 2015. *Modelling and simulation of aircraft nose wheel steering system.* Noida, 2015 39th National Systems Conference (NSC).

Poole, K., Thielecke, F. & Maediger, C., 2013. *Model-Based Development of Health Monitoring Functions for Aircraft Hydraulic Systems.* Sarasota, /BATH 2013 Symposium on Fluid Power and Motion Control .

Pope, J. E., 1996. *Rules of Thumb for Mechanical Engineers.* Houston: Gulf Publishing Company .

Roccatello, A., Mancò, S. & Nervegna, N., 2007. Modelling a Variable Displacement Axial Piston Pump in a Multibody Simulation Environment. *Transactions of ASME,* 129(July 2007), pp. 456-468.

Rokala, M., 2012. *Analysis of Slipper Structures in Water Hydraulic Axial Piston Pumps.* Tampere: Tampere University of Technology.

Rui, H. ym., 1989. The Study of the Gap Characteristics Between the Valve Plate and Cylinder in Swashplate-Type Axial Piston Motor. *Proceedings of the International Conference on Fluid Power Transmission and Control*, p. 773.

Ruixiang, Z., Tingqi, L., Jianding, H. & Dongchao, Y., 2002. *Fault Diagnosis oif Airplane Hydraulic Pump.* Shanghai, Institute of Electronics and Electrical Engineers, pp. 310-3152.

SAE International, 2008. *AIR5829 Air in Aircraft Hydraulic Systems,* Warrendale PA: SAE international, A-6C3 Fluids Committee.

SAE International, 2011. *SAE AS 5440 - Hydraulic Systems, Aircraft, Design and Installation Requirements For.* s.l.:SAE International.

Singh, K. & Upendranath, V., 2013. *Dynamic Simulation of a Landing Gear System for Retraction and Deployment.* Katra, 2013 International Conference Machine Intelligence and Research Advancement (ICMIRA).

Skormin, V. A. & Apone, J., 1995. *On-line Diagnostics of a Variable Displacement Pump of a Flight Actuation System.* Dayton, OH , USA, Institute of Electrical and Electronics Engineers, pp. 503 - 510.

Staack, I. & Krus, P., 2013. *Integration of On-Board Power Systems Simulation in Conceptual Aircraft Design.* Linköping, Proceedings of the 4th CEAS Conference in Linköping, 2013. International Conference of the European Aerospace Societies.

Terry, F., 1998. Actuation Systems Development. *Aircraft Engineering and Aerospace Technology,* 70(4), pp. 265-270.

Tuttle, F. L., Kisslinger, R. L. & Ritzema, D. F., 1990. *F-15 S/MTD IFPC Fault Tolerant Design.* Hayton, Ohio, USA, Institute of Electrical and Electronics Engineers, p. 501.

US Department of Defence, 1999. *MIL-H-5440 - Hydraulic Systems, Aircraft, Design and Installation Requirements for.* Philadelphia: DLA Document Services.

Wicke, V., Edge, K. A. & Vaughan, N. D., 1998. Investigation of the Effects of Swashplate Angle and Suction Timing on the Noise Generation Potential of an Axial. *ASME Fluid Power Systems and Technology,* p. 77.

Xin, L. & Shaoping, W., 2013. Flow field and pressure loss analysis of junction and its structure optimization of aircraft hydraulic pipe system. *Chinese Journal of Aeronautics*, 26(4), p. 1080–1092.

Xu, B., Wang, Q.-n. & Zhang, J.-h., 2015. Effect of case drain pressure on slipper/swashplate pair within axial piston pump. *Journal of Zhejiang University-SCIENCE A*, 16(12).

Yi, F., Kobayashi, S., Matsumoto, K. & Ikeya, M., 1990. Friction Characteristics of a Ball Joint in the Axial Piston Motor. *Fluid Power Control and Robotics - Proceedings of Chengdu 90 ICFPCR*, p. 162.

Yi, F. & Shirakashi, M., 1995. Mixed Lubrication Characteristics Between the Piston and Cylinder in Hydraulic Piston Pump-Motor. *Transactions of the ASME Journal of Tribology*, Osa/vuosikerta 117, p. 80.

Yin, Y. ym., 2015. Fault Analysis and Solution of an Airplane Nose Landing Gear's Emergency Lowering Journal of Aircraft. *Journal of Aircraft*, 53(4), pp. 1022-1032 .

Zeiger, G. & Akers, A., 1985. Torque on the Swashplate of an Axial Piston Pump. *Transactions of the ASME Journal of Dynamic Systems, Measurement, and Control*, Osa/vuosikerta 107, p. 220.

Zhang, B. ym., 2017. Analysis of the flow dynamics characteristics of an axial piston pump based on the computational fluid dynamics method. *Engineering Applications Of Computational Fluid Mechanics* , 11(1).

Zhanlin, W., Qiu, L. & Liming, Y., 2003. *Development Trends of Aircraft Hydraulic Energy Source & Actuation System.* Wuhan, China, s.n., pp. 462-467.

APPENDIX 1: HYDRAULIC SYSTEM OF LOCHEED MARTIN F-16A

This appendix provides an overview to the general arrangement of the typical fourth generation jet fighter hydraulic system. Locheed Martin F-16A is used as an example because reliable technical data in form of documentation released by the manufacturer is widely publicly available for it. (Locheed Martin Corporation, 1994)

The Aircraft and Its General Arrangement

The F -16A is a single-engine, single-seat, multirole tactical fighter with air-to-air and air-to-surface combat capabilities. The wing has automatic leading edge flaps. Flaperons are mounted on the trailing edge of the wing and combine the functions of flaps and ailerons. The horizontal tails provide pitch and roll control through symmetrical/differential deflection. The vertical tail, augmented by twin ventral fins, provides directional stability. All flight control surfaces are actuated hydraulically by two independent hydraulic systems and are controlled by a fly-by-wire system. Figure A1-1 shows the general arrangement of the aircraft and location of some key hydraulic components and hydraulically actuated parts. Parts and components numbering is given in Table A1-1.

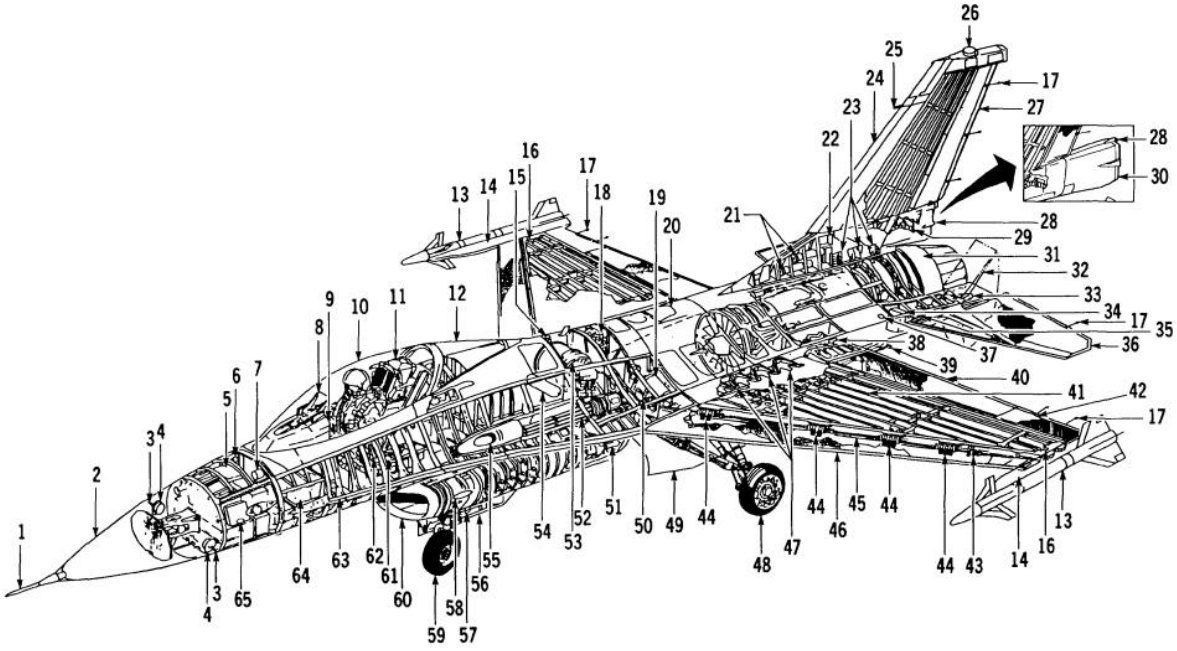

Figure A1-1 General arrangement of F-16A

Table A1-1 Hydraulic components and hydraulically actuated parts numbering for Figure A1-1

18. Leading edge flap (LEF) drive unit	39. Arrestor hook
19. Hydraulic reservoir	40. Flaperon
21. Flight control system (FLCS) accumulators	44. LEF rotary actuator
27. Rudder	46. LEF
29. Rudder integrated servo actuator (ISA)	48. Main landing gear (MLG)
31. Turbofan engine with accessory drive gearbox (ADG)	49. MLG Door
32. Speed brake	52. Gun
33. Speedbrake actuator	54. Emergency power unit (EPU)
35. Horizontal tail ISA	56. Nose landing gear (NLG) door
36. Horizontal tail	59. NLG
38. Flaperon ISA	

The turbofan engine has an engine gearbox which drives the main fuel pump, the oil pump assembly, the engine alternator, and the power take-off (PTO) shaft, which powers the accessory drive gearbox (ADG). The engine arrangement is shown in Figure A1-2. The ADG powers the main generator through the constant-speed drive (CSD), system A and B hydraulic pumps, and FLCS permanent magnet generator (PMG). The jet fuel starter (JFS) is also mounted on the ADG. Figure A1-3 shows the ADG arrangement.

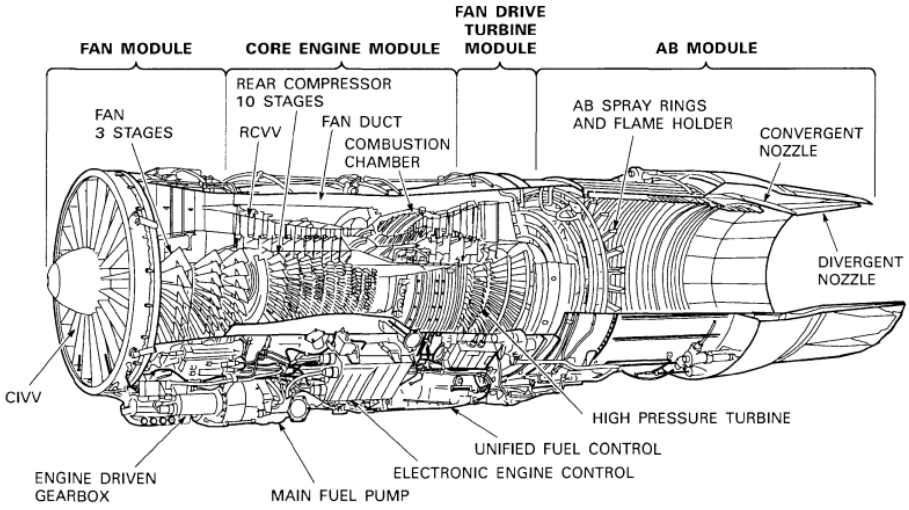

Figure A1-2 The engine arrangement

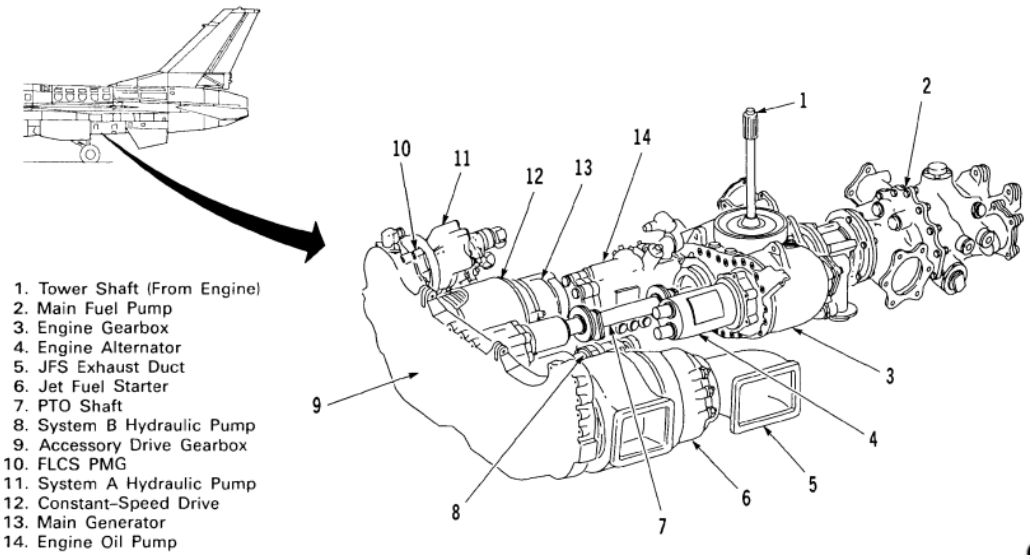

Figure A1-3 ADG arrangement

Hydraulic System Structure and Operation

Hydraulic system diagram is shown in Figure A1-5. Hydraulic pressure is supplied by 210 bar hydraulic systems designated as systems A and B. The systems are powered by two independent EDPs located on the ADG. Both systems have independent reservoir to store hydraulic fluid. The reservoirs are pressurised by their respective hydraulic system to ensure positive pressure at the pump. Reservoir and principle of self-pressurisation is shown in Figure A1-4. Hydraulic system cooling is provided by hydraulic fluid – fuel heat exchanger which uses fuel return flow.

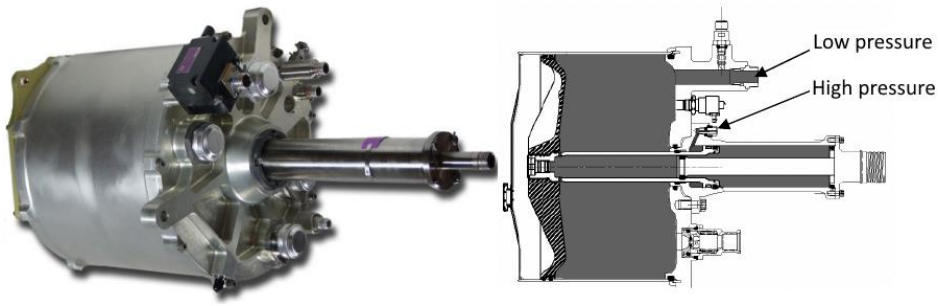

Figure A1-4 Self-pressurised reservoir, outside and cut-away view

Both systems operate simultaneously to supply hydraulic power for the FLCS and LEFs. If one of the systems should fail, the remaining system provides sufficient hydraulic flow and pressure to operate systems with limited maximum actuation rate of the FLCS. System A also supplies power to the hydraulic motor driven fuel flow proportioners (FFP) and the speedbrakes. All remaining utility functions, consisting of

the gun and gun purge door, air refuelling (AR) system, landing gear (LG), brakes, nose wheel steering (NWS), and drag chute system are supplied by system B. System B also charges the brake/JFS accumulators, which provide start power for the JFS and backup pressure for the brakes. System B also contains a drag chute accumulator which provides hydraulic pressure to the drag chute system in case of hydraulic system B failure.

The LG is operated hydraulically, but can be extended pneumatically in the event of hydraulic system B failure. Should both hydraulic systems fail, a third hydraulic pump located on the EPU automatically provides hydraulic pressure to system A.

Each hydraulic system has an FLCS accumulator which is isolated from the main system by check valves. These FLCS accumulators serve a dual function: They provide flow reserve if flow demand exceeds the pump maximum flow rate during rapid control surface movement and if both hydraulic systems fail they provide adequate hydraulic pressure to the flight controls while the EPU comes up to speed.

The EPU is a self-contained system which simultaneously provides emergency hydraulic pressure to system A and emergency electrical power. The EPU is automatically activated when both hydraulic system pressures fall below 1000 psi or when the main generator disconnects from the bus system. The EPU may be operated manually regardless of failure conditions. When operating, the EPU augments hydraulic system A as required. If the normal system A hydraulic pump fails, the EPU is the only source of system A pressure. The EPU uses engine bleed air and/or hydrazine to operate. Normally, engine bleed air is used to maintain operating speed. When bleed air is insufficient, hydrazine augmentation automatically occurs.

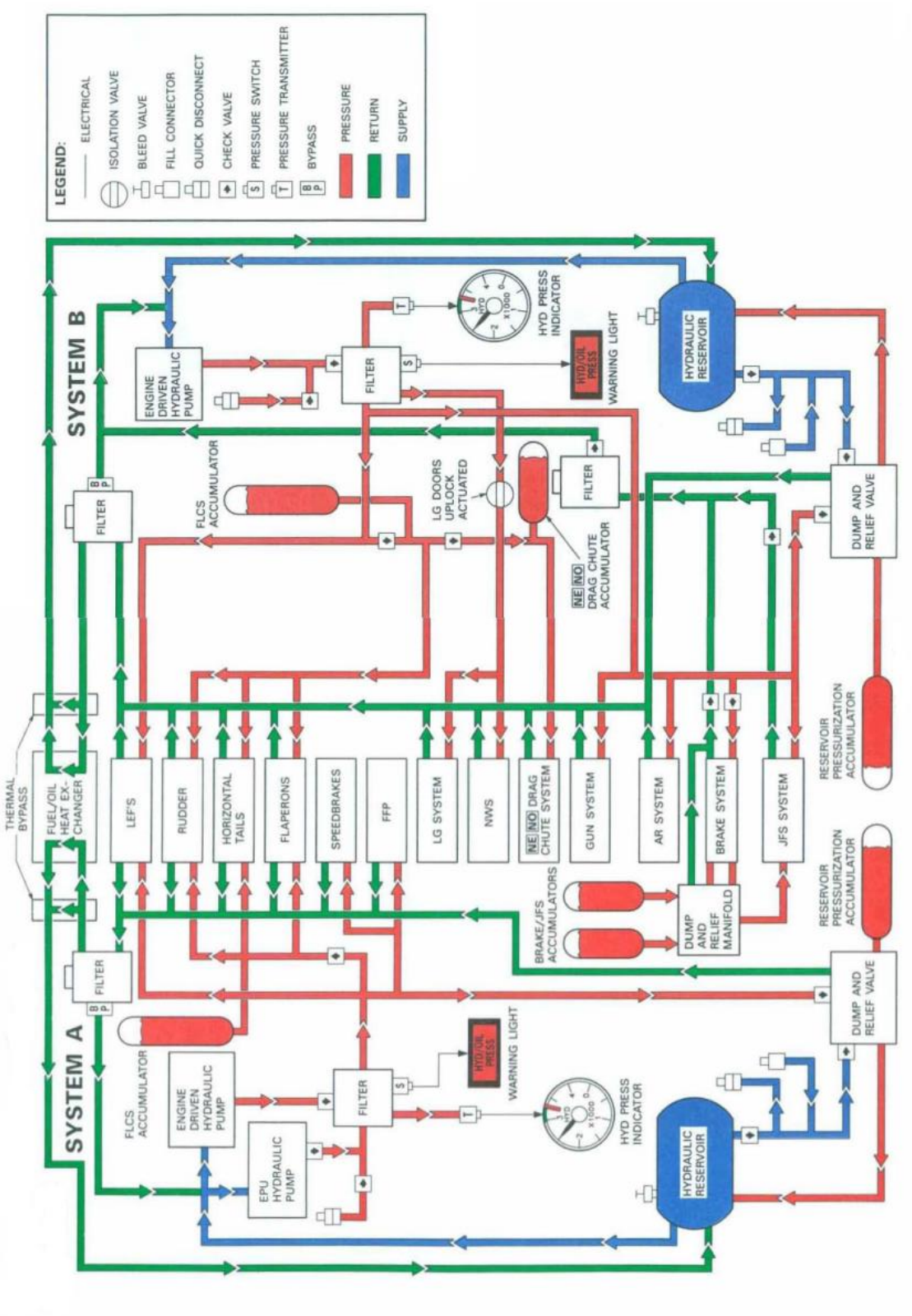

Figure A1-5 Hydraulic system diagram

Tampereen teknillinen yliopisto
PL 527
33101 Tampere

Tampere University of Technology
P.O.B. 527
FI-33101 Tampere, Finland

ISBN 978-952-15-3881-0
ISSN 1459-2045